# INVESTIGATING MECHANISMS UNDERLYING CHEMOTAXIS AND COLONIZATION RESPONSE TO INDOLE IN *ESCHERICHIA COLI*

A Dissertation

by

JINGYUN YANG

Submitted to the Graduate and Professional School of
Texas A&M University
in partial fulfillment of the requirements for the degree of

DOCTOR OF PHILOSOPHY

| | |
|---|---|
| Chair of Committee, | Arul Jayaraman |
| Co-Chair of Committee, | Pushkar P. Lele |
| Committee Members, | Michael D. Manson |
| | Phanourios Tamamis |
| Head of Department, | Arul Jayaraman |

December 2021

Major Subject: Chemical Engineering

# ABSTRACT

Bacterial chemotaxis to microbial-derived metabolites likely plays a key role in shaping the diversity in microbial communities in the gastrointestinal tract (GI tract). Among the important metabolites is indole, which modulates chemotaxis through unknown mechanisms. As indole is produced by the many species in the gut microbiota and as it strongly impacts bacterial physiology, the basis of chemotaxis to indole is of major interest.

In this work, we dissected the mechanisms underlying indole chemotaxis in *Escherichia coli*. We characterized the role of two major chemoreceptors, Tar and Tsr, in sensing indole. Our findings suggest that Tsr and Tar mediate opposite responses to indole, and that the difference in the kinetics of the responses induces biphasic chemotaxis. Biphasic chemotaxis attracts cells that have previously adapted to the metabolite to indole-rich niches. However, it repels cells that have not adapted to the metabolite from indole-rich niches. This causes a bifurcation of the population of cells based on their chemotaxis response. Based on these observations, we propose that indole maintains gut homeostasis by recruiting beneficial commensal bacteria and repelling pathogenic bacteria. We further characterized the structural domains in Tar and Tsr that are responsible for this biphasic chemotaxis response to indole. We have found that the periplasmic domain of Tsr senses indole as a repellent, contradicting earlier reports. Interestingly, our experiments suggest that indole activates all the major domains of Tar: the periplasmic, the HAMP, and the cytoplasmic. Finally, we have investigated the integrated effect of the indole and another important class of microbial metabolites – short chain fatty acids (SCFA), on chemotaxis. Our findings show that the presence of indole can cause an unexpected inversion from repellent to attractant chemotaxis towards SCFAs.

# ACKNOWLEDGEMENTS

I deeply appreciate my advisor Dr. Arul Jayaraman for providing me the great opportunity to study in his lab. The experience of working and living at A&M for six years has incredibly changed my way of thinking, learning, and understanding this world. Without his support, encouragement, and guidance, I would have never grown to become an independent researcher. I would always inspired by his passionate on field of academia and education and benefit from the good training and mentoring from him.

I would like to thank my co-advisor Dr. Pushkar Lele for his great suggestions and help. I would not have such achievements without his insightful comments and advices. I want to acknowledge him for sharing me his tremendous experience and knowledge in the field in the past years. I am also grateful to my committee – Dr. Manson and Dr. Tamamis for their valuable time and advices. I gained so much suggestions and motivations from every committee meeting with them.

I want to thank all past and current lab members in the Jayaraman lab and Lele lab. I want to thank Nitesh, Sasi, Sneha and Nandita for their help when I initially join the lab. I want to thank Ravi for his hard work in our collaborative projects. I want to thank Daniel, Ari, Liangyu, Clint, Farrhin for all their companion and happy moments in the lab these years. I especially appreciate the advice and mentorship from Yufang. Thank you for being my colleagues, my friends, and my family for the past six years. Thanks also go to all my friends at Texas A&M University. Thank you for making my life here such a great and wonderful memory. Thanks to my girls in the dance team to make so much fun here. Thanks to my best friend Kang for her companionship from Dallas.

Thanks Zelun for his support and encouragement at my hardest times. Last, my deepest gratitude goes to my family. I thank my parents and sister for their endless support and love.

# CONTRIBUTORS AND FUNDING SOURCES

This work was supervised by a dissertation committee consisting of Professor Arul Jayaraman (advisor), Professor Pushkar P. Lele (co-advisor), and Professor Phanourios Tamamis in the Department of Chemical Engineering, and Professor Michael D. Manson in the Department of Biology.

The experiments presented in Chapter III were conducted in part by Ravi Chawla and Kathy Y. Rhee of the Department of Chemical Engineering and were published in 2021. The experiments presented in Chapter IV were conducted in collaboration with Anusha Aditya of the Department of Chemical Engineering.

All other work conducted for the dissertation was completed by the student under the advisement of Professor Arul Jayaraman of the Department of Chemical Engineering.

This work was made possible in part by the Ray B. Nesbitt Chair endowment to Arul Jayaraman and from the National Institute of General Medical Sciences United States to Dr. Pushkar P. Lele (R01-GM123085).

TABLE OF CONTENTS

Page

LIST OF FIGURES

Page

LIST OF TABLES

Page

# CHAPTER I

# INTRODUCTION

## 1.1 Background and motivation

The mammalian gastrointestinal (GI) tract harbors a diverse community of microbes, collectively known as the microbiota. The environment is inhabited with up to 100 trillion ($10^{14}$) microbes that belong to over 30 genera (1-3). The microbiota has been shown to be crucial for vitamin and nutrient processing (4), gut physiology (5, 6), maintenance of homeostasis, and development and maintenance of the immune system (7). Another major role for the intestinal microbiota is in host defense against enteric pathogenic infections (8). A diverse group of pathogens contribute to food-borne infections, with the most prevalent strains being *Campylobacter, Listeria, Salmonella, Clostridium, Escherichia coli, Shigella, Vibrio* and *Staphylococcus* (9). Among them, *Salmonella* and *E. coli* account for over 80% of the multi-state outbreaks that have occurred in the US over past several decades (9). Specifically, *enterohemorrhagic E. coli* O157:H7 (EHEC) is responsible for one of the most frequently occurring outbreaks. EHEC is naturally present in cattle and other ruminants, and it is mainly transmitted via contaminated water and food products (10). EHEC colonizes the human colon and enhances attaching and effacing (AE) lesion formation, leading to outbreaks of bloody diarrhea (11). The Shiga toxin produced by the pathogen cause hemolytic uremic syndrome (12), which is the most frequent etiology of pediatric acute renal failure, with a lethality of 3%-5% worldwide (13).

EHEC infections occur through a three step mechanism: migration along the gut lumen and recognition of intestinal epithelium; attaching to and colonizing epithelial cells; infection of host

cells and release of toxin (11). Several studies have identified the factors that modulate EHEC virulence at the host epithelial surface (11, 14, 15). However, less is known about the mechanisms they use to locate and migrate towards the sites of infection. One of the key contributing factors is chemotaxis (16, 17), which refers to the migration of flagellated bacteria towards favorable chemical environments, seeking nutrients and avoiding poisons. It is mediated by modulating an alteration of smooth swimming that is interrupted by tumbles that change the direction of swimming. Chemoattractants promote the smooth swimming while chemorepellents favor tumbling. Flagellar motility and chemotaxis likely help other pathogens, such as *Salmonella enterica*, *Vibrio cholera* and *Helicobactor pylori* establish infections (18-20).

Several studies indicate that motile pathogens use chemotaxis to migrate towards microbial metabolites that guide them to preferred niches in the intestinal tract (21-24). Among these metabolites is fucose, which is a major component of the intestinal mucus. Fucose is sensed by EHEC to differentiate between the lumen and epithelium (25). Prior work from our lab has shown that the enteric neurotransmitter norepinephrine (NE) and its microbiota-derived metabolite dihydroxy mandelic acid (DHMA) are also sensed by EHEC *in vitro* (21). Also of particular interest are short chain fatty acids (SCFAs) such as acetate, propionate, and butyrate, which are sensed by EHEC to locate the proximal colon (22). Another molecule of interest is indole, which is a product of tryptophan metabolism, Indole is an important molecule for chemotaxis in *Salmonella enterica* and *Escherichia coli* (26, 27). Several groups, including our lab, have shown the impact of both SCFAs and indole on motility, biofilm formation, plasmid maintenance, stress responses, and virulence (28-31). In the GI tract, indole is produced in concentrations in the range of 0.2 to 6.5 mM (32), and SCFAs are among the most abundant types of metabolites in the GI tract (31, 33). Indole and SCFA producers thrive in the intestine, especially the proximal colon.

Thus indole and SCFAs are expected to co-exist and to work together to affect bacterial chemotaxis and colonization.

Despite considerable progress in our understanding of bacterial chemotaxis, how these metabolites regulate chemotaxis is poorly understood. Interestingly, some of the molecules that are chemoattractants (e.g., NE, DHMA) also promote virulence of multiple enteric pathogens, including EHEC, *Salmonella*, *Campylobacter* and *Vibrio* (34-37). The positive correlation between chemotaxis and virulence motivates the current work on investigating how metabolites in the GI tract environment modulate colonization and infection.

In our work, we investigated the mechanisms underlying the sensing of indole in *E. coli*. Our overall hypothesis is that the bacterial chemotactic response to indole underlies the attachment and colonization of bacteria to surfaces. Using a non-pathogenic strain of *E. coli* as a model organism, we systematically investigated the mechanisms underlying sensing of indole in terms of the receptors, the signaling mechanisms involved, and the structural domains within chemoreceptors that sense indole. To understand more about the behavior of bacteria when exposed to a chemically complexed environment in which both indole and SCFAs are present, we also investigated how different combinations of indole and SCFAs modulate chemotaxis.

### 1.2 Aims

**Aim 1:** Investigate the mechanisms underlying the chemotaxis response of *E. coli* to indole.

We will employ the tethered cell assay and transwell assays to assess the responses in *E. coli* RP437 to indole. The tethered cell assay monitors the behavior of individual flagellar motors, and the transwell assay shows the response of cell population. We will use Δ*tsr* and Δ*tar* mutants

to characterize the role of these receptors in mediating indole responses. Overall, we will investigate the mechanistic details underlying indole sensing in *E. coli* and discuss the significance of the chemotaxis response to indole in the GI tract.

**Aim 2:** Identify structural domains in the Tsr and Tar chemoreceptors of *E. coli* involved in sensing indole.

To identify the domains of Tsr and Tar that are involved in sensing indole, we will employ hybrid constructs with different combinations of the periplasmic and TM domain, the HAMP domain, and the long four-helix bundle consisting of the methylation helix and kinase control domain. We will express these chimeric receptors in a Δ*tsrtar* mutant. We will conduct Fluorescence Resonance Energy Transfer (FRET) microscopy between CheY-CFP and CheZ-YFP to investigate the activity of the CheA kinase. This approach eliminates any direct effect of indole on the rotational direction of the flagellar motor. We will propose a model to describe how these three structural domains in each receptor contribute to indole sensing and discuss how the responses mediated by the two receptors might interact during colonization of the GI tract.

**Aim 3:** Investigate the interaction of indole and SCFAs during *E.coli* chemotaxis.

In this study, we will discuss the chemotaxis behavior of bacteria in the complex environment in which more than one signaling molecule is present. We will use three different SCFAs as the second stimulus in combination with indole and investigate the integrated effect of the signals on *E. coli* RP437 chemotaxis. The attachment of cells in response to the SCFA gradient with or without indole pre-priming will be quantified with the transwell assay. The rotational bias of the flagellar motor in cells with different combinations of the Tar and Tsr receptors in response

to stimulation with SCFA and indole will be analyzed. We will discuss the integrated responses of these cells and the significance of this response in modulating bacterial colonization of the gut.

### 1.3 Innovation and significance

Several studies have identified microbiota derived molecules that modulate bacterial colonization, but very few have focused on molecular basis of how these metabolites affect the chemotactic signaling that modulates surface colonization. Therefore, understanding the mechanisms underlying the chemotactic responses to these metabolites can be impactful. Our study will link chemotaxis in response to important microbial metabolites with microbial homeostasis in the GI tract. The work proposed here focuses on the chemotactic behavior of *E. coli in vitro*. However, it will also help us understand what may be happening in the *in vivo* environment and thereby advance our understanding of the role of chemotaxis in the formation of commensal bacterial communities and during invasion of the gut by pathogens.

# CHAPTER II

# LITERATURE REVIEW

## 2.1 Gut microbiota

The human body is inhabited by a great number of bacteria, archaea, viruses, and eukaryotes, which are collectively known as the microbiota (38, 39). Microbes thrive on the skin in the respiratory system, and in the genitourinary and gastrointestinal tracts (39-41). However, the gastrointestinal (GI) tract contains over 70% of all the microbes in the human body (1, 42). Estimates of the number of bacterial species varies among studies, but it is generally accepted that over 1000 species exit in the gut (43). The Bacteroidetes and the Firmicutes are dominant phyla, while Proteobacteria, Actinobacteria, Fusobacteria, and Cyanobacteria are present in minor proportions (3). The intestinal microbiota is not homogeneously distributed, with only $10^1$ to $10^3$ cells/gram present at stomach but up to $10^{12}$ per gram in the distal colon(42). The number of individual cells and species varies not only in different sites along GI tract but also longitudinally across the mucus layer (44). For example, the genera *Clostridium*, *Lactobacillus*, and *Enterococcus* are present primarily near epithelial surface and mucus layer, while *Bacteroides*, *Bifidobacterium*, and *Enterobacteriacea* are distributed in the lumen and feces (44).

### 2.1.1 Commensals with flagellar motility

Among the wide range of commensals in the gut, many species, especially Firmicutes and Proteobacteria, have the capacity to produce flagella (45), which are required for swimming motility. In addition to *Escherichia coli*, species belonging to the genera *Clostridium*, *Roseburia*, *Lactobacillus*, *Eubacterium*, *Providencia*, *Citrobacter*, and *Staphylococcus* have the ability to

assemble flagella and are motile (46). Although many of these species are motile when isolated from the host, levels of flagellin, the most abundant protein of bacterial flagella, are low in the healthy gut (47). This might suggest that the host somehow limits the motility of commensals. One study showed that both innate and adaptive immunity quench flagellar motility with anti-flagellin immunoglobulin A (IgA) secreted in the gut (46). The loss of motility for commensals might prevent their breaching epithelial barriers, but that raises the question of why flagellar genes are so widely distributed among commensal species. One study investigated a potential role for motility on inter-species interactions – monocolonization of *Roseburia cecicola* into germ-free mice resulted in the loss of their motility, whereas their motility was maintained when they co-colonized with four other species (48). Motility is possibly important when in the context of a complex environment, in which microbe-microbe interactions occur within different niches (46).

### 2.1.2 Commensal *Escherichia coli* in the GI tract

*Escherichia coli*, the model species for studying bacteria motility, is the predominant facultative anaerobe that resides in the mucus layer of intestine (49, 50). *E. coli* can also persist in the external environment until they enter the host intestine. Following ingestion, *E. coli* survives the acidic environment of the stomach by virtue of their acid-resistance system (51). Upon reaching the colon, they need to find nutrients to end the lag phase and successfully colonize the colon (52). Multiple factors contribute to successful colonization by *E. coli*, including the ability to compete for nutrients and to penetrate the mucus layer (52, 53). However, motility was not found to play any role in colonization of *E. coli* in large intestine of streptomycin-treated mice (54). In contrast, in other studies, the swimming ability of *E. coli* has been shown to be vital for biofilm formation

and host colonization of *E. coli*, especially when they initially enter the lumen and must locate favorable sites for colonization (55, 56).

### 2.2 Chemotaxis and foodborne pathogenesis

The intestinal tract is a complex environment that is encountered by enteric pathogens as they transit through gastrointestinal tract of the host. According to the Centers for Disease Control and Prevention, foodborne illnesses are common in the United States (9). It has been estimated that around 10 million cases of foodborne illness are reported each year, and several major bacterial pathogens are usually implicated (57).

The swimming ability of pathogenic bacteria toward and through the mucus layer of the gut, which is greatly aided by chemotaxis, is believed to be an important contributing factors for infection and virulence (58, 59). It has been shown that around half of animal/human pathogens have chemosensory signaling genes (60). Specifically, the majority of gastrointestinal pathogens, including *Campylobacter, Salmonella, Escherichia coli,* and *Vibrio* spp., possess chemosensory genes (60) and benefit from chemotaxis to locate niches favorable for colonization (58). The potential link between chemotaxis and pathogenicity is summarized in **Fig. 2. 1**. *Helicobacter pylori* is a bacterium that colonizes the gastric epithelium in the stomach and causes multiple severe diseases. Multiple studies have shown the importance of motility and chemotaxis in successful colonization by *H. pylori* (61). *Campylobacter jejuni*, a pathogen that causes gastroenteritis, requires chemotaxis to penetrate the mucus layer and colonize the epithelium (62). Mutants missing chemoreceptors Tlp3 and Tlp4 are severely compromised in their ability to colonize the jejunal mucosa of mice. Complementation with the genes encoding these receptors restored the ability to colonize, emphasizing the importance of chemotaxis to bile and sodium

deoxycholate (24). For *Salmonella enterica*, a competitive colonization assay was conducted using a mixture of the wild-type and a *cheY* mutant strain to assess role of chemotaxis. Although both stains could colonize the intestine of streptomycin-treated mice, the *cheY* strain was out-competed by wild-type by 3 days post-infection (20). Interestingly, chemoreceptor Aer and Tsr are involved in energy taxis of *Salmonella* towards tetrathionate and nitrate, which are released upon infection, indicating *Salmonella enterica* energy taxis seems to support host infection (23). Specifically, *Enterohemorrhagic E. coli* O157:H7 (EHEC), one of the most frequently occurring causes of multistate outbreaks of food poisoning that have occurred in the US over past decade (9), shows strong chemoattraction to epinephrine and norepinephrine and an increased cell attachment to HeLa cells because of this response (28). EHEC is also attracted to the quorum-sensing molecule AI-2 and the presence of AI-2 has been shown to promote cell attachment to HeLa cells (63).

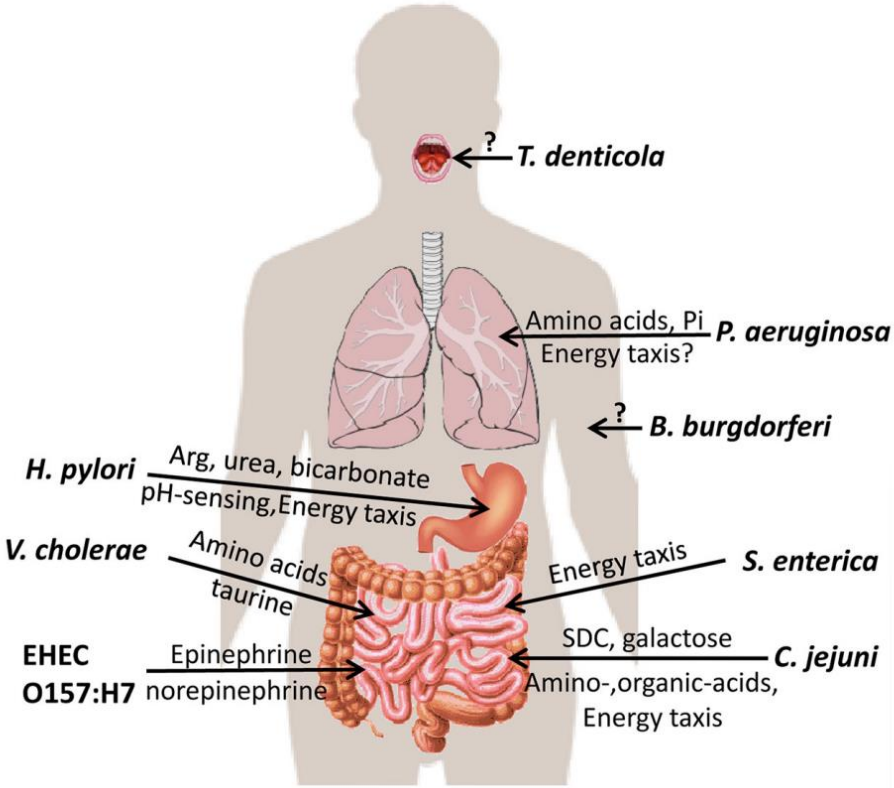

**Figure 2. 1 Diagram of the sites of infection by human pathogens in which chemotaxis has been described to play a key role in colonization and disease development, adapted from Ref. 58 (58).** Descriptions have been generated using different cell, animal and human models.

### 2.3 The *E. coli* chemotaxis system

Bacteria face significant challenges in navigating towards niches. To overcome constraints imposed by random Brownian motion and the high viscous forces prevalent at low Reynolds numbers, bacteria have evolved a strategy to migrate towards favorable chemical environments – termed as chemotaxis (64). The model bacterial species for understanding chemotaxis, *Escherichia coli*, biases a random walk consisting of a combination of runs and tumbles to migrate in chemical gradients (**Fig. 2. 2**.). Each cell rotates its multiple flagella counterclockwise (CCW) to swim forward in a straight line, termed as a 'run' (65). Switching the direction of rotation of the flagella to clockwise (CW) disrupts the flagellar bundle, leading to a 'tumble'. The tumble reorients the cell, allowing it to select a new swimming direction. The cell decreases its frequency of tumbling when it moves in a 'favorable' direction in a chemical gradient.

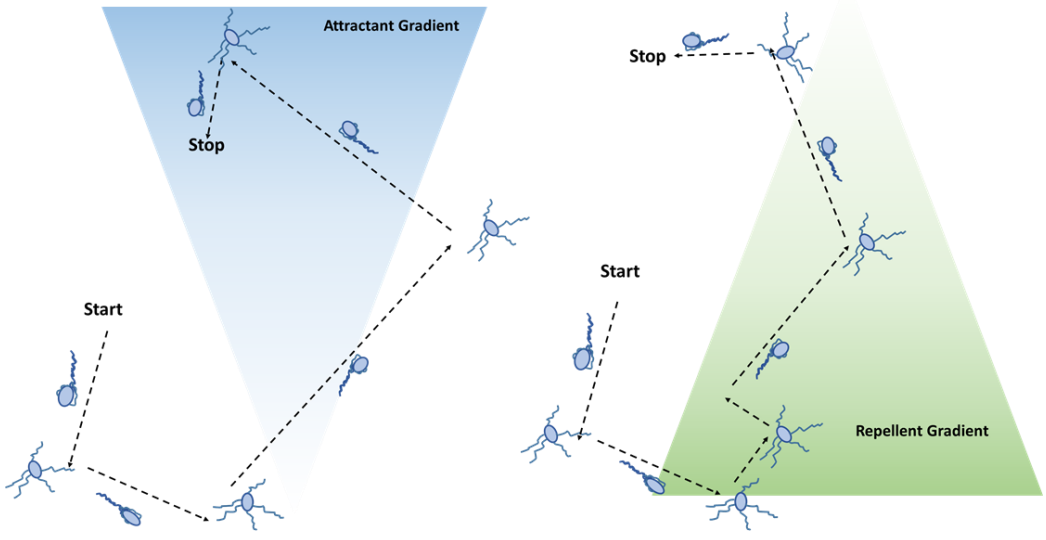

**Figure 2. 2 Chemotactic behavior of *E. coli*.** Bacteria move in a 3-dimensional random walk consisting of alternating runs and tumbles. Attractants favor longer runs while repellents promote more frequent tumbles. Bacteria move up attractant gradients and move down repellent gradients.

### 2.3.1 The bacterial chemotaxis network in *E.coli*

A two-component system controls the switching between the CCW and CW directions of flagellar rotation. The network sensitively detects small changes in the concentration of ligands even when the background concentrations vary over five orders of magnitude (66, 67). **Fig. 2. 3** shows a schematic view of the chemotaxis signaling network. A ligand is detected by a chemoreceptor. Chemoreceptors form hexagonal arrays composed of trimers of receptor homodimers at the cell poles, with the older pole typically having a larger array (68, 69). Five types of chemoreceptors are known in *E. coli*: Tsr, Tar, Trg, Tap, and Aer. The first four are called methyl-accepting chemotaxis proteins (MCPs) because they undergo covalent methylation. An adaptor protein, CheW, helps to link the MCPs to the cytoplasmic kinase CheA, whose activity is closely controlled by the chemoreceptor signaling states (70). CheY, the response regulator, can be phosphorylated by CheA. CheY-P binds to the FliM subunits within the flagellar motor to promote CW rotation in an otherwise CCW-rotating motor (71, 72). The phosphatase CheZ dephosphorylates CheY-P and terminates the signal from the chemoreceptor patch to the flagellar motor (73). The antagonistic activities of CheR (a methyltransferase) and CheB (a methylesterase) are responsible for adaptation to the background level of signals. CheR is constitutively active in methylating the MCPs at specific glutamyl residues using cytoplasmic pool of S-adenosylmethionine as the methyl donor (74). When phosphorylated by CheA, CheB-P remove methyl groups from MCPs (75, 76).

Repellent-binding to the receptors (or decreased binding of attractant) stimulates CheA autophosphorylation, which results in an increase in the concentration of CheY-P. As a

consequence, CheY-P binds to the motor to promote tumbles, allowing the cell to change its course toward the repellent (or away from the attractant). At the same time, CheA phosphorylates the methylesterase CheB, resulting in increased demethylation of the MCPs. This restores CheY-P back to the pre-stimulus levels. The motors respond by resuming CCW rotation, and the cell resumes smooth swimming in a different direction. One study showed that the phosphotransfer to CheY is faster than the phosphotransfer to CheB, which ensures that a response can occur before adaptation nullifies it (77). An attractant binding to the receptor (or a decreased concentration of repellent) inhibits the autophosphorylation of CheA, reducing CheY-P levels. The methyltransferase CheR constitutively methylates MCPs to restore CheA activity to the pre-stimulus values.

The probability of CW motor rotation changes steeply over a narrow range of CheY-P levels. The relationship obeys a Hill function with a Hill coefficient of around 11 (78). The clustering of the receptors at one pole of the cell body facilitates signal amplification because of highly cooperative interactions among the receptors within the cluster (79). This amplification of the signal confers the ability to detect small changes in chemoeffector concentrations and to modify the swimming behavior of the cell in response (80).

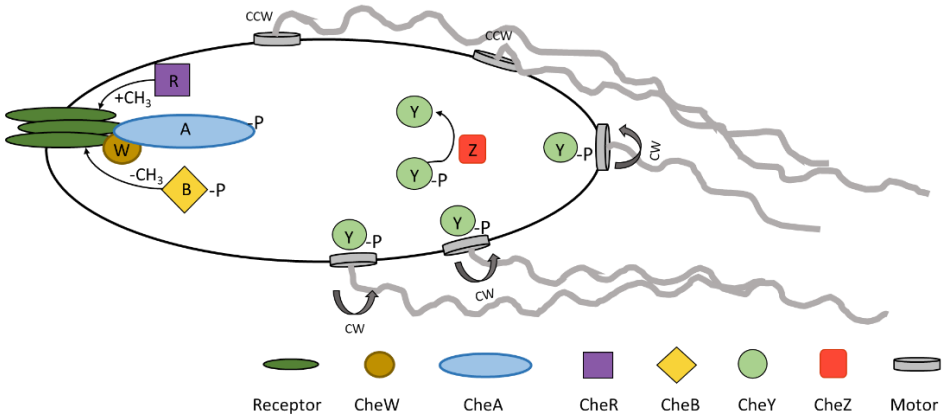

**Figure 2. 3 Schematic of chemotaxis signal transduction in *E. coli.*** Chemoreceptors interact with CheW and CheA to form stable complex at a pole of the cell. Signals are generated by the transfer of phosphoryl groups from the CheA kinase to the response regulator CheY. Phospho-CheY promotes CW rotation of the flagellar motors. CheZ greatly accelerates the dephosphorylation of CheY-P. CheR (methyltransferase) and CheB (methylesterase) are responsible for adaptation through modulation of the methylation state of the receptors.

### 2.3.2 Chemoreceptors

In *E. coli*, four of the five chemoreceptors are MCPs that form homodimers spanning the bacterial cell membrane (81). Tar and Tsr are two most abundant receptors and are present in 5- to 10- fold greater amounts than the two low abundant receptors, Trg and Tap (82). The fifth chemoreceptor, Aer, is not an MCP, but it works with the receptors to mediate a positive aerotactic response sensed by oxidation of its flavin adenine dinucleotide (FAD) group (83).

The cytoplasmic domain of chemoreceptors is rather highly conserved among bacteria and archaea, while the periplasmic domain varies in sequence and structure to accommodate the binding of different types of the ligands (84). The periplasmic domain is the dimer of four-helix bundles (α1–α4, α1'–α4'), whereby two helices from each subunit extend into the bilayer and form a transmembrane four-helix bundle (TM1, TM2, TM1', TM2')(**Fig. 2. 4**) (85-87). A structurally conserved HAMP domain with a four helix, parallel coiled-coil structure (AS1, AS2, AS1', AS2'), connects the transmembrane helices to the cytoplasmic signaling domains (88, 89). The two helices in each HAMP domain are joined by a non-helical connector (CTR) (90). HAMP domain is known to play central role in signal transmission (91). A five-residue junction between TM2 and AS1, known as the control cable, forms a short helix at the membrane-cytoplasm interface (92). The HAMP domain connects with the methylation helices (MH1, MH1') that form an antiparallel four-helix bundle with their C-terminal counterparts(MH2, MH2') (85). The highly conserved glycine hinge forms a flexible connection between the MH helices and the CheA/CheW interaction region

at the membrane-distal tip of the receptor. This regions forms another anti-parallel hour-helix bundle that extends from MH1 to MH2 and is essential for modulating the kinase activity (93). Later work showed the important role of the glycine hinge in facilitating the transition between signaling states at the receptor trimer level (94). At the extreme C-termini of the two most abundant chemoreceptors, Tsr and Tar, a pentapeptide motif (NWETF) binds CheR and localizes it to a region near the MH helices (95).

Signal transduction upon ligand binding to the chemoreceptors is mediated by subtle conformational changes. It is believed that attractant binding results in a 1-2 Å inward piston displacement of the α4-TM2 helix (96, 97) that pushes the N terminus of TM2 into the hydrophobic phase of the membrane. Because the aromatic anchor at the C-terminus of TM2 (WY in Tar, EF in Tsr) has a high affinity for the hydrophobic/hydrophilic interface region of the cytoploasmic face of the membrane, TM2 bends and triggers the inward lateral sliding of the aromatic anchor along with the control cable (98, 99). Both experimental data and molecular simulation have shown that helicity of the control cable is crucial to the signal transmission from TM2 to HAMP domain (100, 101).

The signals from the transmembrane region are then passed through the HAMP domain. The mechanisms for signal transduction by the HAMP domain have been extensively studied, and several models have been proposed. The static two-state model suggests that the HAMP domain interconverts between two rigid conformations that represent opposite signaling states, which include a cogwheel model (89), a helix rearrangement model, and a scissor-like model (reviewed in (102)). Growing evidence, however, based on studies of the Tsr HAMP domain, suggests a biphasic dynamic bundle model that proposes the HAMP domain have a dynamic range of packing stabilities (103-105). The kinase-ON output state corresponds to a dynamic, less-tightly packed

HAMP domain, which leads to a stably packed MH bundle. The kinase-OFF state represents a stable HAMP domain and a dynamic MH bundle. According to a yin-yang model for the interaction of the MH helix with the kinase-control region, a loose packing MH bundle leads to a tight packing of protein interaction region, which inhibits CheA activity (106). Therefore, the attractant-induced kinase-OFF state represents a tightly packed HAMP domain, a loosely packed MH bundle, and a tightly packed protein contact region. The repellent induced kinase-ON state would have the opposite conformation. It has been shown that the packing of MH bundle could provide a structural basis for adaptation modifications (104, 107). The loose packing of MH bundle in the kinase-OFF state may favor interaction with CheR, while the tighter packing of MH bundle in the kinase-ON state may favor interaction with CheB (107). To adapt to an attraction response (kinase-OFF state), methylation of the glutamyl residues at the MH bundle neutralizes the negative charges of the region and favors a tighter packing of MH bundle and looser helix packing at the hairpin tips that interact with CheA, thereby restoring the kinase-ON state (108, 109).

As mentioned earlier, the MCPs are found in closely packed arrays at one pole of the cell body (69). Recent electron-cryotomography studies provide a detailed structure of the clusters (110-112). The receptor dimers group into timers and assemble with CheW and CheA regulatory domains to form hexagons arrays via multiple hydrophobic interactions. This architecture enables the lateral spread of the signals initiated by ligand binding to one receptor to promote signal integration and amplification (79, 113-115). The clustering of the signaling complexes enhances the CheA activity by about a hundred fold and increases the sensitivity and dynamic range of the chemotaxis sensory system (116, 117).

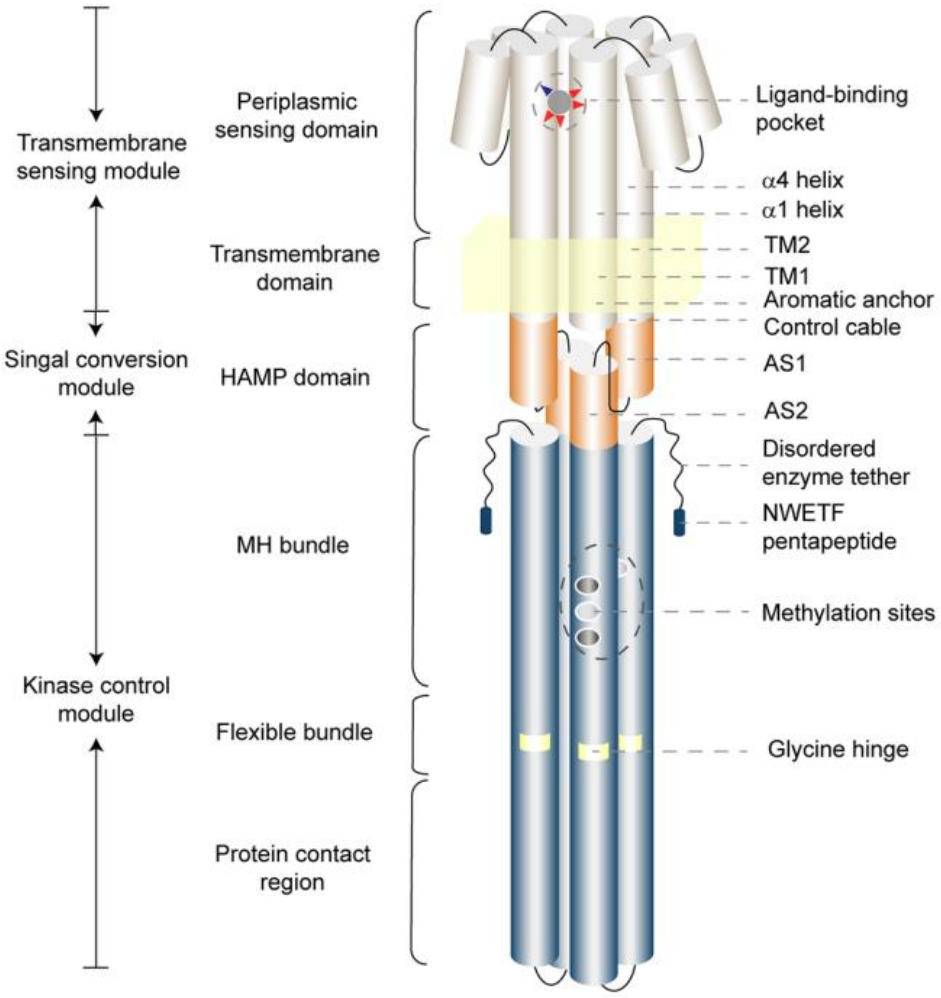


**Figure 2. 4 Structural features of a conventional chemoreceptor homodimer in *E. coli,* adapted from Ref. 102 (102).** The specific features and motifs are noted to the sides of the dimer.

### 2.3.3 The diversity of sensing mechanisms in *E. coli* chemotaxis

Chemoreceptors in *E. coli* use a variety of sensing mechanisms to detect diverse stimuli. These have been divided into four groups (**Fig. 2. 5.)** (118). Tsr and Tar sense serine and aspartate as attractants by direct binding to their periplasmic domains (119, 120). Tsr also senses DHMA by direct binding to the same site as serine (21). Tar senses maltose indirectly by interaction with the ligand-bound form of the periplasmic maltose-binding protein (121). Tsr senses one form of autoinducer-2 (AI-2) by interaction with the AI-2-bound form of the periplasmic LsrB protein (27,

122). Dipeptides are sensed indirectly by Tap through its interaction with the ligand-bound form of the periplasmic DppA protein (123), and Trg senses galactose, glucose through interaction with the periplasmic MglB protein and senses ribose through interaction with the periplasmic RbsD protein. Variety of sugars are sensed as attractants through the phosphotransferase system (PTS) (124). The PTS-mediated influx of sugars into cells lower phosphorylation state of the PTS, which then inhibits CheA activity (**Fig. 2. 5.)** (118). Some other environmental cues such as pH, temperature, osmolarity, and some aromatic compounds elicit chemotactic responses indirect mechanisms (125-129).

The situation with repellents is less well understood. It is not clear that any of them elicit a response by binding directly to the periplasmic domain of a receptor, but it has been reported that spermidine is sensed as a repellent through the interaction of Trg with the PotD periplasmic protein of the spermidine uptake system (130). Many repellents may exert their effect through interaction with parts of the receptor other than the periplasmic domain. Candidates for interaction sites are the TM domain, the HAMP domain, the MH domains, the glycine hinge or the kinase-control domain. Indole, which we show in this work acts both as a repellent sensed by Tsr and as a repellent sensed by Tar, provides a particularly interesting case.

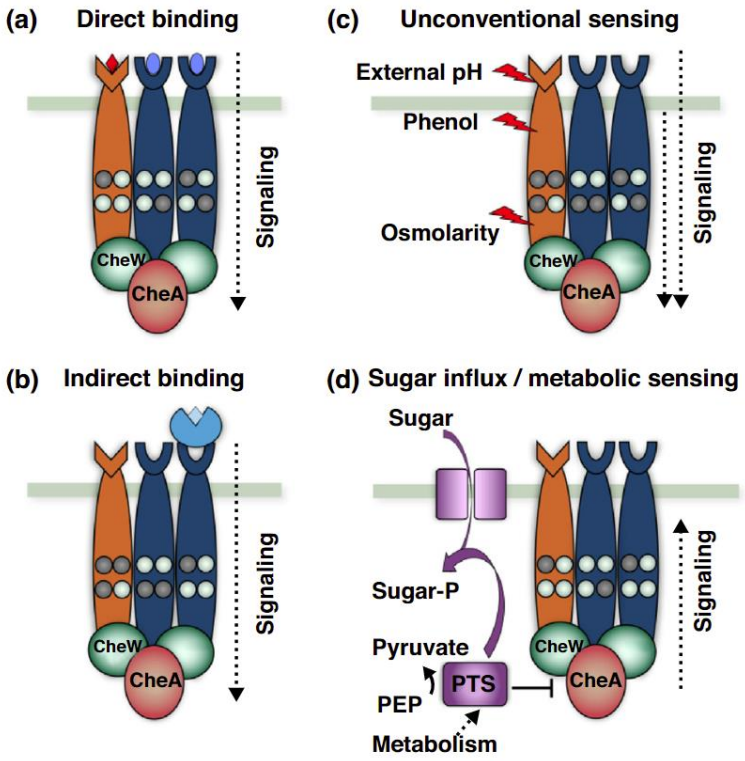


**Figure 2. 5 Diversity of sensing mechanisms in *E. coli* chemotaxis, adapted from Ref. 118 (118).** Chemical ligands bind to the periplasmic sensory domains of chemoreceptors either directly (a) or indirectly via BPs (b), with signaling changes in receptor conformation (dashed arrow) propagating from the sensory domain towards the cytoplasmic tip. (c) Unconventional environmental stimuli are detected by perturbations of different regions of receptors, including the periplasmic domain but potentially also the TM and cytoplasmic domains, as indicated. (d) The PTS links chemotactic response to the uptake of sugars and other metabolites. In this case conformational signals apparently propagate backwards from the signaling tip of receptor towards the methylation region.

## 2.4 Microbial metabolites of interests

Chemotactic responses to microbial metabolites may direct the distribution of bacteria in the gut. Many studies have shown that *E. coli* responds to multiple hormones in the host gut (21, 130). A previous study from our lab characterized an attractant response by *E. coli* to the norepinephrine metabolite DHMA. The Tsr receptor is responsible for sensing DHMA and the residues that interacting its canonical ligand serine is also involved in DHMA sensing. In another study, ten gut-derived compounds were tested, and five of them elicited chemotactic responses in

*E. coli* (130). Melatonin and spermidine were sensed as repellents, while dopamine and DHMA elicited mixed responses with the concentrations that had been tested. The two most abundant bacteria-derived metabolites, indole and SCFAs, have received attention recently because they are important signaling molecules and because they elicit chemotactic responses in *E. coli*.

### 2.4.1 Indole

Indole is produced by degradation of the amino acid tryptophan by tryptophanase. This process releases ammonia and pyruvate, which are used as a source of nitrogen and carbon under starvation conditions (131). At least 85 bacterial species present in the GI tract harbor the *tnaA* gene and can produce indole (30). These bacteria occupy the interface of the mucus layer and lumen. Thus, a large amount of indole could be released into in the lumen. Indole concentrations ranging from 0.25 to 1 mM has been reported in human fecal samples (132), and even higher concentrations are expected to exist in the GI tract.

Indole production in *E. coli* is strongly influenced by environmental conditions (133). For example, the extracellular indole concentration depends on cell population density, and an indole concentration of 0.5 mM has been reported in the stationary-phase of supernatant of *E. coli* growing in rich medium (134, 135). A recent study has shown that, during transitioning to stationary phase, intracellular indole reaches an extremely high concentration (60 mM) through a transient "pulse" (136). Glucose represses indole production by catabolic repression of tryptophanase (137). In addition, other environmental factors, including pH, temperature, and antibiotic stress, also affect indole production. A low pH inhibits indole production, while high pH induce *tnaA* expression (138). More indole is produced in the presence of the bactericidal antibiotics ampicillin and kanamycin (133).

Other studies indicate that indole is a signaling molecule that can affect bacterial phenotypes. Indole inhibits *E. coli* cell growth by preventing cell division (139). At higher concentrations (>3mM), indole acts as an ionophore and disrupts the membrane potential (139). Indole has also been reported to enhance the stress response of bacteria. For example, indole enhances survival of *E. coli* under acidic conditions by upregulating the expression of acid-resistance genes of the glutamine decarboxylase system (140). Indole also increases the expression of multidrug exporters in *E. coli* and thereby contributes its drug tolerance (134). Indole signaling has also been shown important for plasmid maintenance (141).

In addition to bacterial signaling, indole is also an interspecies and interkingdom signal. One study showed that indole could restore the *E. coli* biofilm formation, which was reduced by biochemical inhibition of tryptophanase (135). In contrast, later studies suggest that indole represses the biofilm formation in both non-pathogenic *E. coli* and EHEC (27, 30, 50). These discrepancies might be explained by different growth conditions and different *E.coli* strains (142). Similarly, indole has been reported to elicit different responses in modulating the virulence of EHEC. One report showed that addition of indole restored, and even enhanced, formation of A/E lesions in a *tnaA* deletion mutant EHEC. Indole addition also moderately increased the promoter activity of LEE4 genes, including espA and espB, both of which are important elements for EHEC attachment and colonization on the host cells (143). Later studies suggested indole inhibits virulence gene expression in EHEC (28) as well as in the *tnaA* deletion mutant (32).

In addition to EHEC, it has been reported that indole attenuates virulence gene expression in *Vibrio cholera* (144), *Pseudomonas aeruginosa* (29) and *Salmonella enterica* (26). Indole also modulates indicators of inflammation and promotes barrier integrity in HCT-8 intestinal epithelial cells (145) and in mice *in vivo* (146). Other metabolites derived from tryptophan, such as indole-

3-acetate and tryptamine, also attenuate inflammation responses in RAW264.7 murine macrophages (147).

Despite numerous studies of the roles of indole in bacterial physiology, less is known about how indole functions as a chemoeffector. Indole was first reported as a chemorepellent to *Salmonella* (148). Later studies also implicated indole as a chemorepellent, with a detection threshold of 1 uM (27, 149). As a serine taxis mutant was not able to respond to indole (27), Tsr was believed to sense indole (150, 151). A later study found that *tsr* mutants showed an attractant responses to indole (152), which was attribute to an "error" in chemotaxis sensing (151). Montrone and coworkers further observed that a gutted *E. coli* strain was repelled by indole even though the strain lacks all chemoreceptors and the *cheA-cheZ* genes (153). In general, indole taxis and the chemoreceptors involved are poorly understood, and the mechanisms underlying indole taxis also needed to be elucidated.

### 2.4.2 SCFAs

Short chain fatty acids (SCFA) are produced by the gut microbiota through fermentation of dietary fiber (154). Concentration of SCFAs can reach up to 70-140 mM in the proximal colon and 20-70 mM in the distal colon. The molar ratio of acetate, butyrate, and propionate have been found to be around 3:1:1 for human subjects, although the ratio vary depending on the intake of dietary fiber (31, 154, 155). The pathways of SCFA production have been well studied, and they confirm that the three major products are acetate, butyrate and propionate (156). Acetate is the most abundant SCFA in the gut. It is produced from acetyl-CoA derived from glycolysis (156). Butyrate and propionate are formed through carbohydrate metabolism associated with glycolysis and also from metabolism of amino acids (157). Acetate producers are widely distributed among

bacterial groups, with butyrate and propionate producers are relatively well conserved (158). Many butyrate producing bacteria belong to the phylum Firmicutes, including *Faecalibacterium prausnitzii*, *Eubacterium hallii*, *Eubacterium rectale*, and *Roseburia* spp. (157, 159). The mucin degrading species like *Akkermansia muciniphila* are propionate producers (160).

As a group of the most studied microbial metabolites, SCFAs have been shown to affect gut integrity, mucosal barrier functions, host immunity, and energy metabolism (161-164). SCFAs are important substrates for maintaining the gut epithelium. Butyrate is the fuel for coloncytes and induces the proliferation of healthy cells (161, 165). It has also been shown to regulate the integrity of epithelium through the tight junction protein Claudin-1 (166). SCFAs also play key roles in regulating the immune system and inflammatory responses. Recent studies have highlighted the role of propionate and butyrate in regulating T cell production and function, and elucidated the function of SCFAs in linking cross-talk between the microbiome and the immune system (167, 168). SCFAs are signals that reduce inflammatory responses. Propionate and butyrate have been shown to inhibit production of LPS-induced cytokines in human dendritic cells (169). Clinical studies have used supplementation with SCFAs as therapeutic strategies in inflammatory disease, and butyrate has been observed to play a direct anti-inflammatory role at sites of inflammation (170).

SCFAs have also been shown to inhibit infection by gut pathogens. The acidic environment provided by SCFAs inhibit the growth of *Salmonella* and pathogenic *E. coli* (171, 172). SCFAs are also active against *Clostridium difficile* (173). SCFAs, especially propionate and butyrate, can also suppress the expression of virulence genes in *S. Typhimurium* and pathogenic *E. coli*, although acetate has the opposite effect (174-176).

SCFAs, and especially acetate, are known to be chemoeffectors for *E. coli*. They elicit a chemotactic response by modulating the cytoplasmic pH (128, 129, 177). An early study by the Adler group showed that acetate repels *E. coli* and is likely sensed by the same Tsr receptor as serine (27). Similar activity as repellents was observed also for propionate and butyrate, with Tsr again being the primary receptor. Later studies showed that acetate elicits an attractant response in Δ*tsr* mutant cells (151, 152).

The mechanism of weak acid chemotaxis was elucidated in 1980 (177). It was shown that the responses to were induced by hydrogen ions released inside cells after their diffusion through the cell membrane when protonated. The more detailed mechanism was elaborated later suggesting that the cytoplasmic linker regions of Tsr and Tar sense the change of cytoplasmic pH, and mediate the repellent and attractant responses, respectively (178).

# CHAPTER III

# BIPHASIC CHEMOTAXIS OF *ESCHERICHIA COLI* TO THE MICROBIOTA METABOLITE INDOLE*

## 3.1 Overview

Bacterial chemotaxis to prominent microbiota metabolites such as indole is important in the formation of microbial communities in the gastrointestinal (GI) tract. However, the basis of chemotaxis to indole is poorly understood. Here, we exposed *Escherichia coli* to a range of indole concentrations and measured the dynamic responses of individual flagellar motors to determine the chemotaxis response. Below 1 mM indole, a repellent-only response was observed. At 1 mM indole and higher, a time-dependent inversion from a repellent to an attractant response was observed. The repellent and attractant responses were mediated by the Tsr and Tar chemoreceptors, respectively. Also, the flagellar motor itself mediated a repellent response independent of the receptors. Chemotaxis assays revealed that receptor-mediated adaptation to indole caused a bipartite response—wild-type cells were attracted to regions of high indole concentration if they had previously adapted to indole but were otherwise repelled. We propose that indole spatially segregates cells based on their state of adaptation to repel invaders while recruiting beneficial resident bacteria to growing microbial communities within the GI tract.

---

* Reprinted in part with permission from "Biphasic chemotaxis of *Escherichia coli* to the microbiota metabolite indole" by Jingyun Yang, Ravi Chawla, Kathy Y. Rhee, Rachit Gupta, Michael D. Manson, Arul Jayaraman, and Pushkar P. Lele, 2020, *Proceedings of the National Academy of Sciences*, 117(11),6114-6120. Copyright by National Academy of Sciences

## 3.2 Introduction

Chemotaxis toward environmental cues regulates the formation of bacterial communities and attachment to host cells (179-182). The environmental cues in response to which motile bacteria migrate include nutrients such as amino acids and sugars, oxygen, pH, and temperature gradients (12, 119, 125, 183-186). Bacteria also respond to neurotransmitters and hormones(130) and to metabolites that regulate bacterial physiology and shape the formation of microbial communities (28, 187, 188).

The binding of chemoeffector molecules to the chemoreceptors of *Escherichia coli* modulates the activity of the receptor-associated kinase, CheA. *E. coli* carry five types of chemoreceptors: Tar, Tsr, Trg, Aer and Tap, out of which Tar and Tsr are dominant. The activated CheA autophosphorylates using ATP and in turn phosphorylates the chemotaxis response regulator, CheY. CheY-P binds to a switch in the flagellar motor to promote clockwise (CW) rotation in an otherwise counterclockwise (CCW) rotating flagellum. Such motor reversals mediate alternating runs and tumbles, which enable the cell to steer its direction of swimming in response to a chemical gradient (65).

To continue migrating up a chemical gradient (positive chemotaxis) or down a chemical gradient (negative chemotaxis), cells must constantly reset the activity of CheA. This resetting, known as adaptation, involves the covalent modification of the receptors by two enzymes – CheR and CheB. When an attractant binds and CheA activity falls, the slow constitutive activity of a methyltransferase, CheR, leads to higher methylation of the receptor. Methylation increases the activity of CheA till it reaches pre-stimulus levels. The cells adapt and are ready to respond to higher concentrations of the attractants. When a repellent binds and CheA activity increases, a methylesterase, CheB, becomes phosphorylated. CheB-P rapidly demethylates the receptor to

decrease the activity of CheA back to its pre-stimulus levels. Once again, the cell adapts and is ready to respond to higher concentrations of the repellent.

Among the important metabolites that control chemotactic behavior (65, 148), indole has received wide attention for its role in regulating a broad range of bacterial phenotypes in the GI tract, including motility, stress responses, biofilm formation, antibiotic resistance and virulence (28, 189-192). Indole is a product of tryptophan and is produced by several species that inhabit the GI tract, especially those belonging to the phyla *Bacteroidetes*, *Firmicutes*, *Proteobacteria* and *Actinobacteria* (193). Indole promotes homeostasis in the microbial community of the GI tract by inhibiting virulence and colonization of host cells by several pathogens, including enterohemorrhagic *E. coli* (EHEC) (194, 195), *Salmonella enterica* (26, 192), and *Vibrio cholera* (196). Indole also promotes phenotypes linked to virulence and colonization in other pathogens such as *Pseudomonas aeruginosa* and *Clostridium difficile* (193, 197, 198) . These varying effects of indole probably depend on its concentrations, which can fluctuate over a wide range (0.2 – 6.5 mM) in the GI-tract (32).

Previous reports suggest that indole induces a chemorepellent response in *Salmonella enterica* and *Escherichia coli* (27, 148) and that the response is mediated by the one of the two major chemoreceptors, Tsr (149, 150, 199). Yet, strains of *E. coli* lacking all major chemotaxis genes other than *cheY* also exhibit a repellent response to indole (153). Other studies suggest that indole induces attractant responses instead (199, 200). Thus, the mechanisms underlying these diverse chemotaxis responses to indole remain poorly understood.

In this work, we explored the mechanisms underlying chemotaxis to indole and observed selective partitioning of *E. coli* on the basis of their memory of exposure to indole. Our results

suggest that indole produced by microbial communities retains resident indole-responsive commensals while preventing invading indole-responsive bacteria from joining the community.

## 3.3 Materials and methods

### 3.3.1 Strains and plasmids

All strains were derivatives of *E. coli* RP437 (201) and are listed in **Table 3. 1**. The two-step λ-red–mediated homologous recombination technique (202) was used to generate scarless, in-frame deletions. The deletions were confirmed via sequencing.

### 3.3.2 Cell culture

Overnight cultures were grown at 33 °C in tryptone broth (TB) followed by 1:100 dilution in 25 mL fresh TB for day cultures. The cultures were allowed to grow at 33 °C to an OD600 of 0.5. Antibiotics (100 μg/mL erythromycin and 25 μg/mL chloramphenicol) were added to the cultures where appropriate. Arabinose was added to the day cultures in the range of 0.001 to 0.1% (wt/vol) and IPTG was added to a concentration of 100 μM, where appropriate.

### 3.3.3 Tethered-cell assay

The day cultures were harvested by pelleting cells by centrifugation (1,500 × g, 5 min). Cells were washed 2× in motility buffer (10 mM potassium phosphate buffer, 67 mM NaCl, 0.1 mM EDTA, 1 μM methionine, 10 mM sodium lactate, pH 7.0). The final pellet was resuspended in 1 mL MB. Cells were then sheared to truncate flagellar filaments to stubs following previous approaches, and subsequently tethered to coverslips in perfusion chambers with the aid of sticky FliC filaments (203, 204). Cell rotation was recorded on a Nikon microscope (Optiphot 2) with a

20× phase objective at 60 fps and a digital camera (UI-3240LE-M-GL; IDS Imaging Development Systems). Videos of the rotation of the tethered cells were analyzed with custom-written codes in MATLAB (205). The rotation speeds were determined from Gaussian fits to the speed distributions. The $CW_{bias}$ (fraction of the time that the motor rotates CW) was determined as a function of time by employing a moving filter that averaged over 1.5 cell rotations, as done previously (206).

A three-directional valve (Hamilton, Inc) was employed to exchange the fluid in the perfusion chambers with MB or MB containing indole. The flow rate (260 μL/min) was controlled by a syringe pump (Fusion 200; Chemyx). Separate calibration experiments were performed with a colored fluid to estimate the average time of entry of chemoeffectors into the perfusion chamber after the initiation of flow.

### 3.3.4 pH measurements

A plasmid encoding a pH-sensitive green fluorescent protein (GFP-mut3*) was introduced into the wild-type RP437 strain. The expression level of GFP was controlled with IPTG (100 μM). An LED illumination source (SOLA SE II 365 light engine; Lumencor) and a standard Nikon GFP cube were employed to excite the fluorophores and to filter the emission. One hundred to 200 cells were excited in the field of view with a 60× water-immersion objective (Nikon Instruments). The emission was collected by a sensitive photomultiplier (H7421-40 SEL; Hamamatsu) after passing through a band-pass emission filter (FF01-542/27; AVR Optics). Custom-written LabVIEW codes were employed to record the photon count over time. For calibration purposes, the emission from the cells was measured for 100 s in MB. Then, the medium was exchanged for one containing 40 mM benzoate/MB at pH 6.

During measurements of the effect of indole on internal pH, the emission from the cells was measured for the first 100 s in MB. Then, MB was replaced with MB containing 2 mM indole while continuing the intensity measurements. The cells were allowed to equilibrate for 3 min before switching back to MB.

### 3.3.5 In vitro chemotaxis and attachment assay

A thin agar layer was poured into individual transwell inserts (Nunc cell-culture inserts) and then soaked overnight in motility buffer or in motility buffer containing 2 mM indole. The agar surface was coated with poly-L-lysine to facilitate stable attachment of the cells. The inserts were then carefully transferred to individual wells in a 24-well plate (Carrier Plate Systems; Thermo Fisher Scientific; 141002) carrying a suspension of GFP-expressing *E. coli* (**Figure 3. 1**.). Cells that respond to time-varying chemical gradients established in these reservoirs either migrate toward and attach to the agar pads or are repelled (207, 208). In the primed case, the cell suspension contained 700 μM indole. In the unprimed case, the cell suspension contained no indole. After 5 min, the inserts were carefully removed, gently washed with MB to remove unstuck cells, and then imaged via confocal microscopy. Custom-written MATLAB codes were then employed to count the number of cells adhered to the surface.

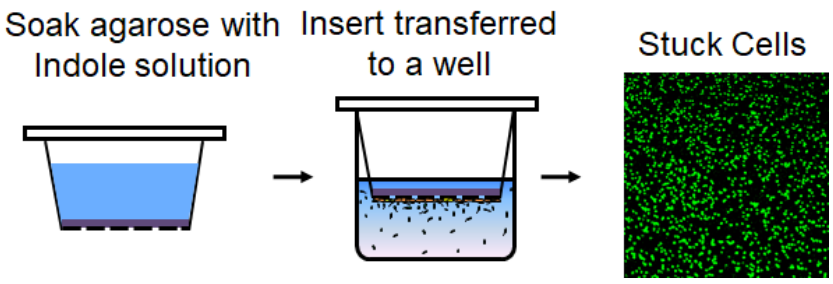

**Figure 3. 1 Transwell insert assay.** Agar was soaked in indole solutions overnight in the insert (left), and the insert was then transferred into a well containing cells (middle). A concentration gradient formed within a few minutes, and the cells actively migrated in response to the indole diffusing out of the agar plug. The insert was carefully removed after 5 min, gently washed in MB, and imaged via confocal microscopy (209).

### 3.3.6 Statistical analysis

All statistical analyses were performed with the Student's t test. Results with $P < 0.05$ were considered statistically significant.

## 3.4 Results

### 3.4.1 Chemotaxis response to a low concentration of indole

We measured the chemotactic response of individual cells by tracking the motor $CW_{bias}$, namely the fraction of the time that it rotates CW, using tethered-cell assays. Perfusion chambers were employed to stimulate tethered cells with indole. An increase in $CW_{bias}$ upon stimulation is indicative of a chemorepellent response, whereas a decrease in $CW_{bias}$ is indicative of a chemoattractant response (210). A strong and reproducible CW repellent response was observed immediately after stimulating wild-type cells with 20 μM indole. The response precisely adapted to the original value within 30 to 50 s (**Figure 3. 2 A**). When indole was replaced with motility buffer, it had the opposite effect; the $CW_{bias}$ decreased initially and subsequently adapted to its pre-stimulus value (**Figure 3. 3**.).

Addition of 20 μM indole to isogenic mutant cells lacking the Tar receptor, which we refer to as Tsr-only because Tsr is their only high-abundance receptor, induced a similar but shorter CW repellent response of only ∼25 s (**Figure 3. 2 A**). Addition of 20 μM indole to isogenic mutant cells lacking the Tsr receptor, which we refer to as Tar-only, did not evoke either a detectable

repellent or attractant response. This result demonstrates that Tsr mediates a repellent response to 20 μM indole and adapts rapidly, presumably through demethylation of Tsr by CheB-P.

### 3.4.2 Chemotaxis responses to higher concentrations of indole

At higher concentrations of indole (200 to 700 μM), wild-type cells continued to exhibit a repellent response that adapted precisely. However, when the cells were treated with 1 mM indole, the repellent response inverted to an attractant response after about 50 s (**Figure 3. 2 B**). A similar time-dependent inversion was observed at 2 mM indole (**Figure 3. 3 A**).

The Tsr-only strain exhibited CW repellent-only responses that adapted precisely to the prestimulus levels with 200 μM to 1 mM indole (**Figure 3. 2 C**). Again, adaptation presumably occurs via CheB-P–mediated demethylation. The increase in the CWbias was relatively insensitive to indole concentrations. The absence of an inverted response after addition of indole, even at 2 mM (**Figure 3. 3 B**), suggested that Tar mediates the delayed attractant response that was observed with the wild type. The Tar-only strain exhibited a strong CCW attractant response to 200 μM to 1 mM indole (**Figure 3. 2 D**), and also to 2 mM indole (**Figure 3. 3 C**). The absence of the repellent response was consistent with the notion that Tsr mediates the initial repellent response that was observed in the wild type. Adaptation in the Tar-only mutant was slower and presumably occurs via CheR-mediated methylation. The adaptation occurred with increasing delays as the concentration of indole increased, likely because the deviation of CheA activity from its basal value increased with indole levels. This suggests that the attractant response does not saturate even at 1 mM indole.

Overall, the biphasic response of wild-type cells to higher concentrations of indole seems to occur due to the combination of a strong but rapidly adapting repellent response mediated by

Tsr and a prolonged, slowly adapting attractant response mediated by Tar. The repellent response masks the attractant response until the cells have adapted via demethylation of Tsr.

### 3.4.3 Responses to the removal of indole

The replacement of indole with motility buffer (MB) had different effects on the wild-type, Tar-only, and Tsr-only cells. The wild type exhibited attractant-like CCW responses when indole at 20 or 200 μM was replaced with MB (**Figure 3. 3 A**). Removal of 700 μM or higher indole induced rapid repellent responses followed by extended attractant responses that did not adapt over 100 s.

The Tsr-only mutant generally exhibited extended attractant responses upon the removal of indole, with adaptation slow because it requires methylation of Tsr. The removal of 2 mM indole induced a biphasic response, with a brief repellent response followed by a strong attractant response that did not adapt over 100 s. We do not know the cause of this brief repellent response. However, it is unlikely to arise due to demethylation-mediated inversion in Tsr's repellent response to indole since no attractant response was ever observed in the Tsr-only strain when indole was added.

The Tar-only mutant exhibited repellent responses that adapted to baseline within 50 to 75 s, presumably via CheB-P–mediated demethylation, when ≥200 μM indole was removed. The Tar-only cells did not give a detectable response to the removal of 20 μM indole, just as they gave no detectable response to addition of 20 μM indole. All of these data are consistent with the notion that indole is sensed by Tsr as a repellent and by Tar as an attractant.

### 3.4.4 Indole responses are not mediated by changes in cytoplasmic pH

Previous work showed that Tar mediates an attractant response when the intracellular pH is decreased, whereas Tsr mediates a repellent response (210). As indole at high concentrations reportedly permeates the membrane and decreases the cytoplasmic pH (139, 211), we tested whether the biphasic response to indole occurs through the known pH-mediated signaling mechanism. To do this, we expressed a pH-sensitive fluorescent protein in the wild-type strain (Materials and Methods). Cells attached to a glass surface in a perfusion chamber were treated with a mix of 40 mM benzoate and buffer (at pH 6.0), following previous approaches (212, 213), and illuminated at an appropriate excitation wavelength. Benzoate in its protonated form permeates the membrane and equalizes the cytoplasmic and extracellular pH. A strong change in emission intensities was observed when pH 7.0 MB was exchanged with a buffer containing 40 mM benzoate at pH 6.0 (**Figure 3. 4, Left panel**). Yet, repeated cycles of exposure to 2 mM indole failed to elicit a measurable change in emission intensity (**Figure 3. 4, Right panel**). This result suggests that, even upon exposure to the highest indole concentration employed in this work, no change occurred in the cytoplasmic pH, at least within the detection limits of our experimental setup.

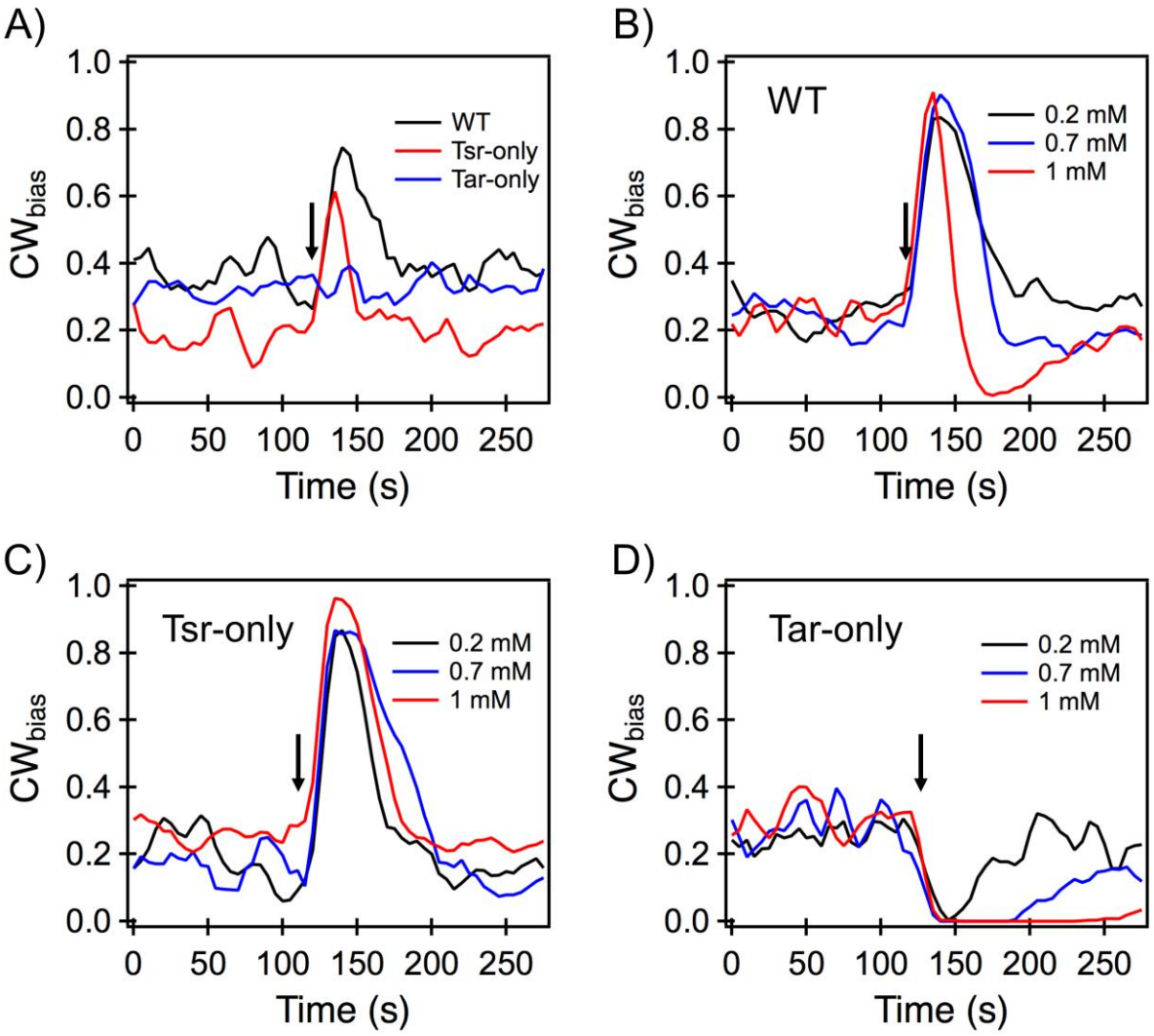


**Figure 3. 2 Cell response to indole in the tethered cell assay.** A) Averaged response of tethered cells to 20 μM indole. The arrow indicates the approximate time of exposure to indole. The wild type (black curve) and the *tar* knockout (red curve) both exhibited a brief increase in $CW_{bias}$, indicating a repellent response. The response precisely adapted such that the pre- and post-stimulus $CW_{bias}$ was similar. The *tsr* knockout showed no response to the stimulation. B) The short-time CW repellent response of wild-type cells was evident over the entire range of concentrations tested, as indicated by the increase in $CW_{bias}$ ~20-50 s following stimulation. At longer times (> 50 s), an attractant response was evident when cells were treated with 1 mM indole. A similar inversion was observed upon treatment with 2 mM indole (see **Figure 3. 3**). C) A strong repellent response was observed in case of the Tsr-only mutant over the entire range of indole concentrations tested. The adaptation was precise in each case. D) Attractant responses were observed in the Tar-only mutant over the 0.2 – 1 mM concentration range. The delay in adaptation to the response increased with indole concentrations. All response curves in A, B, C, and D represent an average over n = 11-21 cells. The average error was 0.01.

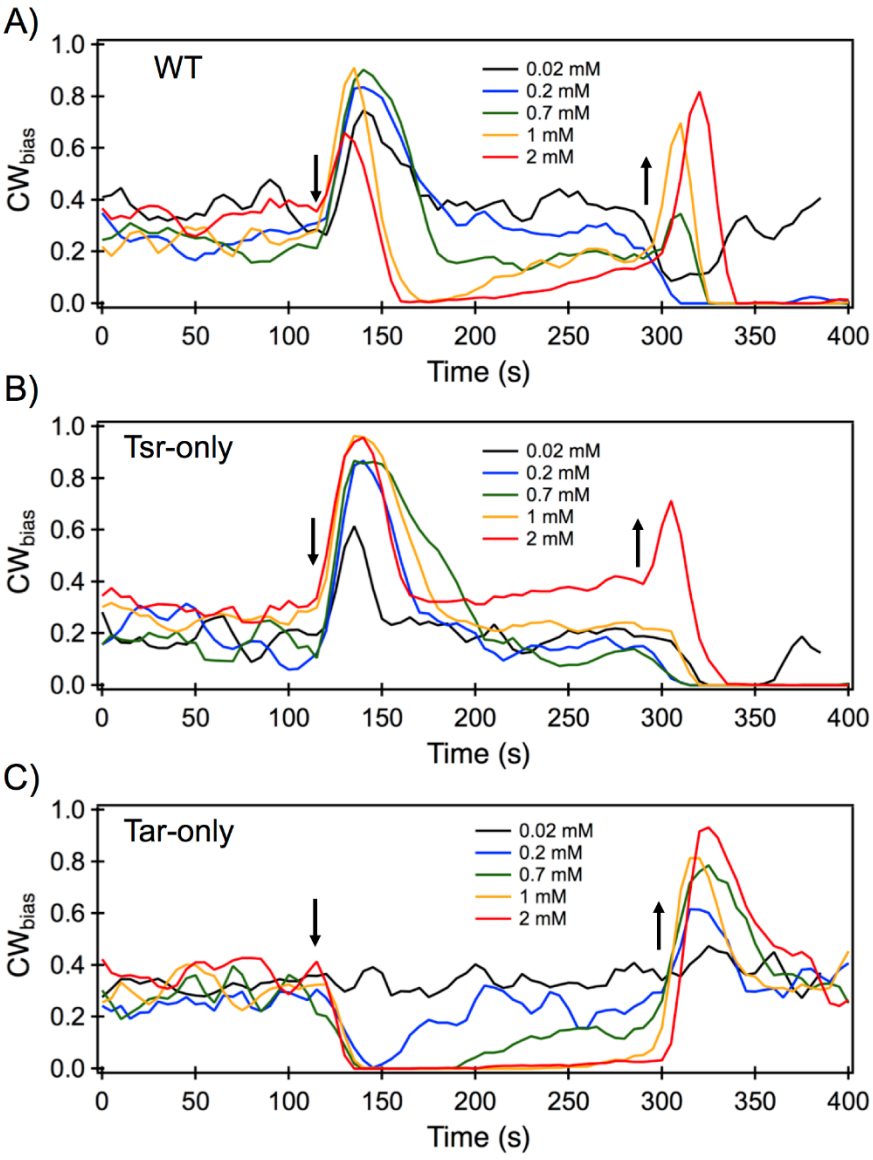


**Figure 3. 3 Responses of tethered cells to the addition and removal of indole.** Indole was replaced with MB in the perfusion chamber at ~ 300 seconds.

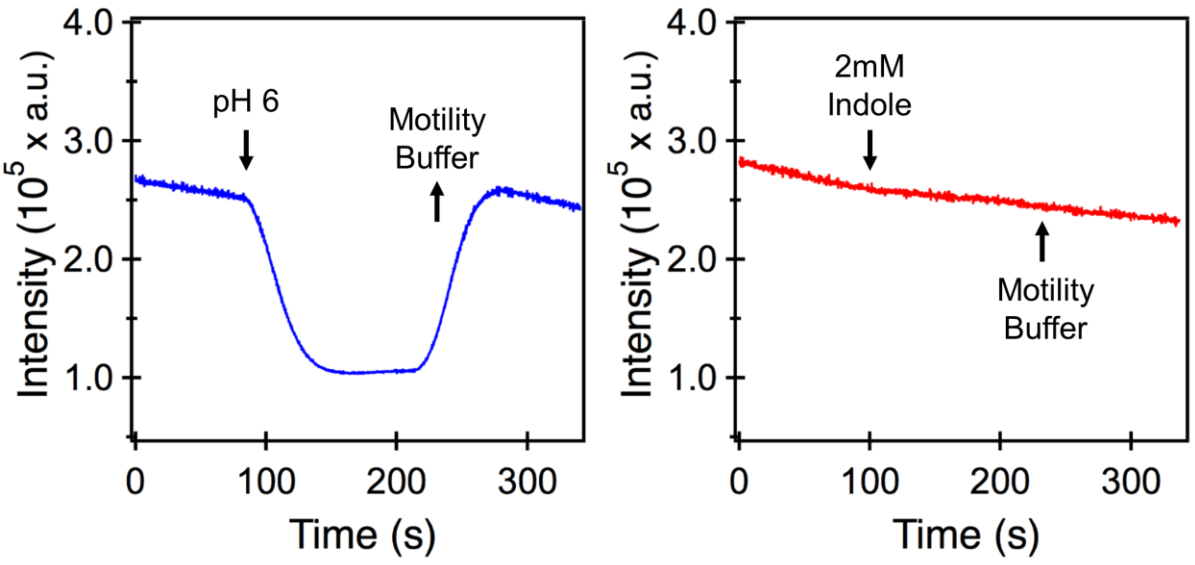


**Figure 3. 4 The change of cytoplasmic pH upon stimulation.** Left panel: Emission intensities of a pH-sensitive fluorophore that was expressed in the wild-type strain are indicated. The cells were initially exposed to a neutral buffer solution (MB, pH 7.0). At ~90 s, the buffer was exchanged with an acidic medium (MB, pH 6.0 plus 40 mM benzoate). The acidification of the intracellular environment reduced the emission intensities. The intensities were restored to the pre-stimulus values when the medium was replaced with MB (pH 7.0) at ~210 s. Right panel: Cells were stimulated with 2 mM indole at ~90 s. No measurable change in the emission intensities was observed. Removal of indole also did not cause a significant change in intensities. Signals were obtained from ~ 100-200 cells.

### 3.4.5 Response to step increments in indole concentrations

Because the repellent response adapted much more quickly than the attractant response (**Figure 3. 2**), we hypothesized that wild-type cells previously adapted to indole would exhibit an attractant-only response upon further stimulation. To test this hypothesis, we repeatedly stimulated the same population of wild-type tethered cells with increasing concentrations of indole (**Figure 3. 5 A**). Each time the cells were stimulated with indole at ≤700 μM, an immediate repellent response that adapted precisely was observed. Once adapted to 700 μM indole, however, the cells exhibited attractant-only responses when exposed to higher concentrations of indole. The brief

Tsr-mediated repellent response that was observed in nonadapted cells (**Figure 3. 2 A**) was absent in these adapted cells.

### 3.4.6 Effect of adaptation to a threshold concentration of indole on chemotaxis to indole-containing surfaces

Because high indole levels (1 mM and above) induced an attractant response in cells that had previously adapted to the threshold level (~700 μM), we hypothesized that such adapted (primed) cells should respond to indole as an attractant and migrate toward indole-rich substrates. To test this idea, we employed an inverted transwell assay previously developed in our laboratory (207, 208), depicted in **Figure 3. 1**. Agar pads presoaked in 2 mM indole were brought into contact with wild-type cells swimming in a 2-mL reservoir of MB. Agar contact with the reservoir fluid rapidly established an indole gradient in the reservoir. The cells in the reservoir that responded to the gradient either migrated away (negative chemotaxis) or toward (positive chemotaxis) the indole-rich agar pads. The number of cells attached to the poly-L-lysine–coated agar pads was quantitatively determined following 5 min of exposure (Materials and Methods). In the primed case, the 2-mL MB reservoir contained ~700 μM indole, and the cells were allowed to adapt to it for 30 min prior to being placed in contact with agar. In the unprimed case, the 2-mL MB reservoir contained no indole during the 30-min incubation. The basal attachment expected due to chance encounters of motile cells with the agar surface over 5 min was determined in separate measurements in which no indole was added to the agar or the reservoir. To rule out the possibility that the primed cells attached in greater numbers because of non– chemotaxis-related effects of indole, an additional gradient-less control was included in which primed cells were exposed to agar that contained the same concentration of indole (700 μM).

As shown in **Figure 3. 5 B**, primed wild-type cells that were exposed to agar pads containing 2 mM indole (positive gradient) attached in higher numbers relative to the basal value (in the absence of indole), indicating an attractant response. Primed wild-type cells exposed to a positive gradient of indole also attached in higher numbers relative to primed wild-type cells that were exposed to uniform indole concentrations (gradient-less control; **Figure 3. 5 C**). This result confirmed that the increased attachment of the primed cells was due to positive chemotaxis (chemoattraction) toward the indole source. In contrast, the unprimed wild-type cells attached in lower numbers than the basal value, indicating a repellent response to indole. The raw data are shown in **Figure 3. 6**.

The chemotaxis assays were repeated with mutants lacking Tsr, Tar, or both Tsr and Tar. With the Tsr-only mutant, unprimed as well as primed cells exhibited negative chemotaxis (repellent response), consistent with the results with tethered cells (**Figure 3. 5 B**). As shown in **Figure 3. 5 C**, the primed Tsr-only cells exhibited negative chemotaxis relative to the gradient-less control. In the Tar-only mutant, unprimed cells exhibited an attractant response (**Figure 3. 5 B**), as in the tethered-cell assay. The primed cells appeared to exhibit a weak repellent response, but the result was not significant relative to the corresponding gradient-less control (**Figure 3. 5 C**). A repellent response was clearly seen in the *Δtar Δtsr* double mutant, whether the cells were primed or unprimed (**Figure 3. 5 B**). The response was significant even when compared with the gradient-less control (**Figure 3. 5 C**). These repellent responses occurred despite the absence of either high-abundance receptor. As will become apparent later, we believe that a part of the repellent response arises from a receptor-independent mechanism rather than a response mediated by the low-abundance receptors Trg, Tap, and Aer.

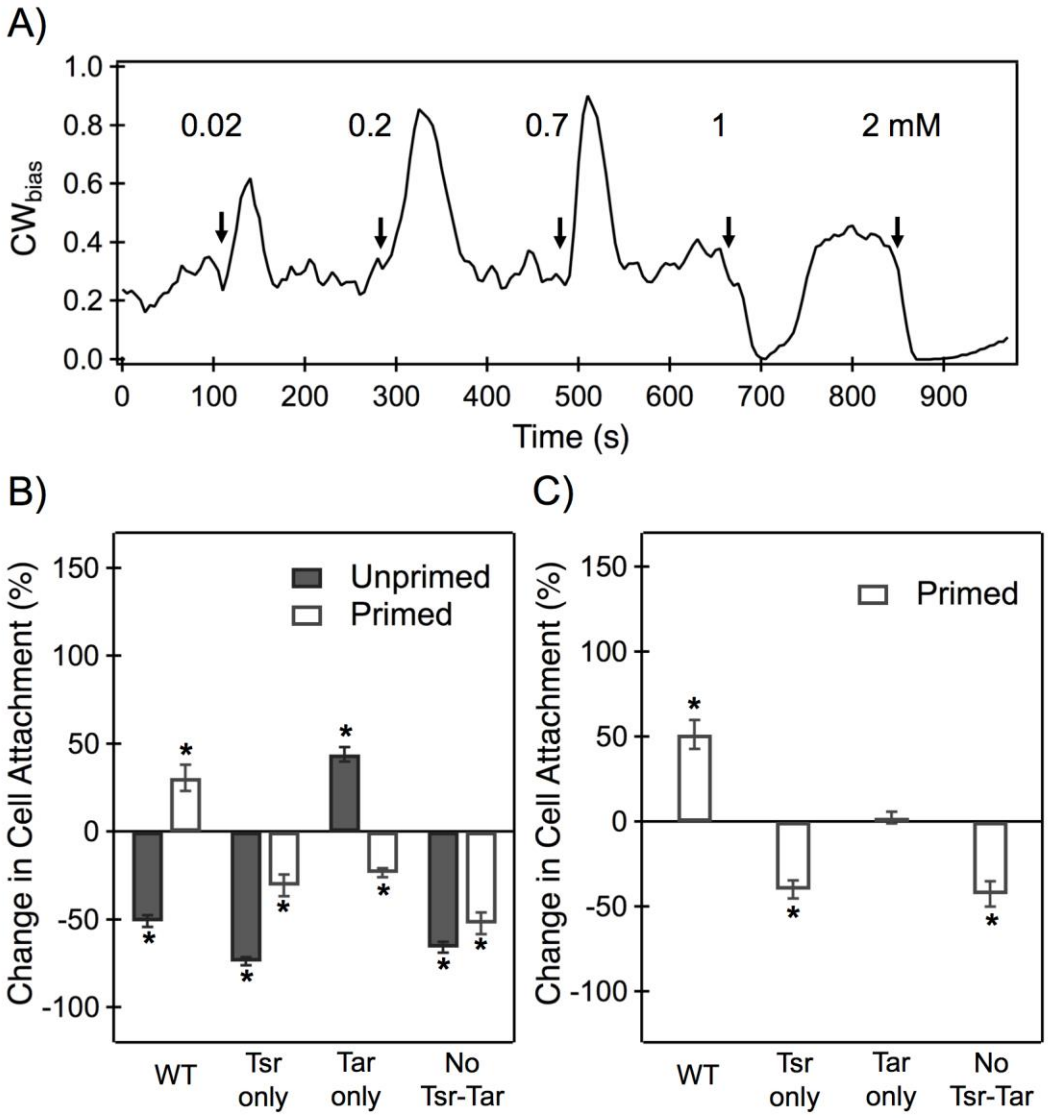


**Figure 3. 5 Wild-type cells were stimulated with step increments in the concentration of indole at the times indicated by the arrows.** Upon adaptation to 0.7 mM indole, attractant-only responses were observed at higher stimulation levels. The average error was 0.07 (n = 11 motors). B and C) The nature and magnitude of the chemotaxis response in the transwell-based chemotaxis assay is indicated for several strains. The ordinate in B) reflects the percentage difference in cell attachment to the agar source containing 2 mM indole relative to the basal attachment. The basal attachment is determined from the number of *unprimed* cells adhered to agar pads that contain no indole (agar pads and reservoir contain MB-only). The basal value depends on chance encounters and attachment of the cells with the polylysine-coated agar surface in the absence of chemical signals, and it has been normalized to 0 for each strain. Positive (negative) attachment values indicate positive (negative) chemotaxis. A +100% value indicates that recruitment to the agar surface is twice that seen through random chance. The ordinate in C) reflects the percentage difference in the attachment of *primed* cells to the agar source containing 2 mM indole relative to

the attachment of *primed* cells in the gradient-less control. The gradient-less control includes agar pads soaked in the same concentration of indole as the cell reservoir (700 μM). Two biological and three technical replicates were carried out for each condition. The mean attachment values were calculated over 4,000-10,000 cells.

### 3.4.7 Is there a receptor-independent response to indole?

To determine the reason for the repellent response in the *Δtsr Δtar* strain, we stimulated tethered cells of the double mutant with indole. These cells exhibited a strong repellent response that showed little adaptation over 200 s (**Figure 3. 7 A**). The small and slow adaptation suggested that kinase (CheA) activity itself was not perturbed significantly and that the majority of the observed repellent response might be receptor-independent.

The flagellar switch consists of the FliM and FliN complexes, to which CheY-P binds, and the FliG ring, which forms the track on which the stators act to rotate the motor (214). We hypothesized that indole permeates the membrane and interacts with the flagellar switch, either directly or indirectly, to promote CW rotation. To test the hypothesis, we generated a *ΔcheY* strain in which the motors are still capable of switching. Although motors usually rotate only CCW in a *ΔcheY* strain, they are able to switch in the presence of a few mutant $FliG^{CW}$ subunits in an otherwise wild-type FliG ring (215). These mutant subunits are locked in the CW conformation (216), and they destabilize the FliG ring to allow switching to occur through cooperative interactions when they are present in the right proportion relative to wild-type FliG subunits (215). Mixed FliG motors were generated by expressing the mutant subunits from an IPTG (isopropyl β-D-thiogalactoside) inducible vector (induced with 5 μM IPTG), while the native FliG subunits were expressed from the genomic locus. The *ΔcheY* cells with mixed FliG motors rotated predominantly CCW, but when stimulated with 2 mM indole they exhibited a strong repellent response that did not adapt over 250 s (**Figure 3. 7 B**). Tethered cells belonging to a *ΔcheY* strain

that carried wild-type FliG subunits continued to rotate CCW only following the addition of 2 mM indole. Because the absence of CheY cuts all communication between the receptor patch and the flagellar motor, this observation is consistent with the hypothesis that part of the repellent response to high concentrations of indole is receptor-independent.

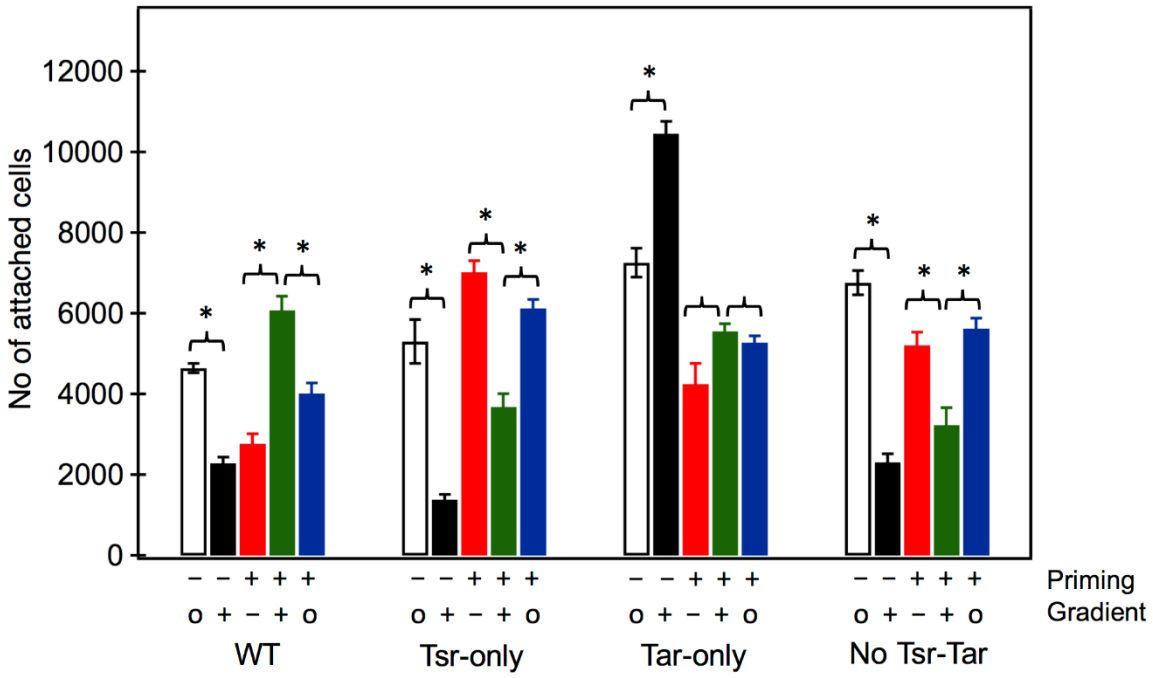


**Figure 3. 6 Transwell agar assays.** *Primed* cells are indicated by '+' and *unprimed* cells are indicated by '-'; Positive gradient (+) indicates that the agar plug contains indole but the reservoir does not. Negative gradient (-) indicates that the agar plug contains no indole and the reservoir contains indole. In case of the *unprimed* cells, zero gradient (o) indicates a uniform concentration of MB in the agar and the reservoir – termed as the basal level. In case of the *primed* cells, the zero gradient (o) indicates a uniform concentration of indole in the agar and the reservoir – termed as the *gradient-less* control. Asterisk indicates statistically significant result (p-value < 0.05). Wild-type cells exhibited a repellent response to 2 mM indole-agar as seen by the reduced attachment in the *unprimed* state (-/+) relative to the basal level (-/o). In the *primed* state (+/+), an attractant response was observed towards the 2 mM indole-agar relative to the basal level. The attractant response was not merely due to the presence of indole, since the cell attachment was lower in case of the *primed* cells exposed to MB-containing agar (+/-) as well as the gradient-less control (+/o). A clear repellent response to indole was observed in the *primed* and *unprimed* Tsr-only strain. In case of the Tar-only strain, the *unprimed* cells showed positive chemotaxis to 2 mM indole-agar

relative to the basal level (-/o). The *primed* cells were insensitive to 2 mM indole-agar (+/+) when compared with the gradient-less control (+/o) and showed a slight attractant effect when compared to the case of MB-containing agar (+/-). *Primed* as well as *unprimed* cells belonging to the *tar-tsr* strain exhibited strong repellent behavior to indole.

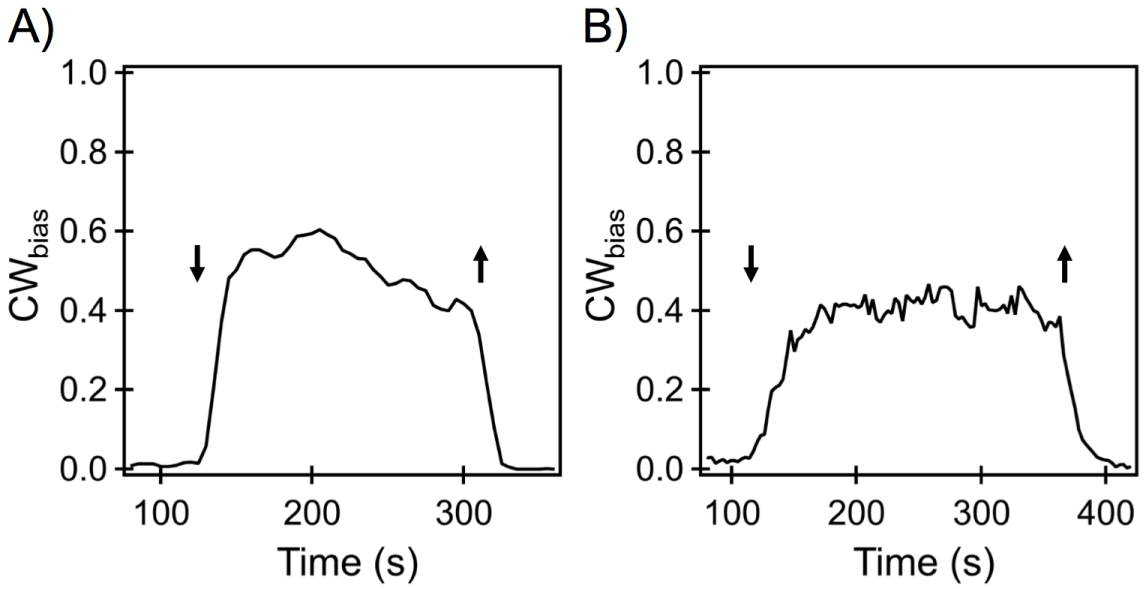


**Figure 3. 7 Averaged response of a Δ*tar* Δ*tsr* double mutant to 1 mM indole.** The entry and exit of indole from the flow cell is indicated by the downward and upward arrows, respectively. A repellent-only response was observed with minimal adaptation. Response curves were averaged over n = 22 cells, and the mean error was 0.01. **B)** The averaged $CW_{bias}$ of the CheY-less $FliG^{CW}$-$FliG^{WT}$ motors that switch is indicated. Stimulation with 2 mM indole at ~110 s increased the $CW_{bias}$, and removal of indole restored the bias to pre-stimulus levels. The curve was averaged over n = 9 cells, and the average error in bias measurements was 0.05.

### 3.5 Discussion

Our experiments quantified the Tsr-mediated repellent response to indole. This is most easily observed in the Tsr-only strain (**Figure 3. 2 A and C**). Cells responded strongly to the addition of 20 μM indole (**Figure 3. 2 A**), and the strength of the response did not increase significantly at concentrations above 200 μM (**Figure 3. 2 C and Figure 3. 3 B**). The adaptation

times, presumably controlled by CheB-P–mediated Tsr demethylation, were relatively short and similar over the range of indole concentrations tested (~30 to 50 s).

We also demonstrated that Tar mediates an attractant response to indole, but only at high concentrations. This is best seen in the Tar-only strain that exhibited strong attractant responses to indole at ≥200 μM or higher (**Figure 3. 2 D**). The time required for adaptation, presumably influenced by the slow Tar methylation by CheR, increased with indole concentration. The $CW_{bias}$ is very sensitive to CheY-P levels (78, 206, 217), and it drops to 0 even for small reductions in CheY-P levels. It takes longer for CheY-P levels, and consequently the CWbias, to recover to the basal value when the reduction in CheY-P is more significant. Therefore, the increasing delays in adaptation in **Figure 3. 2 D** suggest that higher indole levels cause greater reductions in CheY-P levels in the Tar-only strain. Based on this, we conclude that the attractant response to indole requires concentrations of at least 1 mM, and probably higher, to saturate. We also conclude that Tsr has a higher affinity for indole than Tar.

The response of wild-type cells to indole is a combination of the repellent response mediated by Tsr and the attractant response mediated by Tar. At 20 and 200 μM, the wild-type cells sense indole as a repellent through Tsr, and the response adapts quickly (**Figure 3. 2 A**). At indole concentrations of ≥1 mM (**Figure 3. 2 B**), the Tsr-mediated repellent response initially masks the Tar-mediated attractant response until the rapid receptor demethylation by CheB-P deactivates CheA adequately for the attractant response to be revealed. The attractant response then adapts slowly due to CheR-mediated methylation of the receptors. Thus, the binding affinities of Tsr and Tar for indole and the asymmetric kinetics of methylation and demethylation play a key role in the biphasic wild-type response.

Tsr-mediated repellent and Tar-mediated attractant responses are known to occur when the cytoplasmic pH decreases. However, experiments with a pH-sensitive fluorescent protein revealed that even at the highest concentration tested (2 mM), indole did not produce a measurable change in cytoplasmic pH (**Figure 3. 4**). Thus, sensing of changes in cytoplasmic pH in our study is not involved in the receptor responses to indole. The following two questions remain: How does indole interact with the two receptors, and do the indole-binding sites localize to the same region of the proteins in Tsr and Tar? A previous study reported that *E. coli* cells devoid of periplasm continued to exhibit repellent responses to indole, which suggests that the soluble periplasmic protein is not involved, at least in repellent sensing by Tsr (218). However, the interpretation is not straightforward, due to the observed motor-mediated effects (**Figure 3. 7 B**). Another confounding factor is that the strength of the allosteric coupling interactions within the signaling complex arrays in the wild type are unlikely to be preserved in the Tsr-only or Tar-only strains, where one or the other major receptor is lacking (219). Thus, the wild-type response may not be a simple summation of the Tsr-only and Tar-only responses. The mechanisms of indole sensing are the subjects of ongoing investigations.

An important consequence of the rapid adaptation of the repellent response at intermediate indole concentrations and the slow dynamics of the attractant response is that cells preadapted to a threshold concentration of indole exhibit an attractant-only response at higher concentrations. Tethered wild-type cells previously adapted to ~700 μM indole sense it as an attractant at 1 mM and higher concentrations; the brief repellent responses seen at these concentrations in nonadapted cells (**Figure 3. 2 B**) are not seen in adapted cells (**Figure 3. 5 A**). Cells previously adapted to 200 μM or lower concentrations of indole continue to sense it as a repellent. These data suggest that a

threshold indole concentration of ~700 μM bifurcates the cell response depending on its recent exposure to the molecule.

The above argument also suggests that wild-type swimming cells adapted to the threshold indole level (~700 μM) will be attracted to sources of higher indole concentrations, whereas those not adapted to ~700 μM indole will be repelled from those sources. This was confirmed by our in vitro attachment assay (**Figure 3. 5 B and C**). Wild-type cells not previously exposed to the threshold level (unprimed cells) actively avoided agar plugs soaked in 2 mM indole. However, cells adapted to the threshold level (primed cells) were attracted to those agar plugs. This attraction depended on the presence of the Tar receptor, as primed and unprimed Tsr-only cells actively avoided the plugs. The unprimed Tsr-only cells avoided the plugs more than the primed Tsr-only cells, presumably because they had a larger proportion of indole-free, nonadapted Tsr receptors. The unprimed Tar-only cells were attracted to the indole-soaked agar plugs, but the primed Tar-only cells were not. In the case of the strains lacking both Tar and Tsr, the primed as well as the unprimed cells avoided the indole-soaked agar plugs, and tethered cells of this strain exhibited strong, nonadapting repellent responses to indole (**Figure 3. 7 A**).

To determine if the repellent response seen in the *Δtar Δtsr* double mutants was independent of input from chemoreceptors, we measured the responses of tethered cells belonging to a strain that lacked the chemotaxis response regulator CheY and carried a mix of wild-type and CW-locked FliG subunits in its C ring (216, 220). Motors in strains lacking CheY rotate CCW only because the large free energy difference between the CW and CCW conformations of the flagellar switch makes it unlikely that the motor will rotate CW, even for a short time (221). Motors containing both types of FliG subunits exist in a metastable state that can switch, as the CW-locked FliG subunits lower the energy difference between the two rotational states (215). We

hypothesized that indole acts on the motor, directly or indirectly, to further reduce the difference in free energy between the two conformations of the switch, thereby increasing the $CW_{bias}$ in a receptor-independent manner. Indeed, upon addition of 2 mM indole to such cells, a strong and nonadapting repellent response was observed (**Figure 3. 7 B**). It is unclear whether indole interacts directly with the switch complex or through another molecule. However, this finding suggests that indole may act as a chemorepellent even to flagellated bacteria that lack a specific chemoreceptor for sensing it.

The *E. coli* Tsr and Tar receptors mediate opposite responses to several types of signals, including temperature, pH, leucine, and certain neurotransmitters (125, 127, 130, 215, 222-224). In the cases of temperature and pH, the result is to bring cells to optimal environments of neutral pH and physiological temperatures. It is intriguing that the different responses to indole may have exactly the opposite effect, partitioning cells into "extreme" environments. Cells that have adapted to the threshold level (~700 μM) will be attracted to still higher concentrations of the metabolite. In unadapted cells, such as those encountering an indole gradient for the first time, the repellent response will cause cells to swim away from indole-rich regions.

A direct consequence of the above mechanism is that bacteria that produce indole have a higher likelihood of adapting to it, and therefore will be attracted to indole-rich microbial communities. These niches are likely to be those inhabited by other indole-producing bacteria as well. As bacterial species that lack the tryptophanase-encoding *tnaA* gene do not produce indole, their receptors are unlikely to have adapted to the molecule, and therefore will likely be repelled by indole-rich regions. Bacteria lacking a specific chemoreceptor for indole may also be repelled through a receptor-independent repellent response.

The interplay of repellent and attractant responses to indole may help guide the development of microbial niches in regions such as the GI tract. Indole-producing commensal microbes thrive in proximity to the mucosal interface in the GI tract; the concentrations of indole at these sites of production are expected to be much higher than the threshold level, considering that the diluted bulk concentrations in fecal samples can be as high as 6.5 mM (32). Commensal bacteria adapted to the threshold indole level will likely be retained in existing microbial communities because of attractant chemotaxis—although the precise number of motile species in the gut is unknown, several members of the phyla *Firmicutes* and *Proteobacteria* produce flagella (45). Away from the mucosal interface and toward the lumen of the GI tract, where indole levels are lower than the threshold (32), motile bacteria will be repelled by negative chemotaxis (**Figure 3. 8**). Thus, foreign ingested bacteria, including invading pathogens such as *E. coli* O157:H7 and *S. enterica*, are likely to be prevented by indole from gaining a foothold in the mucosa.

It is likely that the GI-tract microbial communities complement the natural defense mechanisms of the host. They might do so by tuning the production of indole and exploiting the biphasic chemotaxis response to retain resident commensal bacteria and to prevent colonization by invading motile pathogens. If the receptor-independent repellent response is a general property of flagellar motors across bacterial species, motile bacteria lacking indole-specific chemoreceptors may also be discouraged from colonizing the intestinal mucosa. However, there exists a spatially varying mix of different microbial and host metabolite signals within the GI tract, some of which are potent chemoattractants (28, 225). The integrated chemotaxis response to a combination of different GI-tract signals may ultimately determine the efficacy of this defense strategy. Combinatorial studies on integrated signaling and chemotaxis response to a combination of metabolites and metabolic derivatives are needed to provide further insights.

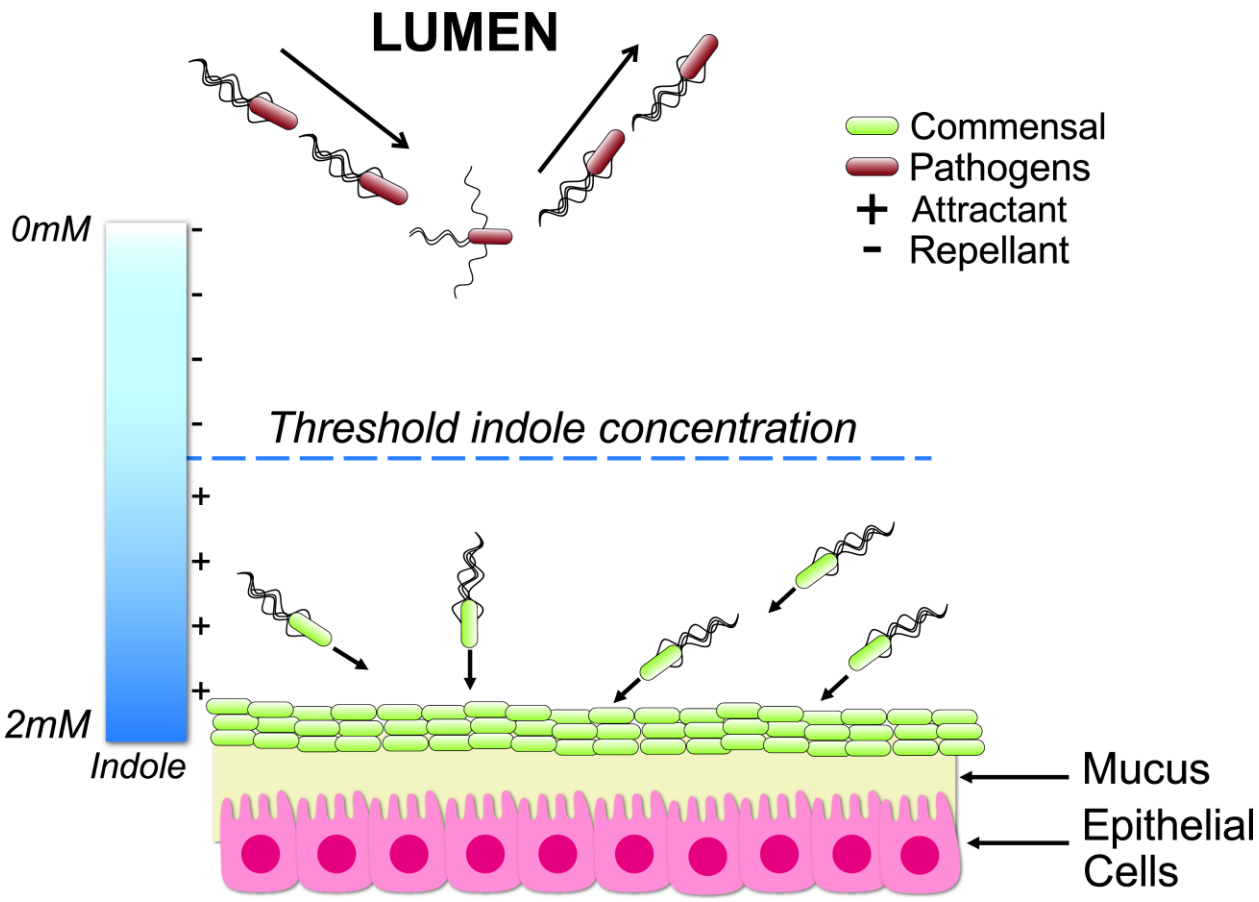


**Figure 3. 8 Distributional sorting by indole in the GI-tract.** The indole levels near the mucosal layers are shown as being above the threshold concentration. *Primed* cells will be attracted to the source, leading to retention of commensal bacteria in existing microbial communities. Away from the source, indole concentrations are shown as being lower than the threshold. Low indole concentrations prevent cells from becoming *primed*, inducing a repellent response. *Unprimed* cells will be induced to migrate towards the lumen.

**Table 3. 1 Bacterial strains and plasmids used in this study**

| Strains | Relevant genotype | Source |
|---|---|---|
| PL15 | HCB33 (RP437), sticky *fliC* allele | (205) |
| PL 221 | PL15 *Δtsr* (Δnt 16-1644 ) *Δtar* (Δnt 16-1638) | This work |
| PL 225 | PL15*Δtsr* (Δnt 16-1644) | This work |
| PL278 | PL15 *Δtar* (Δnt 16-1638) | This work |
| PL14 | PL4 (*ΔcheY*, *sticky fliC*) with *pTrc99A- fliG*$^{CW}$ | (215) |
| CV1 | *thr-1*(Am) *leuB6 his-4 metF159*(Am) *rpsL136* [*thi-1 ara-14 lacY1 mtl-1 xyl-5 eda tonA31 tsx-78*] with pCM18 | (223) |
| CV4 | CV1 Δ*tar* | (122) |
| CV5 | CV1 Δ*tsr thr*$^{+}$ | (122) |
| CV11 | Δ*tsr-tar* | M.D.M. laboratory |
| Plasmids | | |
| pPL1 | *pTrc99A- fliG*$^{CW}$ | (152) |
| pCM18 | pTRKL2-PCP25RBSII-gfpmut3*-T0–T1 | (226) |

# CHAPTER IV

# THE STRUCTURAL DOMAIN IN CHEMORECEPTORS OF *ESCHERICHIA COLI* IN INDOLE SENSING

## 4.1 Introduction

Bacteria swim towards favorable environments by detecting chemical signals with a set of transmembrane methyl-accepting chemotaxis proteins or chemoreceptors (81). Chemoreceptors form trimers of dimers and assemble into hexagonal arrays near the pole of the cell body (68, 69). Ligand-binding to a receptor modulates the activity of the chemotaxis histidine kinase, CheA (70). CheA controls the phosphorylation levels of a response regulator, CheY. CheY-P modulates reversals in the direction of rotation of the flagella to enable chemotaxis (65). In *Escherichia coli*, the binding of a ligand that decreases the CheA activity causes the cell to migrate towards the source of the ligand – termed an attractant response. Binding of a ligand that increases the CheA activity causes the cell to migrate away from the source of the ligand – termed a repellent response. There is some redundancy in sensing: the major receptors, Tar and Tsr, both sense several ligands as attractants (150). However, a handful of ligands are sensed as an attractant by one and as a repellent by the other receptor (227). The mechanisms by Tar and Tsr respond oppositely to some signals is of much interest as it can lead to selective colonization of niches by *E. coli* (228).

According to the standard model of chemoreceptor activation, an attractant molecule binds to the periplasmic domain to cause an inward displacement of the periplasmic helixes (96, 97). A control cable relays the displacement to the HAMP domain , which consists of four helixes arranged in a parallel coiled-coil structure (88, 89), inducing changes in its packing (92, 101). Changes in HAMP-packing control the packing of the MH bundle, which lies in the cytoplasmic

domain below the HAMP. The cytoplasmic domain carries the CheA kinase. A loosely-packed (tightly-packed) HAMP domain induces tight (loose) packing of the MH bundle, which causes the autophosphorylation rate of CheA to increase (decrease) (103-105). CheA transfers its phosphoryl groups to the cytoplasmic response regulator CheY. CheY-P binds to the flagellar motor to promote clockwise (CW) rotation in an otherwise counterclockwise (CCW) rotating flagellum[74]. A methyltransferase (CheR) and a methylesterase (CheB) methylate and demethylate glutamyl residues on the MH bundles to continually reset CheA activity. These enzymes together with the phosphatase, CheZ, maintain CheY-P at its basal levels to maximize the sensitivity of the chemotaxis network to a wide-range of extracellular signals (73, 75, 76).

Stimulants other than the canonical ligand can activate the periplasmic domain (21). However, numerous ligands interact with the cytoplasmic or the HAMP domains to induce chemotaxis signaling (102, 118). The mechanism of non-canonical signaling is poorly understood. Stimuli that induce opposite responses from Tar and Tsr include changes in the pH (127, 185), the temperature (125, 126, 229), and ligands such as phenol, which interacts with both the transmembrane region and the HAMP domain (227). Such biphasic responses are predicted to enable precise sensing and migration towards optimal environments (125, 127, 230). Recently, it was observed that indole induces biphasic chemotaxis responses: Tsr senses indole as a potent repellent and Tar senses it as an attractant. The biphasic response induces cells habituated to the metabolite to migrate towards the source of indole while causing unhabituated cells to be repelled from the source (228). Indole is produced by the gut microbiota from tryptophan (30), and the biphasic response to indole is predicted to protect the GI tract against harmful pathogens while promoting colonization by commensal bacteria (228). Determining how Tar and Tsr sense indole is crucial for understanding the role of indole in maintaining homeostasis in the gut.

Here, we determined the domains of Tsr and Tar involved in sensing indole. We employed a FRET assay to quantify the changes in CheA activity in response to indole. To delineate the role of the different chemoreceptor domains in sensing indole, we used hybrid Tsr and Tar receptors in which the periplasmic, HAMP, and the cytoplasmic domain were interchanged (227). Our observations indicate that indole binds to each of the three domains in Tar to induce an attractant response. However, it likely activates only the periplasmic domain of Tsr to induce the repellent response. These results reveal major differences in Tsr and Tar activation by a non-canonical ligand despite the high degree of homology between the receptors.

## 4.2 Materials and methods

### 4.2.1 Strains and plasmids

All strains were derived from *E. coli* RP437 (201). For tethered cell experiments, we transformed a Δ*tsr*Δ*tar* strain with Ampicillin-resistant *ptrc99A*-based vectors that carried alleles for the expression of the hybrid receptors (228). For FRET measurements with the hybrid receptors, a scarless Δ*tsr*Δ*tar*Δ*cheYcheZ* strain was generated with a two-step λ-red recombination technique (202), and confirmed via sequencing – see **Table 4. 1** for primer information. We transformed the strain with hybrid receptor plasmids and a compatible FRET fusion plasmid. The FRET plasmid was generated by amplifying the *cheY-yfp-cheZ-cfp* allele from pVS88 (66) and inserting it in a Chloramphenicol-resistant *pBAD33* vector. All strains and plasmids used in this work are listed in **Table 4. 2**.

### 4.2.2 Cell culturing and preparation

Overnight culture was grown in Tryptone Broth (TB) and inoculated at a 1:100 dilution in fresh 25 mL TB to grow the day culture. Both the overnight and the day culture were grown at 33 °C in a shaking incubator. Antibiotics were added as appropriate (100 µg/mL for Ampicillin and 25 µg/mL for Chloramphenicol). We added 100 µM IPTG (Isopropyl β- d-1-thiogalactopyranoside) to the day cultures to induce the expression of the hybrid receptors. To induce expression from the pBAD-based FRET plasmid, we added 0.2% w/v arabinose to the day culture. The wildtype FRET strain (see **Table 4. 2**), which carried the original pVS88 plasmid in a *cheYcheZ* background, was grown in the presence of 50 µM IPTG. Each day culture was grown to an $OD_{600}$ of 0.5 and centrifuged at 1,500 × g for 5 min (5702/R A-4-38, Eppendorf, Inc.). The supernatant was discarded and the cell pellet was washed twice by re-suspending and pelleting in motility buffer (MB, 10 mM potassium phosphate buffer, 67 mM NaCl, 0.1 mM EDTA, 1 µM methionine, 10 mM sodium lactate, pH 7.0).

### 4.2.3 FRET assay

Following the multiple washes, cells were resuspended in 1 mL MB. We then added 40 µL of the cell suspension to a circular coverslip (12 mm diameter, Fisher Scientific) pretreated with poly-L-lysine (0.01 % w/v, Sigma-Aldrich). After allowing the cells to settle and adhere for ~ 15 min, the coverslip was mounted face-down on a perfusion chamber (231). A syringe pump (Fusion 200, Chemyx, Inc.) was employed to maintain a continuous flow of MB at 260 µL/min in the chamber. We used a three-way valve (HVP3-2, Hamilton) to switch the flow between MB and MB containing ligands. Our FRET setup was designed based on earlier works (66). Briefly, we coupled an LED white light source (SOLA SE Light Engine, Lumencor, Inc.) into the backport of an

upright microscope (Ti-E, Nikon, Inc.). We used a blue emission filter (435/20x) to filter the white light and reflected it with a 455 nm dichroic mirror (Chroma Technology Corp.) onto the back-aperture of a water-immersion objective (60x, NA 1.2, Nikon, Inc). The emissions were relayed to a pair of photomultipliers (H7421-40 SEL Hamamatsu Corp.) after splitting the cyan and yellow emissions. To split the emissions, we used a 500 LP Dichroic. The yellow emission was passed through a 542/27 nm Bandpass (Semrock, Inc.) before entering the yellow PMT and the cyan emission was passed through a 480/3m Bandpass before entering the cyan PMT. The signals were recorded at 10 Hz sampling frequency with custom-written LabVIEW codes. The ratio of YFP/CFP was analyzed as previously described (66).

### 4.2.4 Tethered cell assay

Cells washed and resuspended in MB, similar to the cell preparation in the FRET assay. Then the cells were sheared to truncate flagellar filaments and subsequently tethered to a cover glass, as previously described (228). Then the cover glass were mounted on the perfusion chamber with a flow controlled by the switchable valve. The rotation of the cells was recorded by a digital camera (UI-3240LE-M-GL; IDS Imaging Development Systems) and analyzed with MATLAB. The rotation bias (fraction of the time that the motor rotates CW) was determined as a function of time, termed $CW_{bias}$.

## 4.3 Results

### 4.3.1 Indole is sensed as a repellent by Tsr's periplasmic domain

To probe how indole activates Tar and Tsr, we employed a FRET (Fluorescence Resonance Energy Transfer) (66) assay that monitors CheA activity indirectly based on the interactions between CheY-P and its phosphatase, CheZ. We first expressed the wild-type Tar in the *tsrtar* strain from an inducible plasmid. The ratio of the emissions in the yellow and the cyan channel decreases during an attractant response and increases during a repellent response (66). In our experiments, the ratio decreased when the Tar-only cells were stimulated over a range of indole (0.2 mM, 0.6 mM and 1 mM), as shown in **Figure 4. 1 A**. When only Tsr was expressed in the cells, the ratios increased upon stimulation over a range of indole (**Figure 4. 1 B**). These measurements confirmed our earlier result that Tar exhibits an attractant response and Tsr exhibits a repellent response to the metabolite (228).

Next, we determined the role of the periplasmic domain of Tsr in the repellent response to indole. To do this, we expressed a Tsr mutant that lacks its periplasmic domains in the *tsrtar* mutant strain (**Figure 4. 1 E**). This mutant failed to show any response to indole, even at 1 mM concentration. The motor itself displayed a repellent response in the presence of this Tsr mutant, which likely occurred due to the activation of the flagellar switch by indole (**Figure 4. 5 left panel**). A control measurement indicated that the Tsr mutant did exhibit a weak repellent response to 50 mM sodium acetate (**Figure 4. 6 left panel**) – sodium acetate decreases the cytoplasmic pH, which is sensed by the cytoplasmic domain of Tsr (90). These results suggest that Tsr's periplasmic domain is necessary for the repellent response to indole.

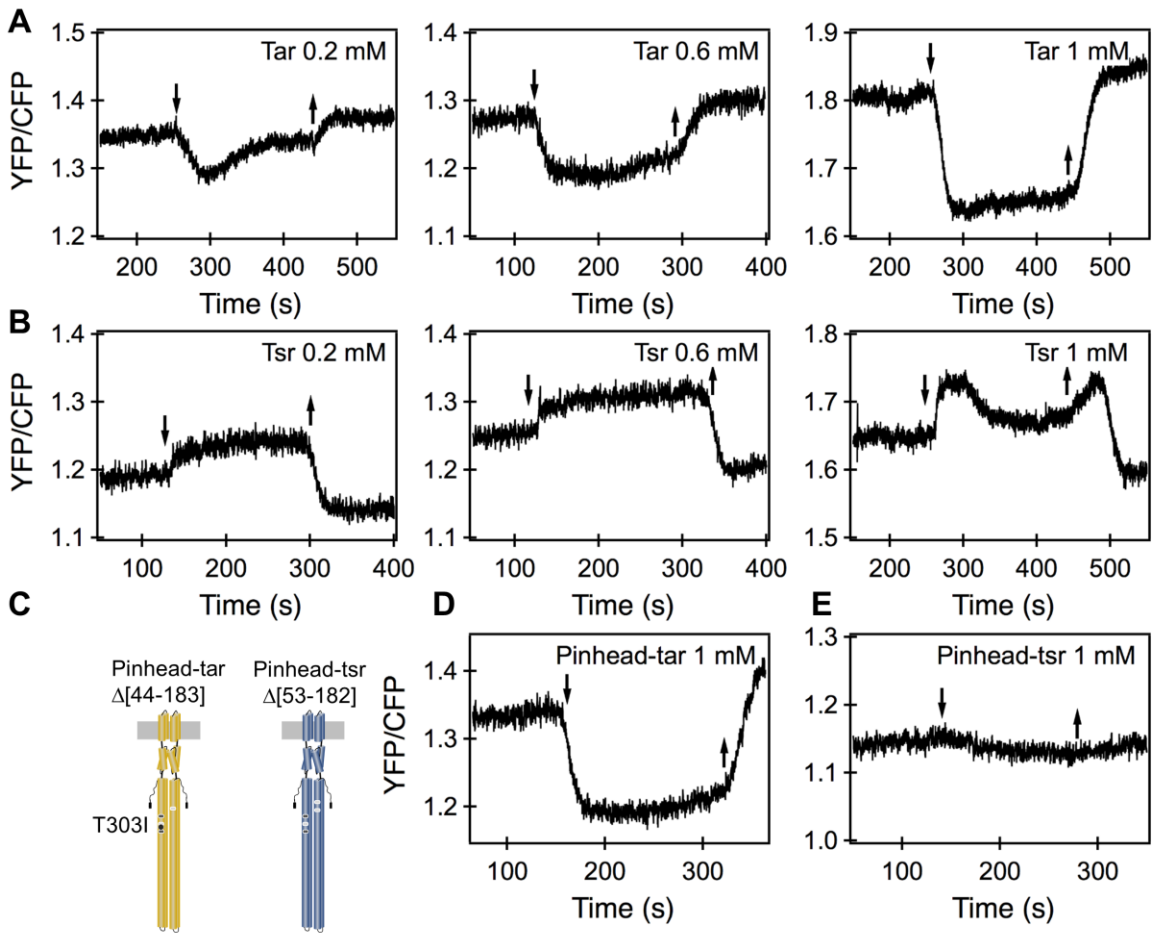


**Figure 4. 1 Indole responses mediated by Tar, Tsr and pinhead receptors.** Dose indole concentrations were employed to stimulate wild-type Tar (A) and Tsr (B). C. The construction of pinhead-tsr and pinhead-tar receptor. D. Pinhead-tar response to 1 mM indole. E. Pinhead-tsr response to 1 mM indole. The down and up arrows indicate the start and end of indole perfusion.

### 4.3.2 Indole is sensed as an attractant by Tar's periplasmic domain

To determine the role of Tar periplasmic domain in sensing indole, we tested the response of a Tar mutant that lacks its periplasmic domain (227). This mutant carries a single amino acid mutation (T303I) that restore the CW signaling ability of the initial pinhead construction, which lost its ability in stimulating kinase. When stimulated with indole, this Tar mutant exhibited a strong attractant response (**Figure 4. 1 D**). While this suggested that the other domains of Tar are likely involved in indole response, it did not eliminate the possibility that the periplasmic domain

senses indole. Hence, we stimulated a hybrid mutant in which the periplasmic domain of Tsr was replaced with Tar's periplasmic domain (called the Tassr mutant) with indole. This particular mutant also exhibited attractant responses to the metabolite, especially at higher concentrations (**Figure 4. 2 A**). This strongly indicated that multiple domains of Tar, including the periplasmic domain, sense indole as an attractant.

To confirm the role Tsr's periplasmic domain in the repellent response and Tar's HAMP and (or) the cytoplasmic domains in the attractant response in indole, we tested the response of a hybrid receptor in which the periplasmic domain of Tar was replaced with that of Tsr. This mutant exhibited a repellent response at low concentrations of indole, indicating that the periplasmic domain was activated first and had a strong affinity for indole (**Figure 4. 2 C**). At medium concentrations, an initial repellent response inverted to an attractant response in a few seconds. The delay in the attractant response is likely because indole has to diffuse through the membrane to gradually build up to a concentration at which it can induce a response from the other receptor domains of Tar. At the highest concentration we studied (1 mM), the response was purely attractant, indicating that the HAMP and/or cytoplasmic domain dominate the indole response of Tar (**Figure 4. 2 D**). These results confirm the kinetic signatures of the indole responses we had observed earlier in the wild-type Tsr and Tar receptors.

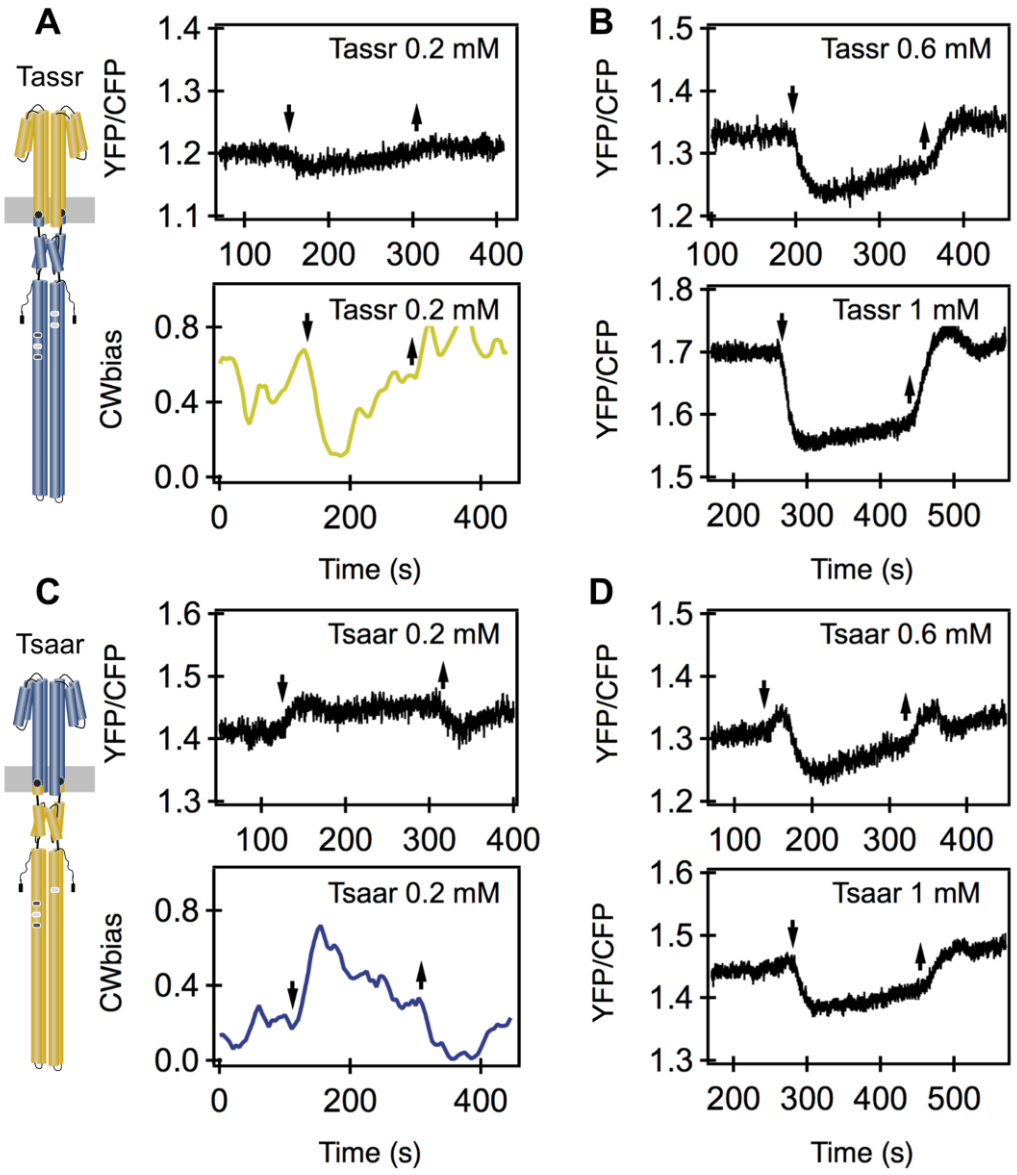


**Figure 4. 2 Response to indole mediated by hybrid Tsr-Tar receptors exchanging periplasmic domain.** A. Response to 0.2 mM indole mediated by Tassr in FRET (up panel) and tethered cell assay (down panel). B. Tassr mediated response to 0.6 mM and 1 mM indole in FRET assay. C Response to 0.2 mM indole mediated by Tsaar in FRET (up panel) and tethered cell assay (down panel). D. Tsaar mediated response to 0.6 mM and 1 mM indole in FRET assay. The down and up arrows indicate the start and end of indole perfusion.

### 4.3.3 The HAMP domain of Tar senses indole as an attractant

To determine if Tar's HAMP domain was involved in sensing indole, we employed a hybrid receptor in which the HAMP domain in Tsr was replaced with that from Tar (called Tsasr

hybrid) (227). When stimulated with 0.2 mM indole, no detectable response was observed. However, at higher concentrations (0.6 and 1 mM indole), the mutant exhibited clear attractant responses (**Figure. 4. 3 A**). As Tsr's periplasmic domain senses indole as a repellent and there is no evidence to support the notion that its cytoplasmic domain senses indole (see **Figure 4. 1**), the only likely domain that could mediate this attractant response is the Tar HAMP domain. We conclude therefore, that Tar's HAMP mediates an attractant response to indole similar to its periplasmic domain.

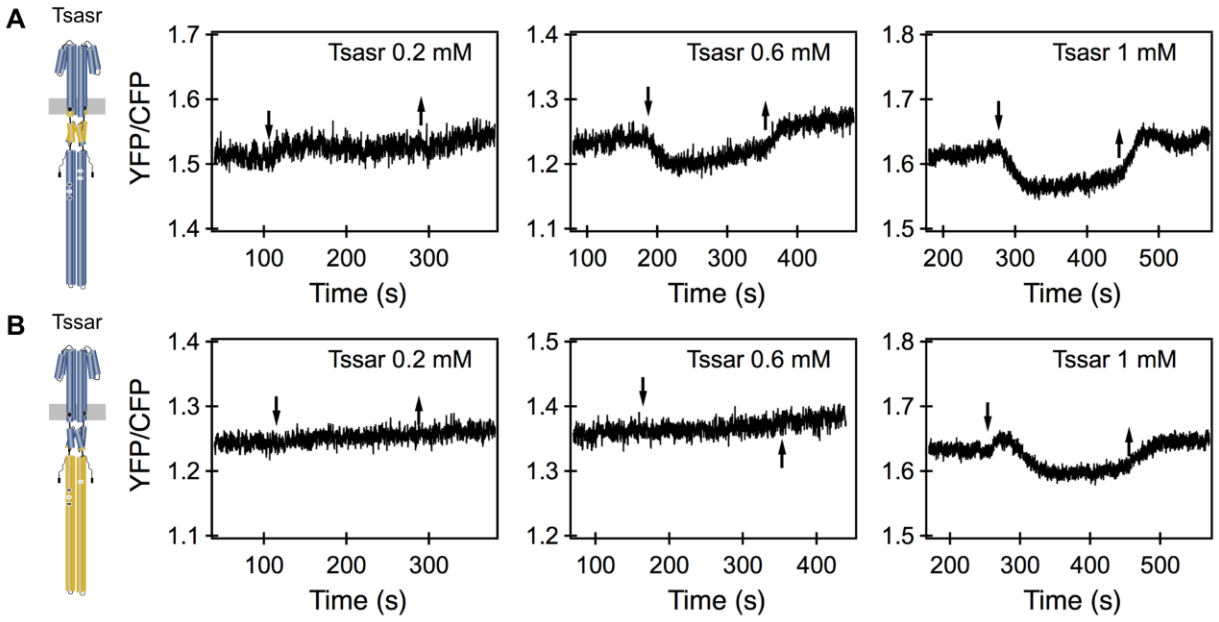


**Figure 4. 3 The role of Tar HAMP domain and MH/KC region in sensing indole.** Cells were stimulated with dose concentration of indole mediated by Tsasr (A) and Tssar (B). The down and up arrows indicate the start and end of indole perfusion.

### 4.3.4 The cytoplasmic domain of Tar senses indole as an attractant

Finally, we investigated whether Tar's cytoplasmic domain played a role in the response to indole. We employed a hybrid receptor in which the Tsr's cytoplasmic domain has been replaced with Tar's cytoplasmic domain. The mutant exhibited no significant response to indole at 0.2 and

0.6 mM (**Figure 4. 3 B left and middle panel**). At 1mM indole, a biphasic response was observed in which a weak repellent response inverted to an attractant response (**Figure 4. 3 B right panel**). The repellent response is likely due to the Tsr periplasmic domain. The attractant response is likely due to the cytoplasmic domain of Tar. These data suggest that all the three domains of Tar – periplasmic, HAMP, and cytoplasmic are likely involved in the sensing of indole as an attractant. See **Table 4. 3** for the entire characterization of receptor/hybrid receptor responses to indole.

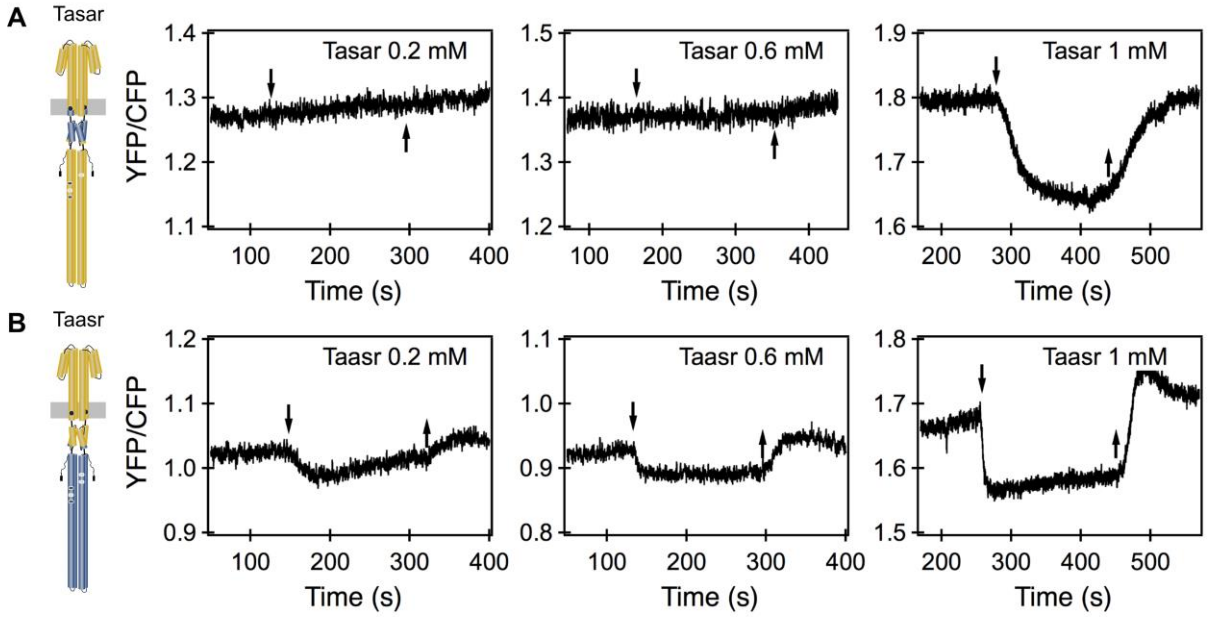


**Figure 4. 4 Response to indole mediated by hybrid receptors of Tasar and Taasr.** Cells were stimulated with dose concentration of indole mediated by Tasar (A) and Taasr (B). The down and up arrows indicate the start and end of indole perfusion.

For Tasar, no response was observed at 0.2 and 0.6 mM indole (**Figure 4. 4 A left and middle panel**) while a strong attractant response occurred at 1 mM indole (**Figure 4. 4 A right panel**). Tasar might have less sensitivity in responding the input signals. In fact, in the tethered cell experiments, most cells with Tasar have a pre-stimulus CWbias of ~1 while that of cells with

wild-type Tsr and Tar were ~ 0.4 (**Figure 4. 7 right panel**). That indicates that the initial kinase activity of Tasar was very different from wild-type receptors with the same 100 µM IPTG induction level, therefore has different dynamic range for responses compared with wild-type receptors. The 0.2 mM and 0.6 mM indole might not adequate enough to stimulate the kinase. At 1mM, Tar periplasmic domain senses indole as an attractant, therefore initiates attractant signaling and decreases kinase activity. We induced Tasar with a lower IPTG concentration (20 µM) and stimulated with 0.2 mM indole, the repellent only response was observed, which is likely due to the flagellar motor (**Figure 4. 7 left panel**).

Taasr showed attractant only response with the magnitude of the response increase with indole concentration (**Figure 4. 4 B**), which is very similar to WT Tar (**Figure 4. 1 A**). This is expected since both Tar periplasmic and HAMP domain are attractant mediator and no other repellent mediator present in Taasr.

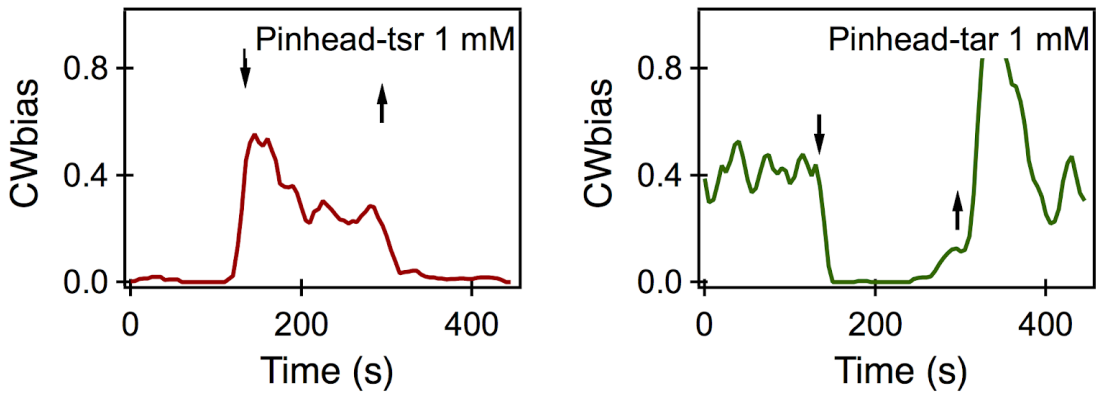


**Figure 4. 5 Responses to indole mediated by pinhead receptors in the tethered cell assay.** Pinhead Tsr (left) and Tar (right) response to 1 mM indole. The down and up arrows indicate the start and end of indole perfusion.

## 4.4 Discussion

The canonical view of a dimeric *E. coli* or *S. enterica* chemoreceptor is that its extracellular, periplasmic domain is responsible for sensing attractants. The periplasmic domain of each receptor monomer is a four-helix bundle, which is flanked by an N-terminal transmembrane helix coming out from the cytoplasm (TM1) and a second transmembrane region passing back into the cytoplasm (TM2). TM2 connects to the two parallel packed helices of the HAMP domain, which in turn connects to the control region consisting of the methylation helix (MH) and kinase control (KC) domains. Each receptor monomer thus consists of four periplasmic helices, two transmembrane regions (TM1 and TM2), two HAMP helices, and two long cytoplasmic helices. Periplasmic helices 1 and 4 of one monomer interact with periplasmic helices 1' and 4' of the other subunit, the two helices of the HAMP domains of each subunit come together to form a parallel 4-helix structure, and the long cytoplasmic helices come together to form an anti-parallel four-helix bundle. The full extent of the dimer, from the membrane-distal tip of the periplasmic domain to the membrane-distal tip of the cytoplasmic domain that interacts with the CheA kinase, is 310Å (232).

Attractants may either interact directly with a binding pocket that spans the dimer interface, or they may first bind to a soluble periplasmic binding protein. The direct-binding ligands that have been well-characterized interact with residues in helix 4 of one subunit and in helix 1' of the other. As more residues in helix 4 are involved in the interaction, that is called the majority binding half-site, whereas the minority half-site is in helix 1'. There is also a second binding site consisting of residues in helix 4' and helix 1. These two sites can be occupied simultaneously, but there is often strong negative cooperativity between them.

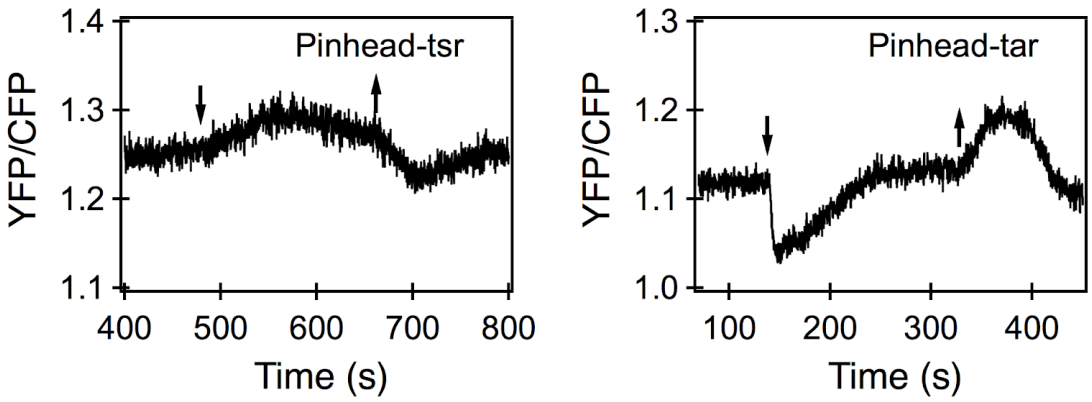


**Figure 4. 6. Responses to sodium acetate mediated by pinhead receptors in the FRET assay.** The pinhead Tsr (left) and Tar (right) mediates responses to 50 mM sodium acetate. The down and up arrows indicates the start and end of indole perfusion.

Ligands that interact with a periplasmic binding protein bind in a cleft between its N-terminal and C-terminal domains. Their binding stabilizes a closed conformation of the protein. In this conformation the protein can interact with residues at or near the membrane-distal tip of the periplasmic domain of the receptor, with the N-terminal domain interacting with one subunit of the dimer and the C-terminal domain interacting with the other subunit (86, 87).

With either directly binding or indirectly binding ligands, the proximal signal is thought to be a one to two ångström displacement of helix 4 of the periplasmic domain toward the membrane (96, 97). This conformational change is transmitted through TM2 to the HAMP domain and then transmitted through the methylation helices to the kinase control domain. The whole process of intrareceptor signaling can thus be thought of as a linearly progressing series of conformational changes from at, or near, the tip of the periplasmic domain to the tip of the cytoplasmic domain that contacts the CheA kinase. The situation is considerably more complicated in reality, as the receptor dimers aggregate to form a trimer of dimers, and the minimal functional signaling unit is two trimers of dimers connected by two CheW molecules and a CheA dimer. Nonetheless, in the

first instance, it is realistic to think of attractant ligand-induced changes being propagated from one end of the receptor dimer to the other.

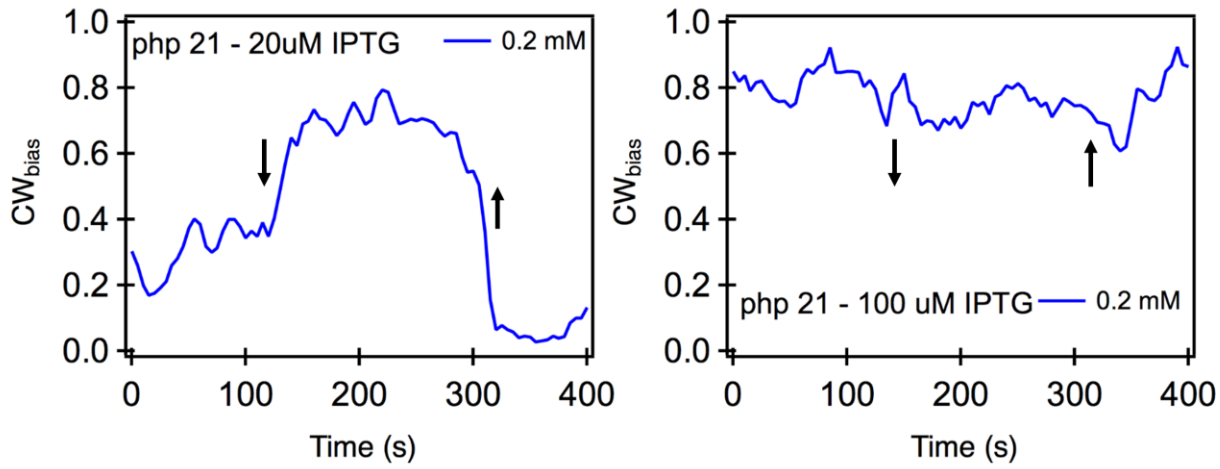


**Figure 4. 7 Responses to 0.2 mM indole mediated by Tasar in the tethered cell assay.** The expression of the receptors were induced with 20 µM (left) and 100 µM (right) IPTG. The down and up arrows indicate the start and end of indole perfusion.

The periplasmic domains of both Tar and Tsr sense attractants by both direct and indirect mechanisms. Tar binds L-aspartate with high affinity, and other certain other amino acids and amino acid analogs with lower affinity, in the interdimer binding pocket described above[248]. Tar of *E. coli*, but not Tar of *S. enterica*, mediates maltose chemotaxis through an interaction with the ligand-bound, closed form of the periplasmic maltose-binding protein (MBP) (233). Tsr binds L-serine with high affinity, and many other amino acids with lower affinity, in its interdimer binding pocket (120). It also mediates chemotaxis to dihydroxymandelic acid (DHMA), a derivative of norepinephrine, at the same site that binds serine, although with higher affinity and with different residue interactions (21). Tsr also mediates chemotaxis to autoinducer-2 (AI-2; tetrahydroxy-*R*-methylfuran) by interacting with the ligand-bound form of the periplasmic LsrB protein (122). All of these interactions have been characterized in considerable detail.

The mechanism of sensing repellent ligands is much less well understood. Only an artificial construct joining the periplasmic, TM, and HAMP domains of the NarX two-component nitrate/nitrate sensor with the MH/KC domain of Tar (the Nart receptor) has been shown to recognize nitrate and nitrite as repellents when they bind to the periplasmic ligand-binding domain of NarX (234). Many other repellents may be sensed through interactions with membrane or cytoplasmic regions of the receptor. In principle, input that changes the conformation of the kinase control domain can be exerted at any point along the intramolecular chain of signal propagation. This is particularly true of ligands that can permeate into or through the lipid bilayer of the cell membrane. Of course, some attractant molecules may also provide input through membrane of intracellular or membrane-associated domains of the protein.

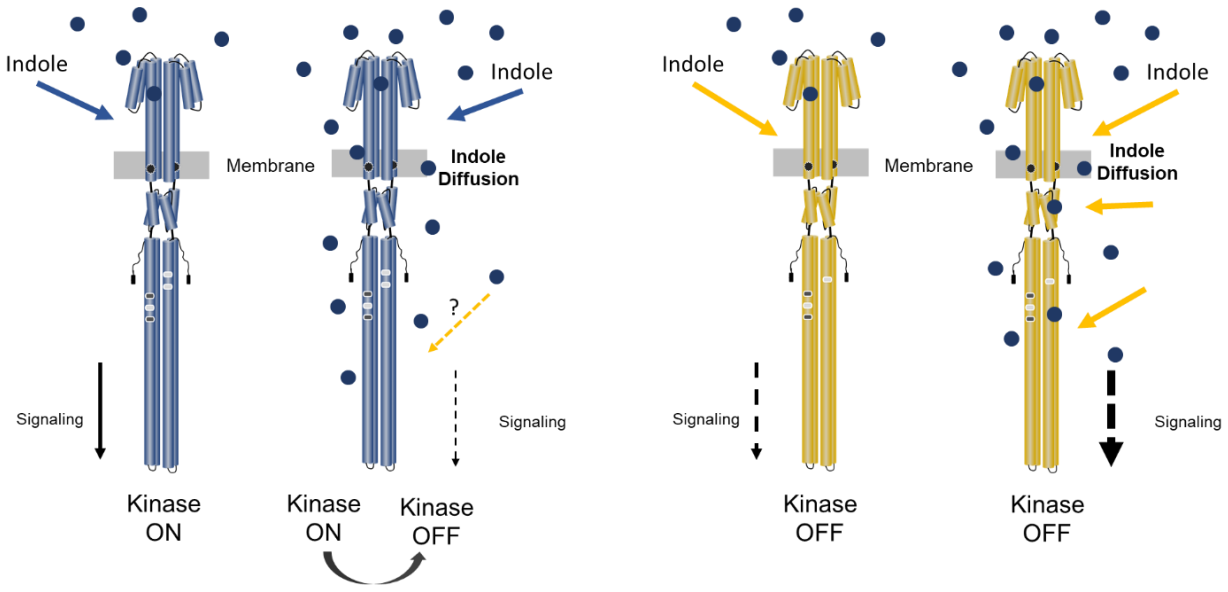


**Figure 4. 8 Possible mechanism of indole sensing through Tsr and Tar.** Indole molecules are indicated by blue solid circles. Blue arrow and yellow arrow indicates repellent and attractant stimuli respectively. Solid black arrow indicates the kinase on stimulation and dotted black line arrow indicates the kinase off stimulation. The weight of the black arrows indicates the strength of the stimulation.

Indole represents a particularly interesting case. As we have shown previously, indole is sensed as a repellent by *E. coli* Tsr and an attractant by Tar (228). The Tsr-mediated repellent response dominates the response of wild-type cells to low concentrations of indole. At intermediate concentrations, an initial repellent response is followed by a longer attractant response. At high concentrations, only an attractant response is observed. As indole permeates freely into cells, the biphasic response led us to hypothesize that the rapid response to lower concentrations of indole might be mediated by the periplasmic domain of Tsr and the slower attractant response might require the permeation of indole into the membrane or into the cytoplasm, a process that would take some time (**Figure 4. 8**).

Although the current study shows that scenario to be roughly accurate, it is clear that reality is more complicated. Multiple domains of the two proteins are involved. These complications were revealed through the analysis of cells expressing various chimeric constructs of Tar and Tsr in which different domains of the proteins were deleted or exchanged. All of these constructs were provided by the laboratory of J. S. Parkinson (227). An important complication in assessing indole chemotaxis is that the flagellar motor in a Δ*cheY* strain, in the absence of any input from the receptors, produces a CW flagellar rotation (i.e., repellent) response to high concentrations of indole. For that reason,we used the FRET response obtained from the interaction of CheY-CFP with CheZ-YFP to record the chemotaxis response in terms of CheY-P produced at the chemoreceptor patch.

The domain compositions of these constructs are shown as cartoons in **Figures 4. 1-4. 4**. Receptors in which the periplasmic domains of Tar and Tsr have been deleted are called pinhead Tar and pinhead Tsr, respectively. Other hybrids in which the periplasmic/TM domain, the HAMP domain, and the MH/KC domain have been exchanged are named according to the donor of the

individual domains, with the first two letters designating the donor of the periplasmic/TM domain, the middle letter designating the origin of the HAMP domain, and the last two letters the source of the MH/KC domain. Thus, Tsaar, has the periplasmic/TM domain of Tsr and the HAMP and MH/KC domains of Tar. Tassr is the complement of that, and Tsasr has the periplasmic/TM and MH/KC domain of Tsr and the HAMP domain of Tar. In all, counting the wild-type receptors and pinhead constructs, we studied the indole responses mediated by ten different receptors.

The data generated from cells expressing each of these constructs in cells deleted for all of the chromosomally encoded chemoreceptors are presented in **Figure 4. 1** through **Figure 4. 4**. As expected, cells expressing only Tar responded to indole as an attractant, indicated by a decrease in the ratio of YFP to CFP fluorescence, to addition of 0.2, 0.6, or 1.0 mM indole (**Figure 4. 1**). They showed a repellent response, indicated by an increase in the ratio of YFP to CFP fluorescence, when indole was removed. In contrast, cells expressing only Tsr responded to indole as a repellent at these concentrations, and they responded to the removal of indole as an attractant stimulus. These results confirm our earlier conclusion that Tar senses indole as an attractant and Tsr senses indole as a repellent. It is worth noting that Tsr-only cells also respond to 20 μM indole as a repellent, as do wild-type cells, whereas Tar-only cells show no response to 20 μM indole (228).

When the responses mediate by the pinhead receptor constructs were analyzed, pinhead Tar mediated a strong attractant response to indole and a return to the baseline YFP/CFP ratio, or perhaps a weak repellent response, after its removal. Thus, the periplasmic domain of Tar is not essential for its ability to mediate an attractant response, a result in accord with our hypothesis. The plasmid expressing pinhead Tsr did not yield easily interpretable results; cells expressing pinhead Tsr rotated only CCW, indicating that its ability to stimulate CheA kinase activity was poor. It did not exhibit a significant FRET response to either the addition or removal of indole.

Although this result may simply mean that it is unable to support significant CheY-P production even after sensing a repellent, it is also consistent with the possibility that the periplasmic domain of Tsr is essential for the repellent response to indole.

The two hybrid receptors Taasr and Tssar also gave results that were consistent with our hypothesis. Taasr gave rise to rather weak attractant responses to 0.2 and 0.6 mM indole and repellent responses to their removal, but it gave a strong attractant response to the addition of 1 mM indole and a strong repellent response to its removal (**Figure. 4. 4 B**). These results indicate that the periplasmic/TM and HAMP domains of Tar are capable of producing a strong attractant responses to indole. The Tssar receptor did not mediate any detectable response to 0.2 or 0.6 mM indole and mediated only a weak biphasic repellent followed by attractant response to 1 mM indole (**Figure. 4. 3 B**). This result is potentially consistent with the Tsr periplasmic domain mediating the repellent response to indole but suggests in addition that the MH/KC domain of Tar can support an attractant response to indole.

The results with chimeras combining the periplasmic/TM domain of one receptor with the the HAMP and MH/KC domains of the other implicate the TM domain of Tar in sensing indole as an attractant (**Figure. 4. 2**). Tassr supported an attractant-only response to 0.2, 0.6, and 1 mM indole, with the responses being weak, intermediate, and strong, respectively. Thus, either the periplasmic or TM domain of Tar senses indole as an attractant. Cells expressing Tsaar showed biphasic FRET responses to 0.2 and 0.6 mM indole and an attractant-only response to 1 mM indole. This result is consistent with the periplasmic/TM domain of Tsr mediating a repellent response to indole that can be overridden at high indole concentrations by an attractant response mediated by the HAMP and/or MH/KC domains of Tar.

The results obtained with receptors in which only the HAMP domains were exchanged reinforce some of our previous conclusions. Cells expressing the Tsasr protein, in which the HAMP domain is derived from Tar and the remainder of the protein is Tsr, give a marginal repellent response to 0.2 mM indole, a weak attractant response to 0.6 mM indole, and an intermediate attractant response to 1 mM indole. This result demonstrates that the Tar HAMP domain alone can mediate an attractant response to indole. Cells expressing the Tasar protein exhibit no detectable response to 0.2 or 0.6 mM indole but show a strong attractant response to 1 mM indole. Thus, the periplasmic/TM and/or MH/KC domains of Tar can produce an attractant signal.

To summarize, taken together our results suggest that the periplasmic and/or TM domains of Tsr can generate a repellent signal. We did not test a construct in which the periplasmic domain was donated by Tsr and the TM domain by Tar, nor vice versa, so we cannot distinguish between repellent responses originating with either of these two portions of the periplasmic/TM domain.

The attractant response to indole seems to have multiple inputs, as receptors with only the periplasmic/TM domain, only the HAMP domain, or only the MH/KC domain are all capable of generating an attractant response. Perhaps this reflects that it is easier to down-regulate CheA stimulation to give an attractant response than to up-regulate it to give a repellent response. Any interaction with indole that alters the normal helix packing in any of these three regions could have the latter effect. It will take the construction and testing of additional receptor constructs in which the periplasmic and TM domains and the MH and KC domains are interchanged to further refine the location within Tar in which attractant responses to indole can be generated. However, the caveat must be made that the more mixing and matching of domains that is attempted through

genetic engineering, the more likely it is that serious mismatching will lead to non-functional proteins.

Chemoreceptors can be considered transmembrane allosteric enzymes, with the regulatory site outside the cell and the active site at which phosphorylation of CheY occurs in the cytoplasm (235). The biochemical lesson from this study is that signal input to a protein that depends on allosteric effects can occur at the allosteric ligand-binding site or anywhere between it and the active site along the intramolecular signal transduction pathway, which is extensive in chemoreceptors. Most studies of ligand recognition have focused on interactions of attractants with a well-defined allosteric binding site in the periplasmic domain. This study represents an attempt to begin to come to grips with non-canonical mechanisms for responding to chemoeffectors without well-defined binding sites.

The biological takeaway from this study is an extension of one that we made previously. The interplay of countervailing responses to a chemoeffector, or a physical signal like temperature or pH, can produce sophisticated responses by bacteria. In the case of indole, in wild-type cell, Tsr senses low concentrations of indole to give a repellent response and Tar senses higher concentrations of indole to give an attractant response. At first glance, this may seem counterintuitive. However, the Tsr-mediated repellent response adapts rapidly and converts to an attractant response at higher concentrations of indole. Our earlier work showed that wild-type cells pre-adapted to concentrations of indole of 0.7 mM or higher showed an attractant response to higher concentrations of indole (228). Thus, cells that had become "accustomed" to the higher indole concentrations that exist within dense populations of indole-producing bacteria, which include *E. coli*, would be attracted and remain within that population. An example would be commensal *E. coli* living at high density within the intestinal mucosa or at the intestinal lining.

Meanwhile, invading cells in the lumen of the intestine, including pathogens, would be repelled by the lower concentrations of indole diffusing out of the intestinal mucosa and would not colonize the intestinal lining. Thus, the biphasic repellent/attractant response to indole shown by *E. coli* might prove to be highly adaptive to the resident bacteria as well as a promoter of host intestinal homeostasis.

**Table 4. 1 Primers used in this study**

| Primer | Function | 5’ to 3’ sequence |
|---|---|---|
| ptrc99A SacI FWD | Amplifying fusion insert (cheY-YFP-cheZ-CFP) | ATTGAGCTCTGCAGGTCGTAAATCACTGC |
| ptrc99A HindIII REV | Amplifying fusion insert (cheY-YFP-cheZ-CFP) | CGTAAGCTTCTGGCAGTTCCCTACTCTCG |
| Red_CheYCheZ_P1 | Replacing cheYcheZ with Kan-ccdB box | GACAGGCGATACGTATTTAAATCAGGAGTGTGAAATGGCGTCAGAAGAACTCGTCAAGAA |
| Red_CheYCheZ_P2 | Replacing cheYcheZ with Kan-ccdB box | GCCTGATATGACGTGGTCACGCCACATCAGGCAATACAAATTTATATTCCCCAGAACATC |
| CheYCheZ-kan ccdB 1 FWD | Removing Kan-ccdB box | CGGAGAGCATGCCCGACAATCG |
| CheYCheZ-kan ccdB 2 REV | Removing Kan-ccdB box | GGCATGGACCCTTGCGCAAAAC |

**Table 4. 2 Bacterial strains and plasmids used in this study**

| Strains | Relevant genotype | Source |
|---|---|---|
| PL 221 | PL15 *Δtsr* (Δnt 16-1644 ) *Δtar* (Δnt 16-1638) | (228) |
| | PL15 *Δtsr* (Δnt 16-1644 ) *Δtar* (Δnt 16-1638) *ΔcheYcheZ* | This work |
| Plasmids | | |
| pVS88 | CheY-EYFP / CheZ-EYFP expression plasmid, pTrc99a derivative, $Amp^R$ | (66) |
| pBAD33-FRET | CheY-EYFP / CheZ-EYFP expression plasmid, pACYC-184 derivative, $Chl^R$ | This work |
| pPA791; Pinhead Tar | *tar* (Δ44-183) T303I | Gift from Sandy Parkinson |
| pPA910; Pinhead Tsr | *tsr* (Δ53-182); pRR53 derivative | Gift from Sandy Parkinson |
| pHP2; Tar | *Tar* VVV200-202AAA | Gift from Sandy Parkinson |
| pHP4; Tsr | *Tsr* VVL202-204AAA | Gift from Sandy Parkinson |
| pHP17; Tsaar | | Gift from Sandy Parkinson |
| pHP18; Tsasr | | Gift from Sandy Parkinson |
| pHP19; Tssar | | Gift from Sandy Parkinson |
| pHP20; Tassr | | Gift from Sandy Parkinson |
| pHP21; Tasar | | Gift from Sandy Parkinson |
| pHP22; Taasr | | Gift from Sandy Parkinson |

**Table 4. 3 FRET responses to addition and removal of indole**

| Receptor | Indole conc. | Add | Adapt | Remove | Adapt |
|---|---|---|---|---|---|
| Tar | 0.2 mM | Kinase off + | Yes | Kinase on + | No |
| | 0.6 mM | Kinase off ++ | Partial | Kinase on ++ | No |
| | 1.0 mM | Kinase off +++ | No | Kinase on +++ | No |
| Tsr | 0.2 mM | Kinase on + | No | Kinase off ++ | No |
| | 0.6 mM | Kinase on + | No | Kinase off ++ | No |
| | 1.0 mM | Kinase on ++ | Yes | Kinase on ++ | Yes |
| Pinhead Tar | 1.0 mM | Kinase off +++ | No | Kinase on +++ | No |
| Pinhead Tsr | 1.0 mM | No response | --- | No response | --- |
| Tassr | 0.2 mM | Kinase off + | Yes | No response | --- |
| | 0.6 mM | Kinase off ++ | Partial | Kinase on ++ | No |
| | 1.0 mM | Kinase off +++ | No | Kinase on +++ | Partial |
| Tsaar | 0.2 mM | Kinase on + | No | Kinase off + | Yes |
| | 0.6 mM | Biphasic on/off | Partial | Biphasic on/off | Yes |
| | 1.0 mM | Kinase off ++ | Partial | Biphasic on/off | Partial |
| Tasar | 0.2 mM | No | --- | No | --- |
| | 0.6 mM | No | --- | No | --- |
| | 1.0 mM | Kinase off +++ | No | Kinase on +++ | No |
| Tsasr | 0.2 mM | Kinase on + | No | No | --- |
| | 0.6 mM | Kinase off + | Yes | Kinase on | No |
| | 1.0 mM | Kinase off ++ | No | Kinase on ++ | No |
| Taasr | 0.2 mM | Kinase off + | Yes | Kinase on + | No |
| | 0.6 mM | Kinase off + | No | Kinase on ++ | No |
| | 1.0 mM | Kinase off +++ | No | Kinase on +++ | Partial |
| Tssar | 0.2 mM | No | --- | No | --- |
| | 0.6 mM | No | --- | No | --- |
| | 1.0 mM | Biphasic on/off | No | Kinase on + | No |

# CHAPTER V

# INVESTIGATING THE INTEGRATED EFFECT OF INDOLE AND SCFAS ON *E. COLI* CHEMOTAXIS AND SURFACE COLONIZATION

## 5.1 Introduction

The mammalian gut is one of the most populated microbial ecosystems (38, 39). In the gut, microbes are resident in the mucus on the intestinal epithelium, and can influence the host by modulating metabolism, immune responses, and other physiological functions (39, 236). Several bacterial species such as *Clostridium ramosum*, *Roseburia intestinalis*, and *Lactobacillus brevis* that are present in the GI tract have genes that encode for proteins involved in flagellar assembly (45, 46). Although the chemotaxis and motility of commensals is believed to be largely inhibited by the immune system in healthy hosts (46), they are nevertheless important in the context of microbe-microbe interactions in the GI tract (48).

Microbial derived metabolites have been shown to modulate bacterial chemotaxis (21, 48, 130, 237). Tryptophan-derived microbial metabolites are increasingly being recognized as a class of microbial metabolites that play a significant role in several aspects of host physiology, including in the modulation of pathogen infections and regulation of inflammatory responses in different tissues (28, 143, 147). Metabolites such as indole are well characterized to be elicit chemotaxis responses in *E. coli* (27, 149, 228). Indole is produced from tryptophan by bacteria including *E. coli* that harbors *tnaA*, the gene that encodes for tryptophanase. Indole is abundant in the GI tract, with concentrations ranging from 0.25 to 6.5 mM in human feces (132). In our recent study, we have shown that indole elicit biphasic chemotaxis response in *E. coli*, which is mediated oppositely by Tsr and Tar (228).

The short chain fatty acids (SCFA), which are produced from fermentation of dietary fiber by anaerobic bacteria resident in the colon, are among the abundant microbial metabolites in the GI tract. The total concentration of the three main SCFAs (acetate, butyrate, and propionate) can reach up to 140 mM in the proximal colon and up to 70 mM in the distal colon (31, 154, 155). SCFAs are known to be chemoeffectors in *E. coli* and elicit a repellent response through decreasing the cytoplasmic pH (177, 185, 213). Subsequent studies demonstrated that the change in cytoplasmic pH upon exposure to SCFAs is mediated by Tsr and Tar (178).

While the chemotaxis response of *E.coli* individually to molecules like indole and SCFAs are well studied, little is known about how the *E. coli* chemotaxis network senses and responds to different stimuli that are present together. This is especially true when molecules that elicit attractant, repellent, or bidirectional responses are present together. Tsr and Tar are two receptors that mediate the majority of bidirectional chemotaxis responses to molecules such as aromatic compounds, pH, temperature, and weak acids (125, 127, 178, 227, 238). Although some studies have elucidated the mechanisms underlying the response to bidirectional taxis and investigated the cooperative signaling within Tsr and Tar receptors (239, 240), few studies have focused on the integrated effect of multiple stimuli

Based on the abundance of indole and SCFAs in the GI tract, as well as their established roles in host physiology and function, we investigated the chemotaxis response of *E. coli* exposed to both indole and SCFA. Using acetate as the model SCFA, we also investigated the mechanisms underlying the response when *E. coli* are exposed to both indole and SCFAs. Our results represent a first step in understanding how two metabolites from the same or different niches can modulate the chemotaxis and colonization of bacteria in the GI tract.

## 5.2 Materials and methods

### 5.2.1 Bacterial strains and grow conditions

All strains were derivatives of *E. coli* RP437 (201) and are listed in **Table 3. 1**. The two-step λ-red–mediated homologous recombination technique (202) was used to generate scarless, in-frame deletions. The deletions were confirmed via sequencing.

Overnight cultures were grown at 33 °C in tryptone broth (TB) followed by 1:100 dilution in 25 mL fresh TB for day cultures. The cultures were allowed to grow at 33 °C to an OD600 of 0.5. Antibiotics (100 μg/mL erythromycin and 25 μg/mL chloramphenicol) were added to the cultures where appropriate. Arabinose was added to the day cultures in the range of 0.001 to 0.1% (wt/vol) and IPTG was added to a concentration of 100 μM, where appropriate.

### 5.2.2 Tethered-cell assay

The day cultures were harvested by pelleting cells by centrifugation (1,500 × g, 5 min). Cells were washed 2× in motility buffer (10 mM potassium phosphate buffer, 67 mM NaCl, 0.1 mM EDTA, 1 μM methionine, 10 mM sodium lactate, pH 7.0). The final pellet was resuspended in 1 mL MB. Cells were then sheared to truncate flagellar filaments to stubs following previous approaches, and subsequently tethered to coverslips in perfusion chambers with the aid of sticky FliC filaments (203, 204). Cell rotation was recorded on a Nikon microscope (Optiphot 2) with a 20× phase objective at 60 fps and a digital camera (UI-3240LE-M-GL; IDS Imaging Development Systems). Videos of the rotation of the tethered cells were analyzed with custom-written codes in MATLAB (205). The rotation speeds were determined from Gaussian fits to the speed distributions. The $CW_{bias}$ (fraction of the time that the motor rotates CW) was determined as a function of time by employing a moving filter that averaged over 1.5 cell rotations, as done

previously (206). A three-directional valve (Hamilton, Inc) was employed to exchange the fluid in the perfusion chambers with MB or MB containing indole. The flow rate (260 μL/min) was controlled by a syringe pump (Fusion 200; Chemyx). Separate calibration experiments were performed with a colored fluid to estimate the average time of entry of chemoeffectors into the perfusion chamber after the initiation of flow.

### 5.2.3 Transwell assay

A thin agar layer was poured into individual transwell inserts (Nunc cell-culture inserts) and then soaked overnight in motility buffer or in motility buffer containing 2 mM indole. The agar surface was coated with poly-L-lysine to facilitate stable attachment of the cells. The inserts were then carefully transferred to individual wells in a 24-well plate (Carrier Plate Systems; Thermo Fisher Scientific; 141002) carrying a suspension of GFP-expressing *E. coli* (**Figure 3. 1**). Cells that respond to time-varying chemical gradients established in these reservoirs either migrate toward and attach to the agar pads or are repelled (207, 208). In the primed case, the cell suspension contained 700 μM indole. In the unprimed case, the cell suspension contained no indole. After 5 min, the inserts were carefully removed, gently washed with MB to remove unstuck cells, and then imaged via confocal microscopy. Custom-written MATLAB codes were then employed to count the number of cells adhered to the surface.

## 5.3 Results

### 5.3.1 *E. coli* RP437 senses SCFAs as repellents

To assess the chemotactic response and surface colonization of *E. coli* to SCFAs, we employed the transwell assay with three main SCFAs produced in the GI tract (acetate, butyrate

and propionate). Different concentrations of SCFAs were introduced into the inserts and a stable gradient was formed inside the cell containing reservoirs as described in our prior work[242]. As shown in **Figure 5. 1**, number of cells attached to 5 mM acetate was decreased compared to the motility buffer control. With 10 mM and 20 mM acetate in the inserts, less cells tended to swim near acetate rich surfaces, and the repellent response increased with increasing concentration. Similar results were also observed for butyrate and propionate (**Figure 5. 1**).

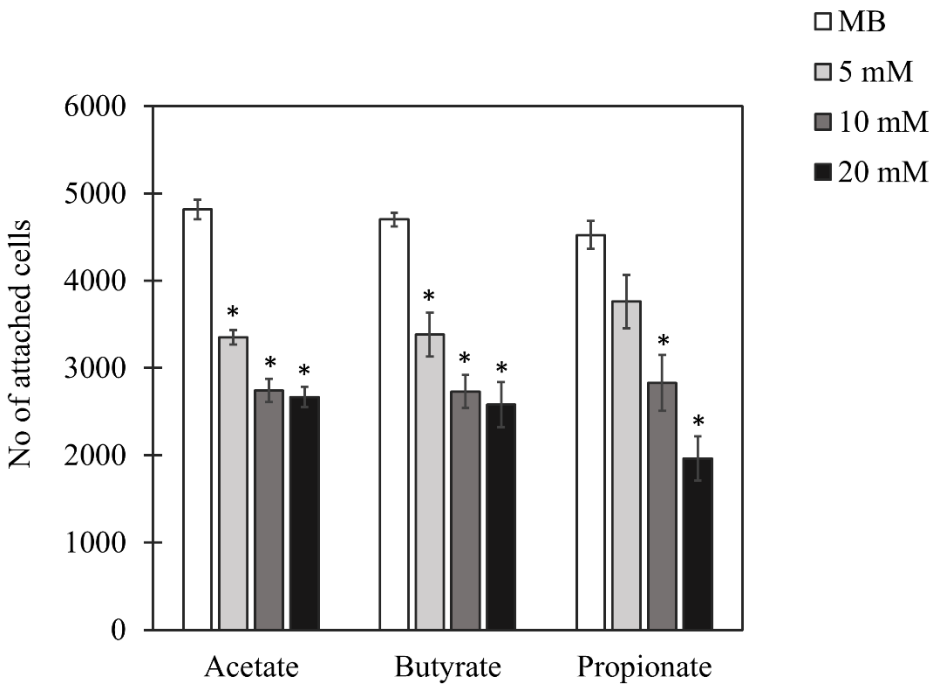


**Figure 5. 1 Wild-type *E. coli* response to SCFAs in the transwell assay.** Different concentrations of SCFAs were introduced in the transwell inserts. The number of attached cells were quantified. * indicates statistically significant difference ($p < 0.05$ using the student t-test).

### 5.3.2 *E. coli* RP437 senses SCFAs as attractants when pre-primed in indole

Since *E. coli* produces indole, they are likely to be pre-adapted to indole in the GI tract. In order to investigate the integrated response of *E. coli* to SCFA and indole, cells were first primed for 5 minutes with 0.7 mM indole, the concentration that we previously observed as a threshold

that bifurcated the cell population based on their position in an indole gradient (228). Primed cells were then introduced in the reservoirs and brought contact with SCFA-soaked agarose pads. To establish only a SCFA gradient in the wells, 0.7 mM indole was introduced in the transwell inserts. Control experiments were done without adding SCFAs to the inserts while keeping the concentration of indole the same in the well and in the insert.

The number of attached cells with SCFAs was normalized to the control (relative attachment) and are shown in **Figure 5. 2**. *E. coli* cells exhibited a repellent response to different concentrations of acetate in the absence of indole priming, as indicated by the negative relative attachment (**Figure 5. 2 left panel**). However, when cells were pre-adapted in 0.7 mM indole, the response to acetate was inverted, as compared to unprimed cells. More cells migrated towards the acetate-rich region with priming, although the swimming speed was reduced with indole priming (data not shown). While indole priming inverted the repellent response to acetate at all three concentrations (5, 10, and 20 mM) tested, the relative attachment at only 10 mM and 20 mM acetate were statistically significant (**Figure 5. 2 left panel**).

A repellent response to butyrate and propionate was observed with unprimed *E. coli*, while the response of *E. coli* primed with indole to butyrate and propionate were different from that observed with acetate. Indole priming reduced the extent of repellent chemotactic response to butyrate at 10 mM and 20 mM; however, an attractant response was not observed at these concentrations (**Figure 5. 2 middle panel**). With propionate, a clear inversion from repellent to attractant response was observed at 20 mM (**Figure 5. 2 right panel).** Although the responses at 5 mM and 10 mM propionate were not significant, the inversion from repellent to attractant response was still observed (**Figure 5. 2 right panel)**.

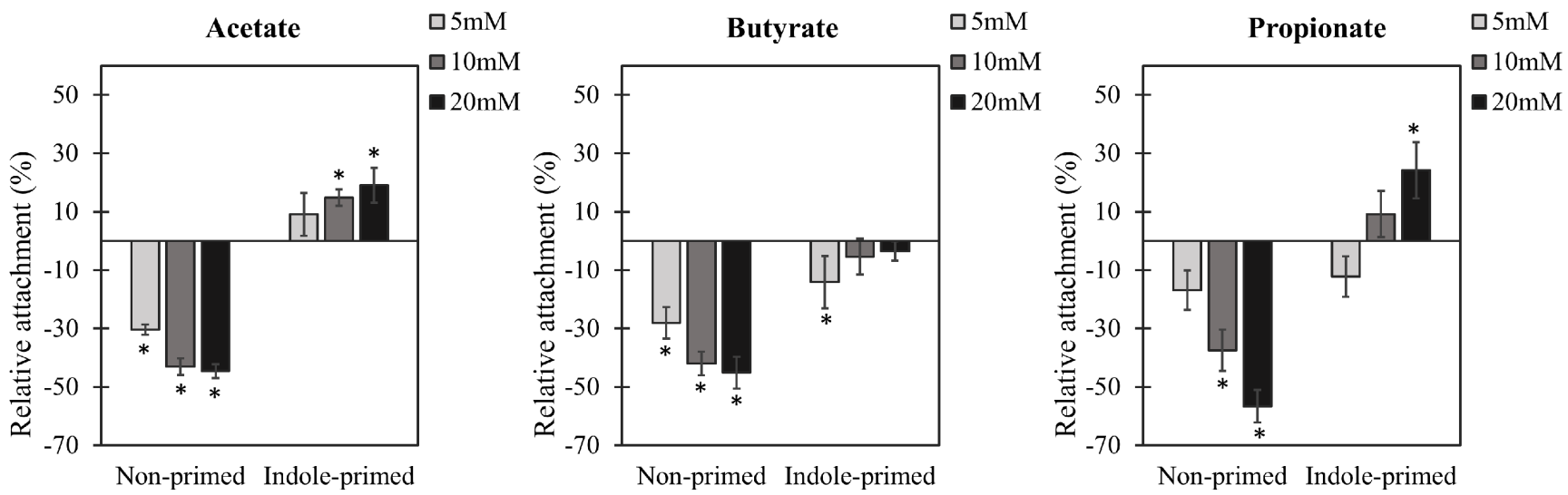


**Figure 5. 2 Wild-type *E. coli* response to SCFAs in the transwell assay.** Different concentrations of SCFAs were introduced in the transwell inserts with or without indole priming, and the number of attached cells were quantified. The response to acetate (left), Butyrate (middle), and propionate (209) with or without 0.7 mM indole priming in the transwell assays are shown. The ordinate axes show the percentage difference in cell attachment to SCFA containing agar relative to the control attachment. * indicates statistically significant difference in cell attachment relative to the control ($p < 0.05$ using the student t-test).

### 5.3.3 Tsr contributes the repellent response to acetate in the wild-type cells without indole priming

We used the tethered cell experiment to investigate the mechanisms underlying the chemotaxis response to both SCFA and indole. These studies were carried out in wild-type and *tsr/tar* mutant *E. coli* using acetate as the model SCFA since it is the most abundant SCFA in the gut, a well-studied signal for weak acid taxis[165], and elicited the highest inversion from repellent to attractant response in *E. coli* primed with indole. In the wild-type cells, acetate elicited an increase in CWbias, indicating a repellent response at the tested concentrations (5 mM and 10 mM) (**Figure 5. 3 left panel)**. The repellent response was followed by an "overshoot" for approximately 20 seconds, after which the CWbias returned to pre-stimulus levels.

With the *tar*-only mutant (Δ *tsr*), acetate elicited an attractant response upon stimulation and adapted after 50 seconds (**Figure 5. 3 middle panel**). With the *tsr*-only strain (Δ *tar*), acetate elicited a repellent response at 5 mM and 10 mM, and quickly adapted back (**Figure 5. 3 right panel**). The "overshoot" in CWbias was also observed with the mutant strains. Similar results were observed in the transwell assays with 20 mM acetate (**Figure 5. 4**), with more cells attached to acetate-rich surfaces with *tar*-only cells and less with *tsr*-only cells. For the *tsrtar* double mutant, no significant responses to acetate were observed (**Figure 5. 4**), suggesting only Tsr and Tar are responsible for sensing acetate, and the repellent response in wild-type cells is likely due to the Tsr receptor.

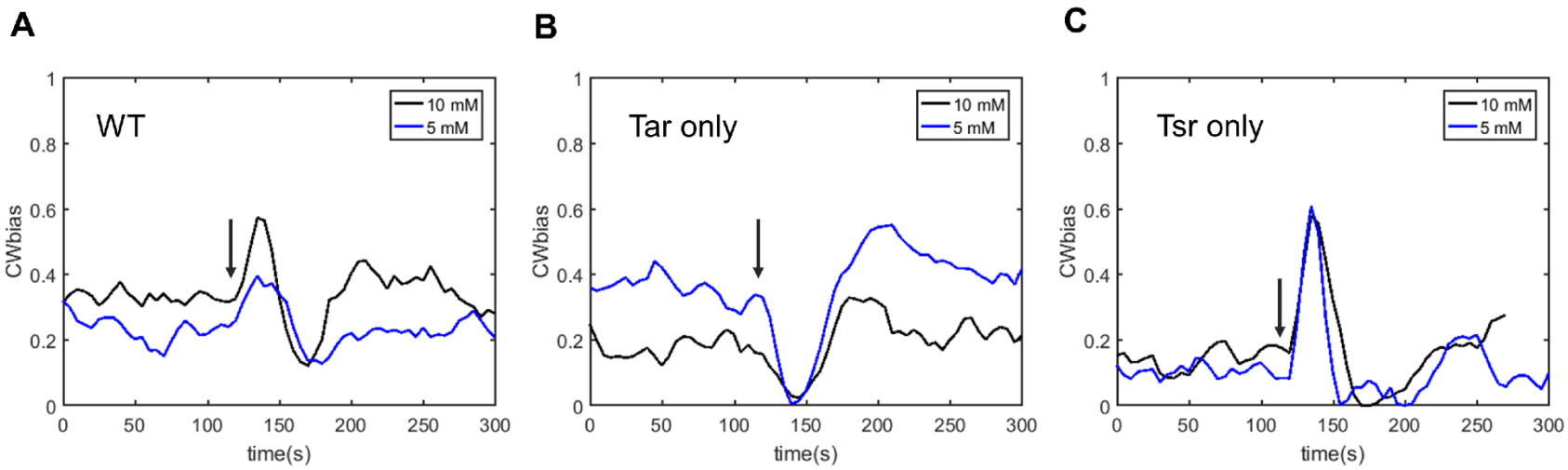


**Figure 5. 3 *E. coli* response to acetate in the tethered cell assay.** The CWbias response to 5 mM (blue lines) and 10 mM acetate (black lines) were tested. Response of A. wild-type strain, B. *tar*-only mutant (Δ *tsr*), and C. *tsr*-only mutant (Δ *tar*) are shown. Arrow indicates the start of acetate perfusion.

### 5.3.4 Tar dominates the attractant response to acetate in wild-type *E. coli* primed with indole

We tested the chemotaxis response of wild-type *E. coli* to acetate primed with indole (**Figure 5. 5 left panel)**. Stimulation of cells with acetate (5 and 10 mM) after exposure to indole resulted in a decrease in the CWbias, which indicated an attractant response to acetate. This was in contrast to the response without indole priming which resulted in a repellent response (see **Figure 5. 3 left panel**). Since there was no indole gradient, the observed attractant response can be attributed as the response to acetate with indole priming.

We also determined the response of behavior of *tsr*-only and *tar*-only mutants under same conditions (priming with indole, followed by exposure to acetate). Interestingly, priming with indole did not affect the response to acetate. *E. coli* with only Tar (Δ *tsr*) showed an attractant response when exposed to acetate after indole priming (**Figure 5. 5 middle panel)**, which was similar to that observed without indole priming (**Figure 5. 3 middle panel**). Similarly, *E. coli* with only Tsr (Δ *tar*) showed a repellent response to acetate, irrespective of whether cells were pre-exposed to indole or not (**Figure 5. 5 right panel)**. But the "overshoot" phenomenon that was observed in the absence of indole priming was not observed with indole priming.

We also investigated the response of wild-type, Δ *tar*, and Δ *tar E. coli* to 20 mM acetate with indole priming using the transwell assay. The response to acetate (both direction and magnitude of response) in all three cases was similar, irrespective of whether cells were primed with indole or not (**Figure 5. 5**). These results suggest that the attractant response observed with wild-type *E. coli* with indole priming is likely mediated by the Tar receptor.

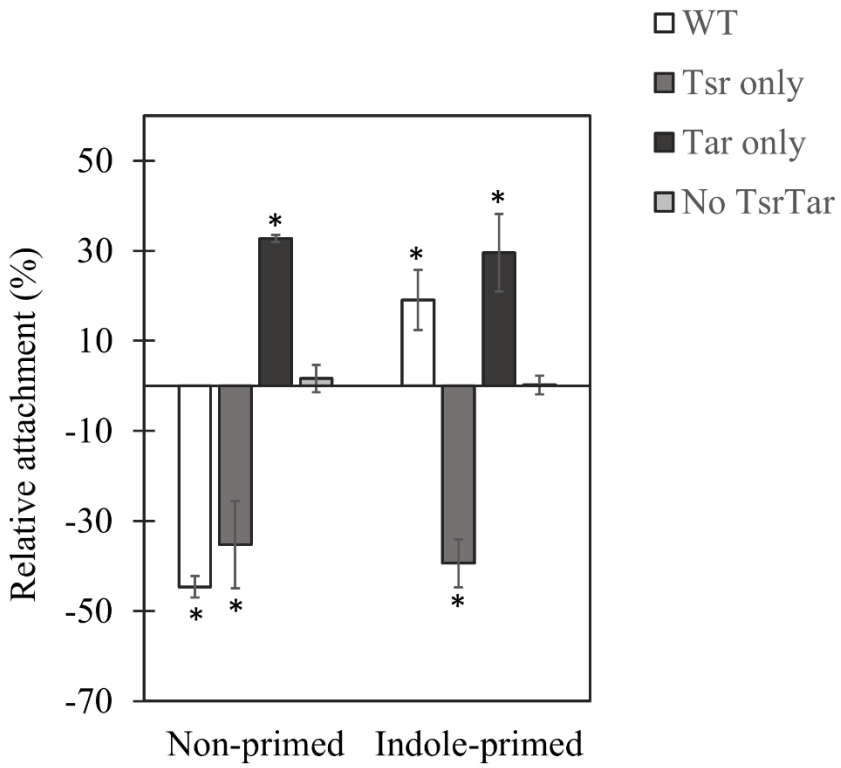


**Figure 5. 4 Chemotaxis response of *E. coli* to to 20 mM acetate with or without 0.7 mM indole priming in the transwell assay.** The ordinates reflect the percentage difference in cell attachment to acetate containing agar relative to that observed with the control. * indicates statistical significance ($p < 0.05$ using the student t-test).

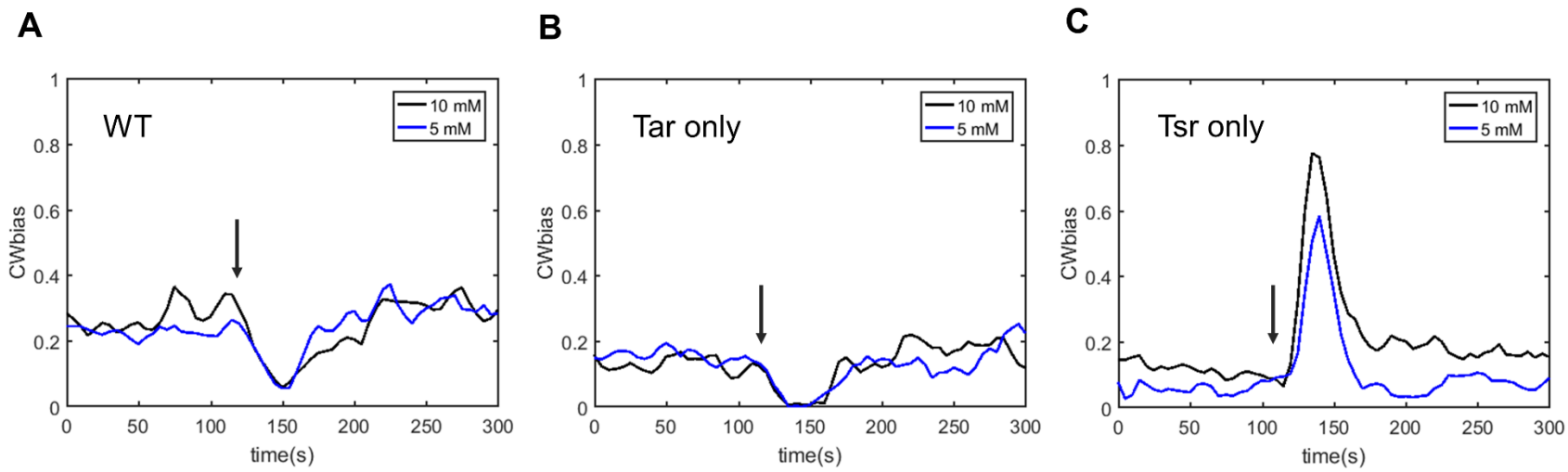


**Figure 5. 5 Chemotaxis response of *E. coli* to acetate with 0.7 mM priming in the tethered cell assay.** The CWbias response to 5 mM (blue lines) and 10 mM acetate (black lines) were tested. Response of A. wild-type strain, B. *tar*-only mutant (Δ *tsr*), and C. *tsr*-only mutant (Δ *tar*) are shown. Arrow indicates the start of acetate perfusion.

## 5.4 Discussion

Several studies have focused on investigating the role of microbial metabolites on host responses and function (236, 237), and the potential role of microbial metabolites in directing bacterial colonization in the GI tract have not been extensively investigated. Since it is challenging to visualize the microbiota and investigate chemotaxis *in vivo,* the link between chemotaxis and microbial community formation has only been indirectly investigated (45, 48, 241). Moreover, a majority of these studies have investigated the effect of a single molecule (e.g., list a few with references) on bacterial chemotaxis. In this work, we investigated the effect of sequential exposure to two microbial metabolites on *E. coli* chemotaxis and colonization. Our results showing that the repellent response to SCFAs can be either completely reversed or attenuated if cells are pre-exposed to indole clearly demonstrates the importance of signal integration in the formation of bacterial niches in microbial communities.

Indole and SCFAs are abundant molecules in the GI tract and are also sensed by the model strain *E. coli* RP437 as chemoeffectors and elicit a repellent response (27). We recently demonstrated that indole can also be sensed as an attractant at concentrations higher than 0.7 mM when *E. coli* is pre-exposed to indole (228). In this study, we demonstrate that a similar biphasic response or inversion of the repellent response is observed in *E. coli* for SCFAs as well. However, in contrast to indole, the biphasic response to acetate is not concentration-dependent but observed when *E. coli* is exposed to 0.7 mM indole prior to SCFAs. This observation was true for the three SCFAs tested in this study, although the butyrate did not elicit a clear inversion of the repellent response, as was observed for acetate and propionate at 20 mM. These results indicate that cells that naturally exposed to indole have a tendency to migrate toward SCFA rich area. This is

contrasted with previous conclusion that SCFA have antimicrobial effect that tend to eliminate bacteria around (162, 163, 172).

*E. coli* is a known indole producer in the GI tract, although it is a not a dominant member of the microbial community in healthy hosts (52, 133). It has been shown that the abundance of *E. coli* can expand when the community is perturbed by environmental factors such as seasons, temperature, living area, and antibiotic treatment (242, 243), and together with increased indole production (198). Thus, it is intriguing to speculate that the chemotactic response to indole might play a role in the expansion of *E. coli* (or other indole-producing bacteria) inside the intestinal tract and promote the formation of communities enriched in these bacteria, especially when in the presence of other abundant metabolites such as SCFAs. Multiple anaerobic bacteria that are present in the GI tract are known to produce SCFAs, and some of them are known to be motile (45, 46, 241), including species from the genera *Clostridium*, *Roseburia*, and *Eubacterium*. Thus, it is also possible that the abundance of these genera could increase if they have the molecular machinery to sense indole.

The *E. coli* chemotaxis network is well characterized in terms of the proteins involved in signal transduction and the molecules that can be sensed. While attractant chemotaxis has been well described, mechanisms underlying the sensing of chemorepellents and other non-canonical signals are not fully understood. Our previous study showed that both Tsr and Tar are involved in indole sensing through the chemotaxis network (228) and contribute to repellent and attractant taxis, respectively. We also identified (see **Chapter 4**) that indole is sensed through the Tsr periplasmic domain as repellent and the Tar periplasmic domain as attractant. In addition, the Tar cytoplasmic domain including HAMP and MH bundle also mediate the attractant response to indole. For SCFAs, a previous study showed that acetate is sensed through modulation of the

cytoplasmic pH and three amino acid residues linking the HAMP and MH bundle of Tsr and Tar are responsible for sensing the change in pH. In our study, we have shown that acetate elicits repellent response in *tsr*-only cells and attractant response in *tar*-only cells. Pre-priming with indole did not invert or decrease cells responses to acetate in the two mutants (**Figure 5. 3 and 5. 5**). However, indole priming inverted the response to acetate in the wild-type *E. coli*. Acetate is sensed by wild-type cells as a repellent, which is likely mediated by Tsr. It is possible that the Tar-mediated attractant response is masked by the repellent response, and priming cells with indole brings out the Tar-mediated attractant response in wild-type cells. Such differential sensing occurs when both Tsr and Tar are present at physiological levels in the receptor patch (**Figure 5. 6**).

The cross-talk between Tsr and Tar as well as the affinity of indole to the two receptors likely determines the receptor that is engaged by indole. Prior work by Sourjik *et al*. has characterized the mechanisms in external pH taxis in *E. coli* RP437 (127). Similar to the chemotactic response to the change of cytoplasmic pH, Tsr and Tar oppositely sense the change of external pH and cooperatively regulate cell response to an external pH gradient. This bidirectional tuning is partially achieved through the methylation level of Tsr and Tar depending on the ambient pH. At acidic pH, Tsr has fewer methylated glutamyl residues thus has higher sensitivity to changes in pH. Therefore Tsr dominates the response to the increase of pH and causes the cells to migrate towards higher pH values. At basic pH, Tar is less methylated and dominates the response to the decrease of pH, causing the cells to swim towards lower pH values. As a result, this push-pull mechanisms enables *E. coli* cells to accumulate at their optimal pH value. Another contributing factors in this bidirectional tuning is the relative ratio of Tsr and Tar receptors. When cells were grown to an $OD_{600}$ of 0.2, Tar/Tsr ratio was around 0.5. The ratio was around 1.2 at $OD_{600}$ of 0.8. Since more Tar receptors were express at OD 0.8, the cells were more sensitive to

the decrease of pH. In our study with acetate, although we did not fully characterize the effect of receptor methylation level and Tar/Tsr expression ratio on the cell responses, the mechanisms underlying cell response to acetate might similar to that of response to external pH. However, the response to acetate in the cells that are pre-primed in indole is more complicated. Although indole priming was expected to change the methylation level of Tsr and Tar, it did not desensitize the receptors to acetate. In *tsr*-only cells, indole would elicit a repellent response that leads to stimulation of CheA kinase activity. When adapted, the chemoreceptors receptors would be demethylated and hence become less sensitive to additional repellent stimuli. Similarly, with *tar*-only cells, indole would result in an increase in receptor methylation and hence be less responsive or sensitive to further stimulation with chemoattractants. However, we did not observe such behavior in our priming experiments, in which pre-primed *tsr*- and *tar*-only cells responded to acetate with the same extent compared with un-primed conditions. The level of Tsr and Tar and their affinity to acetate might be more important and in the inverted response to acetate in wild-type *E. coli* when primed indole. A previous study from Soujik *et al.* suggested cooperativity between Tsr and Tar and showed that serine/aspartate binding to one receptor affects the affinity of the other receptor to the ligands (239, 244). However, it must be noted Tsr-Tar cooperativity has been almost exclusively described based on the sensing of attractants such as serine and aspartate. Further studies are required to investigate receptor cooperativity with biphasic signals such as acetate and indole. It is likely that indole interacting with one type of receptor changes the affinity of the other receptor to acetate. For example, Tsr interacting with indole possibly increases the affinity of Tar in sensing acetate. As a result, priming wild-type cells with indole promotes Tar mediated attractant response to acetate.

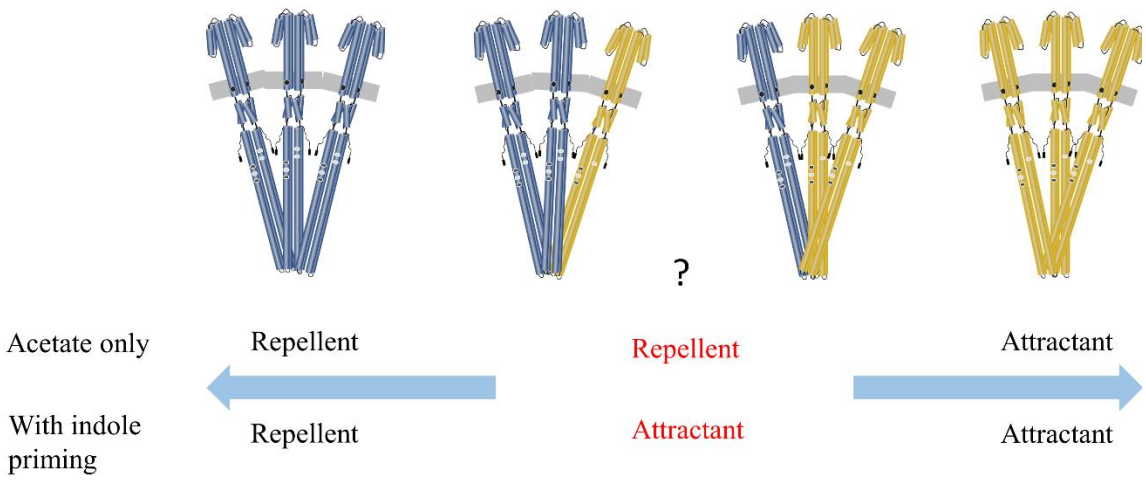


**Figure 5. 6 The integrated response of indole and acetate in cells with different Tsr/Tar level.** Blue receptor indicates Tsr and Yellow receptor indicate Tar.

Understanding the mechanistic basis of the chemotactic responses to a combination of different microbial signals might help us to elucidate the migration behavior of bacteria in the complex environment of the intestinal tract. Motile bacteria from its original niches possibly senses multiple cues and searches for sites to colonize, thus promotes formation of new microbial community. This process could be modulated by tuning the production of microbial metabolites like indole and acetate. Therefore, the disturbance of gut homeostasis would result in the change of microbial metabolite profiles, which in turn modulate microbial communities.

# CHAPTER VI

# SUMMARY AND FUTURE DIRECTIONS

Prior studies have shown that microbial metabolites play key roles in modulating the formation of microbial communities and pathogen infections (236, 237). Our results shed light on potential role for microbial metabolites in bacterial chemotaxis, which directly impacts both microbial community formation and pathogen colonization.

Using the model stain *E. coli* RP437, we investigated the chemotaxis response of bacteria to the microbial metabolite indole. We elucidated the role of different *E. coli* chemoreceptors in sensing indole and identified the key subunits within chemoreceptors that are involved. Tsr and Tar, as two dominant chemoreceptors in *E. coli*, oppositely sense indole and mediate chemotactic responses in a concentration-dependent manner. The differential binding affinity of indole to the two receptors likely results in a biphasic response. At low concentrations of indole, Tsr dominates and results in repellent response to indole, while at higher concentrations of indole, cells show attractant response to indole through the Tar receptor. This biphasic response to indole also directs the swimming behavior of wild-type *E. coli* cells in an indole gradient. Using a transwell assay, we generated an indole gradient that simulated the indole gradient likely generated in the microenvironment surrounding indole producing microbial communities. When introduced into this gradient, *E. coli* was repelled by indole, unless they were previously adapted to 0.7 mM indole. Based on these observations, we proposed a model describing the potential role of indole in maintaining microbial communities through modulation of bacterial chemotaxis. Using hybrid Tsr/Tar receptors, we characterized the function of each subunit in Tsr and Tar in sensing indole. We found that the periplasmic domain of the Tsr is essential to sense indole as a

repellent, while Tar's periplasmic domain sense indole as an attractant. Interestingly, Tar's cytoplasmic region, including HAMP domain and MH/KC region also mediate attractant signaling in indole sensing.

While our studies elucidated how indole mediates the chemotaxis behavior of non-pathogenic *E. coli*, it would also be worthwhile to investigate the chemotactic response of pathogenic *E. coli* strains to indole. Preliminary results of the transwell assay suggest that a pathogenic enterohemorrhagic strain *E. coli* O157:H7 (EHEC) exhibits a different chemotaxis response to indole compared with the non-pathogenic *E. coli* strain used in this study. EHEC cells were repelled by 2 mM indole no matter what concentrations they were pre-primed in, while *E. coli* RP437 cells were attracted toward 2 mM indole when pre-primed in 0.7 mM and 1 mM indole. Given that the Tsr and Tar receptors play a key role in biphasic indole sensing, a systematic analysis of Tsr/Tar expression levels in the different *E. coli* strains is needed to understand the different responses to indole.

Since the GI tract environment is a complex ecosystem with hundreds of species and their metabolite products, any organism in the GI tract is likely to be exposed to more than a single signaling molecule. Therefore, we further extended our model by introducing SCFAs as a second class of putative chemotaxis ligands and investigated the integrated effect of indole and SCFAs in modulating chemotaxis. We found that although adapting cells to SCFAs didn't alter the repellent response to indole, pre-adapting cells to indole switched the response to SCFAs from repellent to an attractant response. While pre-adapting cells to indole decrease the cell response to higher concentration of indole in Tsr/Tar mutant cells, we didn't observe the phenomenon in Tsr/Tar mutant strains in SCFA responses, which indicates that preadaptation to indole saturated the receptors for more indole binding but did not prevent SCFA binding. Also, the switch in

chemotaxis response to SCFAs with indole priming was observed only in wild-type cells and not in Tsr- or Tar-only mutants, suggesting that Tsr and Tar might cooperatively mediate the chemotaxis response to SCFAs when cells are pre-adapted to indole. Therefore, the response of *E. coli* to SCFA with indole pre-adaptation needs to be examined with different expression levels of Tsr/Tar so that the relationship between receptor cooperativity and integrated chemotaxis response to multiple stimuli can be systematically investigated.

It is intriguing to speculate if the phenomenon of inverted or switched *E. coli* chemotaxis response is limited to indole and SCFAs, or is a more generalized phenomenon that affects responses that are inherently sensed oppositely by Tsr and Tar (i.e., bidirectional stimuli). Future studies investigating the effect of indole with other repellents such as leucine, phenol, and external pH can lead to a better understanding of integrated repellent signaling in *E. coli*.

The molecular mechanisms underlying repellent sensing in *E. coli* is poorly understood; therefore, mechanistic studies on the interaction of indole with specific residues in different chemoreceptors can help better understand repellent sensing mechanisms in *E. coli*. Such mechanistic studies of bacterial chemotaxis would also provide additional evidence in support of the connection between bacterial chemotaxis and colonization in the gut. It would be interesting to elucidate how bacteria process simultaneous exposure to multiple attractant and repellent cues, and integrate them to swim through the mucus in the GI tract. Moreover, determining if the chemotaxis response to a few classes of signals dominates the response to other signals can help in developing novel approaches for controlling bacterial colonization in the GI tract.

While our studies were carried out in non-pathogenic *E. coli*, they can be extended to commensals and pathogenic bacteria. The role of motility and chemotaxis ability in commensals such as *Clostridium*, *Roseburia*, *Lactobacillus*, and *Eubacterium* have are being increasingly

studied (48, 120). Similarly, motility and chemotaxis systems have also been described in multiple pathogens including *S. enterica*, *H. pylori*, EHEC, and *C. jejuni* (23, 61, 62). Understanding the role of chemotaxis in these organisms will help understanding the role of the GI tract microbial community in health and disease.

REFERENCES


1. Ley, R.E., D.A. Peterson, and J.I. Gordon, *Ecological and evolutionary forces shaping microbial diversity in the human intestine.* Cell, 2006. **124**: p. 837-848.
2. Bäckhed, F., R.E. Ley, J.L. Sonnenburg, D.A. Peterson, and J.I. Gordon, *Host-bacterial mutualism in the human intestine*, in *Science*. 2005.
3. Eckburg, P.B., E.M. Bik, C.N. Bernstein, E. Purdom, L. Dethlefsen, M. Sargent, . . . D.A. Relman, *Diversity of the Human Intestinal Microbial Flora.* Science, 2005. **308**: p. 1635-1638.
4. Valdes, A.M., J. Walter, E. Segal, and T.D. Spector, *Role of the gut microbiota in nutrition and health.* BMJ (Online), 2018.
5. Hooper, L.V. and J.I. Gordon, *Commensal host-bacterial relationships in the gut*, in *Science*. 2001.
6. Makki, K., E.C. Deehan, J. Walter, and F. Bäckhed, *The Impact of Dietary Fiber on Gut Microbiota in Host Health and Disease.* Cell Host and Microbe, 2018. **23**: p. 705-715.
7. Round, J.L. and S.K. Mazmanian, *The gut microbiota shapes intestinal immune responses during health and disease*, in *Nature Reviews Immunology*. 2009.
8. Sekirov, I. and B.B. Finlay, *The role of the intestinal microbiota in enteric infection*, in *Journal of Physiology*. 2009.
9. CDCP, *Foodborne Germs and Illness.* Food Safety, 2019.
10. O'Brien, A.D. and K.L. Mohawk, *Mouse models of escherichia coli O157:H7 infection and shiga toxin injection*, in *Journal of Biomedicine and Biotechnology*. 2011.

11. Kaper, J.B., J.P. Nataro, and H.L.T. Mobley, *Pathogenic Escherichia coli*, in *Nature Reviews Microbiology*. 2004.

12. Huttenhower, C., D. Gevers, R. Knight, S. Abubucker, J.H. Badger, A.T. Chinwalla, . . . O. White, *Structure, function and diversity of the healthy human microbiome.* Nature, 2012.

13. Loirat, C., J. Saland, and M. Bitzan, *Management of hemolytic uremic syndrome*, in *Presse Medicale*. 2012.

14. Phillips, A., S. Navabpour, S. Hicks, G. Dougan, T. Wallis, and G. Frankel, *Enterohaemorrhagic Escherichia coliO157: H7 target Peyer's patches in humans and cause attaching/effacing lesions in both human and bovine intestine.* Gut, 2000. **47**(3): p. 377-381.

15. Torres, A.G. and J.B. Kaper, *Multiple elements controlling adherence of enterohemorrhagic Escherichia coli O157: H7 to HeLa cells.* Infection and immunity, 2003. **71**(9): p. 4985-4995.

16. Ottemann, K.M. and J.F. Miller, *Roles for motility in bacterial-host interactions.* Molecular Microbiology, 1997. **24**: p. 1109-1117.

17. Josenhans, C. and S. Suerbaum, *The role of motility as a virulence factor in bacteria.* International Journal of Medical Microbiology, 2002.

18. Liu, Z., Y. Wang, S. Liu, Y. Sheng, K.-G. Rueggeberg, H. Wang, . . . B. Kan, *Vibrio cholerae represses polysaccharide synthesis to promote motility in mucosa.* Infection and immunity, 2015. **83**(3): p. 1114-1121.

19. Ottemann, K.M. and A.C. Lowenthal, *Helicobacter pylori uses motility for initial colonization and to attain robust infection.* Infection and immunity, 2002. **70**(4): p. 1984-1990.

20. Stecher, B., S. Hapfelmeier, C. Müller, M. Kremer, T. Stallmach, and W.D. Hardt, *Flagella and chemotaxis are required for efficient induction of Salmonella enterica serovar typhimurium colitis in streptomycin-pretreated mice.* Infection and Immunity, 2004. **72**: p. 4138-4150.

21. Pasupuleti, S., N. Sule, W.B. Cohn, D.S. MacKenzie, A. Jayaraman, and M.D. Manson, *Chemotaxis of Escherichia coli to norepinephrine (NE) requires conversion of NE to 3,4-dihydroxymandelic acid.* Journal of Bacteriology, 2014. **196**: p. 3992-4000.

22. Tobe, T., N. Nakanishi, and N. Sugimoto, *Activation of motility by sensing short-chain fatty acids via two steps in a flagellar gene regulatory cascade in enterohemorrhagic Escherichia coli.* Infection and Immunity, 2011.

23. Rivera-Chávez, F., C.A. Lopez, L.F. Zhang, L. García-Pastor, A. Chávez-Arroyo, K.L. Lokken, . . . A.J. Bäumler, *Energy taxis toward host-derived nitrate supports a salmonella pathogenicity island 1-independent mechanism of invasion.* mBio, 2016. **7**.

24. Li, Z., H. Lou, D.M. Ojcius, A. Sun, D. Sun, J. Zhao, . . . J. Yan, *Methyl-accepting chemotaxis proteins 3 and 4 are responsible for Campylobacter jejuni chemotaxis and jejuna colonization in mice in response to sodium deoxycholate.* Journal of Medical Microbiology, 2014. **63**: p. 343-354.

25. Pacheco, A.R., D. Munera, M.K. Waldor, V. Sperandio, and J.M. Ritchie, *Fucose sensing regulates bacterial intestinal colonization*, in *Nature*. 2012.

26. Kohli, N., Z. Crisp, R. Riordan, M. Li, R.C. Alaniz, and A. Jayaraman, *The microbiota metabolite indole inhibits Salmonella virulence: Involvement of the PhoPQ two-component system.* PLoS ONE, 2018. **13**: p. e0190613.

27. Tso, W.W. and J. Adler, *Negative chemotaxis in Escherichia coli.* Journal of Bacteriology, 1974. **118**: p. 560-576.

28. Bansal, T., D. Englert, J. Lee, M. Hegde, T.K. Wood, and A. Jayaraman, *Differential effects of epinephrine, norepinephrine, and indole on Escherichia coli O157:H7 chemotaxis, colonization, and gene expression.* Infection and Immunity, 2007.

29. Lee, J., C. Attila, S.L.G.G. Cirillo, J.D. Cirillo, and T.K. Wood, *Indole and 7-hydroxyindole diminish Pseudomonas aeruginosa virulence.* Microbial Biotechnology, 2009.

30. Lee, J.H. and J.H. Lee, *Indole as an intercellular signal in microbial communities*, in *FEMS Microbiology Reviews*. 2010.

31. Cummings, J.H., E.W. Pomare, H.W.J. Branch, C.P.E. Naylor, and G.T. MacFarlane, *Short chain fatty acids in human large intestine, portal, hepatic and venous blood.* Gut, 1987.

32. Kumar, A. and V. Sperandio, *Indole signaling at the host-microbiota-pathogen interface.* mBio, 2019. **10**.

33. Macfarlane, G.T., G.R. Gibson, and J.H. Cummings, *Comparison of fermentation reactions in different regions of the human colon.* Journal of Applied Bacteriology, 1992.

34. Lyte, M., B. Arulanandam, K. Nguyen, C. Frank, A. Erickson, and D. Francis, *Norepinephrine induced growth and expression of virulence associated factors in*

*enterotoxigenic and enterohemorrhagic strains of Escherichia coli.* Advances in Experimental Medicine and Biology, 1997.

35. Cogan, T.A., A.O. Thomas, L.E.N. Rees, A.H. Taylor, M.A. Jepson, P.H. Williams, . . . T.J. Humphrey, *Norepinephrine increases the pathogenic potential of Campylobacter jejuni.* Gut, 2007.
36. Nakano, M., A. Takahashi, Y. Sakai, and Y. Nakaya, *Modulation of Pathogenicity with Norepinephrine Related to the Type III Secretion System of Vibrio parahaemolyticus* The Journal of Infectious Diseases, 2007.
37. Pullinger, G.D., S.C. Carnell, F.F. Sharaff, P.M. Van Diemen, F. Dziva, E. Morgan, . . . M.P. Stevens, *Norepinephrine augments Salmonella enterica-induced enteritis in a manner associated with increased net replication but independent of the putative adrenergic sensor kinases QseC and QseE.* Infection and Immunity, 2010.
38. Simon, G.L. and S.L. Gorbach, *Intestinal flora in health and disease.* Gastroenterology, 1984. **86**: p. 174-193.
39. Neish, A.S., *Microbes in Gastrointestinal Health and Disease.* Gastroenterology, 2009. **136**: p. 65-80.
40. Hull, M.W. and A.W. Chow, *Indigenous Microflora and Innate Immunity of the Head and Neck.* Infectious Disease Clinics of North America, 2007. **21**: p. 265-282.
41. Chiller, K., B.A. Selkin, and G.J. Murakawa, *Skin Microflora and Bacterial Infections of the Skin.* Journal of Investigative Dermatology Symposium Proceedings, 2001. **6**: p. 170-174.

42. O'Hara, A.M. and F. Shanahan, *The gut flora as a forgotten organ.* EMBO Reports, 2006. **7**: p. 688.

43. Xu, J. and J.I. Gordon, *Honor thy symbionts.* Proceedings of the National Academy of Sciences, 2003. **100**: p. 10452-10459.

44. Zhang, Z., J. Geng, X. Tang, H. Fan, J. Xu, X. Wen, . . . P. Shi, *Spatial heterogeneity and co-occurrence patterns of human mucosal-associated intestinal microbiota.* ISME Journal, 2014.

45. Lozupone, C., K. Faust, J. Raes, J.J. Faith, D.N. Frank, J. Zaneveld, . . . R. Knight, *Identifying genomic and metabolic features that can underlie early successional and opportunistic lifestyles of human gut symbionts.* Genome Res., 2012. **22**: p. 1974-1984.

46. Cullender, T.C., B. Chassaing, A. Janzon, K. Kumar, C.E. Muller, J.J. Werner, . . . R.E. Ley, *Innate and adaptive immunity interact to quench microbiome flagellar motility in the gut.* Cell Host and Microbe, 2013. **14**: p. 571-581.

47. Verberkmoes, N.C., A.L. Russell, M. Shah, A. Godzik, M. Rosenquist, J. Halfvarson, . . . J.K. Jansson, *Shotgun metaproteomics of the human distal gut microbiota.* The ISME Journal 2009 3:2, 2008. **3**: p. 179-189.

48. Stanton, T.B. and D.C. Savage, *Motility as a factor in bowel colonization by Roseburia cecicola, an obligately anaerobic bacterium from the mouse caecum.* Journal of General Microbiology, 1984. **130**: p. 173-183.

49. *Escherichia coli at the Intestinal Mucosal Surface.* Virulence Mechanisms of Bacterial Pathogens, Fourth Edition, 2014: p. 175-196.

50. Laux, D.C., P.S. Cohen, and T. Conway, *Role of the Mucus Layer in Bacterial Colonization of the Intestine.* Colonization of Mucosal Surfaces, 2014: p. 199-212.

51. Foster, J.W., *Escherichia coli acid resistance: tales of an amateur acidophile.* Nature Reviews Microbiology 2004 2:11, 2004. **2**: p. 898-907.

52. Freter, R., H. Brickner, J. Fekete, M.M. Vickerman, and K.E. Carey, *Survival and implantation of Escherichia coli in the intestinal tract.* Infection and Immunity, 1983. **39**: p. 686-703.

53. Møller, A.K., M.P. Leatham, T. Conway, P.J.M. Nuijten, L.A.M. De Haan, K.A. Krogfelt, and P.S. Cohen, *An Escherichia coli MG1655 lipopolysaccharide deep-rough core mutant grows and survives in mouse cecal mucus but fails to colonize the mouse large intestine.* Infection and Immunity, 2003. **71**: p. 2142-2152.

54. McCormick, B.A., D.C. Laux, and P.S. Cohen, *Neither motility nor chemotaxis plays a role in the ability of Escherichia coli F-18 to colonize the streptomycin-treated mouse large intestine.* Infection and Immunity, 1990. **58**: p. 2957-2961.

55. Haiko, J. and B. Westerlund-Wikström, *The Role of the Bacterial Flagellum in Adhesion and Virulence.* Biology 2013, Vol. 2, Pages 1242-1267, 2013. **2**: p. 1242-1267.

56. Maki, N., J.E. Gestwicki, E.M. Lake, L.L. Kiessling, and J. Adler, *Motility and chemotaxis of filamentous cells of Escherichia coli.* Journal of Bacteriology, 2000. **182**: p. 4337-4342.

57. Scallan, E., R.M. Hoekstra, F.J. Angulo, R.V. Tauxe, M.-A. Widdowson, S.L. Roy, . . . P.M. Griffin, *Foodborne Illness Acquired in the United States—Major Pathogens.* Emerging Infectious Diseases, 2011. **17**: p. 7.

58. Matilla, M.A. and T. Krell, *The effect of bacterial chemotaxis on host infection and pathogenicity.* FEMS Microbiology Reviews, 2018. **42**: p. fux052.

59. ALLWEISS, B., J. DOSTAL, K.E. CAREY, T.F. EDWARDS, and R. FRETER, *The role of chemotaxis in the ecology of bacterial pathogens of mucosal surfaces.* Nature 1977 266:5601, 1977. **266**: p. 448-450.

60. Wuichet, K. and I.B. Zhulin, *Origins and Diversification of a Complex Signal Transduction System in Prokaryotes.* Science Signaling, 2010. **3**: p. ra50-ra50.

61. Williams, S.M., Y.T. Chen, T.M. Andermann, J.E. Carter, D.J. McGee, and K.M. Ottemann, *Helicobacter pylori chemotaxis modulates inflammation and bacterium-gastric epithelium interactions in infected mice.* Infection and Immunity, 2007. **75**: p. 3747-3757.

62. Chang, C. and J.F. Miller, *Campylobacter jejuni colonization of mice with limited enteric flora.* Infection and Immunity, 2006. **74**: p. 5261-5271.

63. Jani, S., A.L. Seely, G.L. Peabody V, A. Jayaraman, and M.D. Manson, *Chemotaxis to self-generated AI-2 promotes biofilm formation in Escherichia coli.* Microbiology (United Kingdom), 2017. **163**: p. 1778-1790.

64. Thar, R. and M. Kühl, *Bacteria are not too small for spatial sensing of chemical gradients: An experimental evidence.* Proceedings of the National Academy of Sciences of the United States of America, 2003.

65. Larsen, S.H., R.W. Reader, E.N. Kort, W.W. Tso, and J. Adler, *Change in direction of flagellar rotation is the basis of the chemotactic response in Escherichia coli.* Nature, 1974. **249**: p. 74-77.

66. Sourjik, V. and H.C. Berg, *Receptor sensitivity in bacterial chemotaxis.* Proceedings of the National Academy of Sciences of the United States of America, 2002.

67. Kim, C., M. Jackson, R. Lux, and S. Khan, *Determinants of chemotactic signal amplification in Escherichia coli.* Journal of Molecular Biology, 2001.

68. Shimizu, T.S., N. Le Novère, M.D. Levin, A.J. Beavil, B.J. Sutton, and D. Bray, *Molecular model of a lattice of signalling proteins involved in bacterial chemotaxis.* Nature Cell Biology, 2000.

69. Maddock, J.R. and L. Shapiro, *Polar location of the chemoreceptor complex in the Escherichia coli cell.* Science, 1993.

70. Borkovich, K.A., N. Kaplan, J.F. Hess, and M.I. Simon, *Transmembrane signal transduction in bacterial chemotaxis involves ligand-dependent activation of phosphate group transfer.* Proceedings of the National Academy of Sciences of the United States of America, 1989.

71. Welch, M., K. Oosawa, S.I. Aizawa, and M. Eisenbach, *Phosphorylation-dependent binding of a signal molecule to the flagellar switch of bacteria.* Proceedings of the National Academy of Sciences of the United States of America, 1993.

72. Toker, A.S. and R.M. Macnab, *Distinct regions of bacterial flagellar switch protein FliM interact with FliG, FliN and CheY.* Journal of Molecular Biology, 1997.

73. McEvoy, M.M., A. Bren, M. Eisenbach, and F.W. Dahlquist, *Identification of the binding interfaces on CheY for two of its targets, the phosphatase CheZ and the flagellar switch protein FliM.* Journal of Molecular Biology, 1999.

74. Springer, W.R. and D.E. Koshland, *Identification of a protein methyltransferase as the cheR gene product in the bacterial sensing system.* Proceedings of the National Academy of Sciences of the United States of America, 1977.

75. Kehry, M.R. and F.W. Dahlquist, *Adaptation in bacterial chemotaxis: CheB-dependent modification permits additional methylations of sensory transducer proteins.* Cell, 1982.

76. Kehry, M.R., T.G. Doak, and F.W. Dahlquist, *Sensory adaptation in bacterial chemotaxis: Regulation of demethylation.* Journal of Bacteriology, 1985.

77. Hess, J.F., R.B. Bourret, and M.I. Simon, *Histidine phosphorylation and phosphoryl group transfer in bacterial chemotaxis.* Nature, 1988.

78. Cluzel, P., M. Surette, and S. Leibler, *An ultrasensitive bacterial motor revealed by monitoring signaling proteins in single cells.* Science, 2000. **287**: p. 1652-1655.

79. Bray, D., M.D. Levin, and C.J. Morton-Firth, *Receptor clustering as a cellular mechanism to control sensitivity.* Nature, 1998.

80. Goldman, J.P., M.D. Levin, and D. Bray, *Signal amplification in a lattice of coupled protein kinases.* Molecular BioSystems, 2009. **5**: p. 1853-1859.

81. Falke, J.J. and G.L. Hazelbauer, *Transmembrane signaling in bacterial chemoreceptors*, in *Trends in Biochemical Sciences*. 2001.

82. Hazelbauer, G.L., P. Engstrom, and S. Harayama, *Methyl-accepting chemotaxis protein III and transducer gene trg.* Journal of Bacteriology, 1981.

83. Bibikov, S.I., A.C. Miller, K.K. Gosink, and J.S. Parkinson, *Methylation-independent aerotaxis mediated by the Escherichia coli Aer protein.* Journal of Bacteriology, 2004.

84. Ortega, Á., I.B. Zhulin, and T. Krell, *Sensory Repertoire of Bacterial Chemoreceptors.* Microbiology and Molecular Biology Reviews, 2017.

85. Kim, K.K., H. Yokota, and S.H. Kim, *Four-helical-bundle structure of the cytoplasmic domain of a serine chemotaxis receptor.* Nature, 1999.

86. Yeh, J.I., H.P. Biemann, G.G. Privé, J. Pandit, D.E. Koshland, and S.H. Kim, *High-resolution structures of the ligand binding domain of the wild-type bacterial aspartate receptor.* Journal of Molecular Biology, 1996.

87. Milburn, M.V., G.G. Privé, D.L. Milligan, W.G. Scott, J. Yeh, J. Jancarik, . . . S.H. Kim, *Three-dimensional structures of the ligand-binding domain of the bacterial aspartate receptor with and without a ligand.* Science, 1991.

88. Airola, M.V., K.J. Watts, A.M. Bilwes, and B.R. Crane, *Structure of Concatenated HAMP Domains Provides a Mechanism for Signal Transduction.* Structure, 2010.

89. Hulko, M., F. Berndt, M. Gruber, J.U. Linder, V. Truffault, A. Schultz, . . . M. Coles, *The HAMP Domain Structure Implies Helix Rotation in Transmembrane Signaling.* Cell, 2006.

90. Aravind, L. and C.P. Ponting, *The cytoplasmic helical linker domain of receptor histidine kinase and methyl-accepting proteins is common to many prokaryotic signalling proteins.* FEMS Microbiology Letters, 1999.

91. Parkinson, J.S., *Signaling Mechanisms of HAMP Domains in Chemoreceptors and Sensor Kinases.* Annual Review of Microbiology, 2010.

92. Kitanovic, S., P. Ames, and J.S. Parkinson, *Mutational analysis of the control cable that mediates transmembrane signaling in the Escherichia coli serine chemoreceptor.* J Bacteriol, 2011.

93. Coleman, M.D., R.B. Bass, R.S. Mehan, and J.J. Falke, *Conserved glycine residues in the cytoplasmic domain of the aspartate receptor play essential roles in kinase coupling and on-off switching.* Biochemistry, 2005.

94. Yang, W., C. Keith Cassidy, P. Ames, C.A. Diebolder, K. Schulten, Z. Luthey-Schulten, . . . A. Briegel, *In situ conformational changes of the escherichia coli serine chemoreceptor in different signaling states.* mBio, 2019.

95. Wu, J., J. Li, G. Li, D.G. Long, and R.M. Weis, *The receptor binding site for the methyltransferase of bacterial chemotaxis is distinct from the sites of methylation.* Biochemistry, 1996.

96. Hall, B.A., J.P. Armitage, and M.S.P. Sansom, *Transmembrane helix dynamics of bacterial chemoreceptors supports a piston model of signalling.* PLoS Computational Biology, 2011.

97. Yu, D., X. Ma, Y. Tu, and L. Lai, *Both piston-like and rotational motions are present in bacterial chemoreceptor signaling.* Scientific Reports, 2015.

98. Adase, C.A., R.R. Draheim, and M.D. Manson, *The residue composition of the aromatic anchor of the second transmembrane helix determines the signaling properties of the aspartate/maltose chemoreceptor tar of escherichia coli.* Biochemistry, 2012.

99. Manson, M.D., *Transmembrane signaling is anything but rigid,* in *Journal of Bacteriology*. 2011.

100. Ames, P., S. Hunter, and J.S. Parkinson, *Evidence for a Helix-Clutch Mechanism of Transmembrane Signaling in a Bacterial Chemoreceptor.* Journal of Molecular Biology, 2016.

101. Kitanovic, S., P. Ames, and J.S. Parkinson, *A trigger residue for transmembrane signaling in the Escherichia coli serine chemoreceptor.* Journal of Bacteriology, 2015.

102. Bi, S. and L. Lai, *Bacterial chemoreceptors and chemoeffectors*, in *Cellular and Molecular Life Sciences*. 2015.

103. Zhou, Q., P. Ames, and J.S. Parkinson, *Mutational analyses of HAMP helices suggest a dynamic bundle model of input-output signalling m chemoreceptors.* Molecular Microbiology, 2009.

104. Stewart, V., *The HAMP signal-conversion domain: Static two-state or dynamic three-state?*, in *Molecular Microbiology*. 2014.

105. Zhou, Q., P. Ames, and J.S. Parkinson, *Biphasic control logic of HAMP domain signalling in the Escherichia coli serine chemoreceptor.* Molecular Microbiology, 2011.

106. Swain, K.E., M.A. Gonzalez, and J.J. Falke, *Engineered socket study of signaling through a four-helix bundle: Evidence for a Yin-Yang mechanism in the kinase control module of the aspartate receptor.* Biochemistry, 2009.

107. Ames, P., Q. Zhou, and J.S. Parkinson, *HAMP domain structural determinants for signalling and sensory adaptation in Tsr, the Escherichia coli serine chemoreceptor.* Molecular Microbiology, 2014.

108. Lai, W.C., B.D. Beel, and G.L. Hazelbauer, *Adaptational modification and ligand occupancy have opposite effects on positioning of the transmembrane signalling helix of a chemoreceptor.* Molecular Microbiology, 2006.

109. Starrett, D.J. and J.J. Falke, *Adaptation mechanism of the aspartate receptor: Electrostatics of the adaptation subdomain play a key role in modulating kinase activity.* Biochemistry, 2005.

110. Briegel, A., D.R. Ortega, E.I. Tocheva, K. Wuichet, L. Zhuo, C. Songye, . . . G.J. Jensen, *Universal architecture of bacterial chemoreceptor arrays.* Proceedings of the National Academy of Sciences of the United States of America, 2009.

111. Briegel, A., M.L. Wong, H.L. Hodges, C.M. Oikonomou, K.N. Piasta, M.J. Harris, . . . G.J. Jensen, *New insights into bacterial chemoreceptor array structure and assembly from electron cryotomography.* Biochemistry, 2014.

112. Briegel, A., X. Li, A.M. Bilwes, K.T. Hughes, G.J. Jensen, and B.R. Crane, *Bacterial chemoreceptor arrays are hexagonally packed trimers of receptor dimers networked by rings of kinase and coupling proteins.* Proceedings of the National Academy of Sciences of the United States of America, 2012.

113. Hazelbauer, G.L., J.J. Falke, and J.S. Parkinson, *Bacterial chemoreceptors: high-performance signaling in networked arrays*, in *Trends in Biochemical Sciences*. 2008.

114. Shimizu, T.S., S.V. Aksenov, and D. Bray, *A spatially extended stochastic model of the bacterial chemotaxis signalling pathway.* Journal of Molecular Biology, 2003.

115. Parkinson, J.S., G.L. Hazelbauer, and J.J. Falke, *Signaling and sensory adaptation in Escherichia coli chemoreceptors: 2015 update*, in *Trends in Microbiology*. 2015.

116. Li, M. and G.L. Hazelbauer, *Core unit of chemotaxis signaling complexes.* Proceedings of the National Academy of Sciences of the United States of America, 2011.

117. Hazelbauer, G.L. and W.C. Lai, *Bacterial chemoreceptors: providing enhanced features to two-component signaling*, in *Current Opinion in Microbiology*. 2010.

118. Bi, S. and V. Sourjik, *Stimulus sensing and signal processing in bacterial chemotaxis*, in *Current Opinion in Microbiology*. 2018.

119. Mesibov, R. and J. Adler, *Chemotaxis toward amino acids in Escherichia coli.* Journal of Bacteriology, 1972. **112**: p. 315-326.

120. Tajima, H., K. Imada, M. Sakuma, F. Hattori, T. Nara, N. Kamo, . . . I. Kawagishi, *Ligand specificity determined by differentially arranged common ligand-binding residues in bacterial amino acid chemoreceptors Tsr and Tar.* Journal of Biological Chemistry, 2011. **286**: p. 42200-42210.

121. Hazelbauer, G.L., *Maltose chemoreceptor of Escherichia coli.* Journal of Bacteriology, 1975.

122. Hegde, M., D.L. Englert, S. Schrock, W.B. Cohn, C. Vogt, T.K. Wood, . . . A. Jayaraman, *Chemotaxis to the quorum-sensing signal AI-2 requires the Tsr chemoreceptor and the periplasmic LsrB AI-2-binding protein.* Journal of Bacteriology, 2011.

123. Manson, M.D., V. Blank, G. Brade, and C.F. Higgins, *Peptide chemotaxis in E. coli involves the Tap signal transducer and the dipeptide permease.* Nature, 1986.

124. Somavanshi, R., B. Ghosh, and V. Sourjik, *Sugar Influx Sensing by the Phosphotransferase System of Escherichia coli.* PLoS Biology, 2016.

125. Paulick, A., V. Jakovljevic, S. Zhang, M. Erickstad, A. Groisman, Y. Meir, . . . V. Sourjik, *Mechanism of bidirectional thermotaxis in Escherichia coli.* eLife, 2017.

126. Oleksiuk, O., V. Jakovljevic, N. Vladimirov, R. Carvalho, E. Paster, W.S. Ryu, . . . V. Sourjik, *Thermal robustness of signaling in bacterial chemotaxis.* Cell, 2011.

127. Yang, Y. and V. Sourjik, *Opposite responses by different chemoreceptors set a tunable preference point in Escherichia coli pH taxis.* Molecular Microbiology, 2012.

128. Martinez, K.A., *Cytoplasmic pH response to acid stress in individual cells of Escherichia coli and Bacillus subtilis observed by fluorescence ratio imaging microscopy.* Appl. Environ. Microbiol. **78**.

129. Kihara, M. and R.M. Macnab, *Cytoplasmic pH mediates pH taxis and weak-acid repellent taxis of bacteria.* Journal of Bacteriology. **145**: p. 1209-1221.

130. Lopes, J.G. and V. Sourjik, *Chemotaxis of Escherichia coli to major hormones and polyamines present in human gut.* ISME Journal, 2018. **12**: p. 2736-2747.

131. NEWTON, W.A. and E.E. SNELL, *CATALYTIC PROPERTIES OF TRYPTOPHANASE, A MULTIFUNCTIONAL PYRIDOXAL.* Proceedings of the National Academy of Sciences of the United States of, 1964.

132. Darkoh, C., C. Chappell, C. Gonzales, and P. Okhuysen, *A rapid and specific method for the detection of indole in complex biological samples.* Applied and Environmental Microbiology, 2015.

133. Han, T.H., J.H. Lee, M.H. Cho, T.K. Wood, and J.H. Lee, *Environmental factors affecting indole production in Escherichia coli.* Research in Microbiology, 2011. **162**: p. 108-116.

134. Kobayashi, A., H. Hirakawa, T. Hirata, K. Nishino, and A. Yamaguchi, *Growth phase-dependent expression of drug exporters in Escherichia coli and its contribution to drug tolerance.* Journal of Bacteriology, 2006.

135. Di Martino, P., R. Fursy, L. Bret, B. Sundararaju, and R.S. Phillips, *Indole can act as an extracellular signal to regulate biofilm formation of Escherichia coli and other indole-producing bacteria.* Canadian Journal of Microbiology, 2003.

136. Zarkan, A., S. Caño-Muñiz, J. Zhu, K. Al Nahas, J. Cama, U.F. Keyser, . . . D.K. Summers, *Indole Pulse Signalling Regulates the Cytoplasmic pH of E. coli in a Memory-Like Manner.* Scientific Reports, 2019. **9**: p. 3868.

137. Botsford, J.L. and R.D. DeMoss, *Catabolite repression of tryptophanase in Escherichia coli.* Journal of Bacteriology, 1971.

138. Wyeth, F.J.S., *The Effects of Acids, Alkalies, and Sugars on the Growth and Indole Formation of Bacillus coli.* Biochemical Journal, 1919.

139. Chimerel, C., C.M. Field, S. Piñero-Fernandez, U.F. Keyser, and D.K. Summers, *Indole prevents Escherichia coli cell division by modulating membrane potential.* Biochimica et Biophysica Acta - Biomembranes, 2012.

140. Hirakawa, H., M. Hayashi-Nishino, A. Yamaguchi, and K. Nishino, *Indole enhances acid resistance in Escherichia coli.* Microbial Pathogenesis, 2010.

141. Chant, E.L. and D.K. Summers, *Indole signalling contributes to the stable maintenance of Escherichia coli multicopy plasmids.* Molecular Microbiology, 2007.

142. Rossi, E., A. Cimdins, P. Lüthje, A. Brauner, Å. Sjöling, P. Landini, and U. Römling, *"It's a gut feeling"–Escherichia coli biofilm formation in the gastrointestinal tract environment*, in *Critical Reviews in Microbiology*. 2018.

143. Hirakawa, H., T. Kodama, A. Takumi-Kobayashi, T. Honda, and A. Yamaguchi, *Secreted indole serves as a signal for expression of type III secretion system translocators in enterohaemorrhagic Escherichia coli O157 : H7.* Microbiology, 2009.

144. Howard, M.F., X. Renee Bina, and J.E. Bina, *Indole inhibits ToxR regulon expression in Vibrio cholerae.* Infection and Immunity, 2019.

145. Bansal, T., R.C. Alaniz, T.K. Wood, and A. Jayaraman, *The bacterial signal indole increases epithelial-cell tight-junction resistance and attenuates indicators of inflammation.* Proceedings of the National Academy of Sciences of the United States of America, 2010.

146. Whitfield-Cargile, C.M., N.D. Cohen, R.S. Chapkin, B.R. Weeks, L.A. Davidson, J.S. Goldsby, . . . R.C. Alaniz, *The microbiota-derived metabolite indole decreases mucosal inflammation and injury in a murine model of NSAID enteropathy.* Gut Microbes, 2016.

147. Krishnan, S., Y. Ding, N. Saedi, M. Choi, G.V. Sridharan, D.H. Sherr, . . . K. Lee, *Gut Microbiota-Derived Tryptophan Metabolites Modulate Inflammatory Response in Hepatocytes and Macrophages.* Cell Reports, 2018.

148. Tsang, N., R. Macnab, and D.E. Koshland, *Common Mechanism for Repellents and Attractants in Bacterial Chemotaxis.* Science, 1973. **181**: p. 60-63.

149. Parkinson, J.S. and P.T. Revello, *Sensory adaptation mutants of E. coli.* Cell, 1978. **15**: p. 1221-1230.

150. Springer, M.S., M.F. Goy, and J. Adler, *Sensory transduction in Escherichia coli: Two complementary pathways of information processing that involve methylated proteins.* Proceedings of the National Academy of Sciences of the United States of America, 1977. **74**: p. 3312-3316.

151. Muskavitch, M.A., E.N. Kort, M.S. Springer, M.F. Goy, and J. Adler, *Attraction by repellents: An error in sensory information processing by bacterial mutants.* Science, 1978. **201**: p. 63-65.

152. Reader, R.W., W.-W.W. Tso, M.S. Springer, M.F. Goy, and J. Adler, *Pleiotropic aspartate taxis and serine taxis mutants of Escherichia coli.* Journal of General Microbiology, 1979. **111**: p. 363-374.

153. Montrone, M., D. Oesterhelt, and W. Marwan, *Phosphorylation-independent bacterial chemoresponses correlate with changes in the cytoplasmic level of fumarate.* Journal of Bacteriology, 1996. **178**: p. 6882-6887.

154. Topping, D.L., P.M. Clifton, T. DL, and C. PM, *Short-chain fatty acids and human colonic function: Roles of resistant starch and nonstarch polysaccharides*, in *Physiological Reviews*. 2001, Physiol Rev. p. 1031-1064.

155. McOrist, A.L., G.C.J. Abell, C. Cooke, and K. Nyland, *Bacterial population dynamics and faecal short-chain fatty acid (SCFA) concentrations in healthy humans.* British Journal of Nutrition, 2008.

156. Miller, T.L. and M.J. Wolin, *Pathways of acetate, propionate, and butyrate formation by the human fecal microbial flora.* Applied and Environmental Microbiology, 1996. **62**: p. 1589-1592.

157. Louis, P. and H.J. Flint, *Formation of propionate and butyrate by the human colonic microbiota.* Environmental Microbiology, 2017. **19**: p. 29-41.

158. Morrison, D.J. and T. Preston, *Formation of short chain fatty acids by the gut microbiota and their impact on human metabolism*, 2016. **7**: p. 189-200.

159. Louis, P. and H.J. Flint, *Diversity, metabolism and microbial ecology of butyrate-producing bacteria from the human large intestine.* FEMS Microbiology Letters, 2009. **294**: p. 1-8.

160. Derrien, M., E.E. Vaughan, C.M. Plugge, and W.M.d. Vos, *Akkermansia muciniphila gen. nov., sp. nov., a human intestinal mucin-degrading bacterium.* International Journal of Systematic and Evolutionary Microbiology, 2004. **54**: p. 1469-1476.

161. van der Beek, C.M., J.G. Bloemen, M.A. van den Broek, K. Lenaerts, K. Venema, W.A. Buurman, and C.H. Dejong, *Hepatic Uptake of Rectally Administered Butyrate Prevents an Increase in Systemic Butyrate Concentrations in Humans.* The Journal of Nutrition, 2015. **145**: p. 2019-2024.

162. Yao, Y., X. Cai, W. Fei, Y. Ye, M. Zhao, and C. Zheng, *The role of short-chain fatty acids in immunity, inflammation and metabolism*. Critical Reviews in Food Science and Nutrition, 2020: p. 1-12.

163. Besten, G.d., K.v. Eunen, A.K. Groen, K. Venema, D.-J. Reijngoud, and B.M. Bakker, *The role of short-chain fatty acids in the interplay between diet, gut microbiota, and host energy metabolism.* Journal of Lipid Research, 2013. **54**: p. 2325-2340.

164. Saudi, W.S.W. and M. Sjöblom, *Short-chain fatty acids augment rat duodenal mucosal barrier function.* Experimental Physiology, 2017. **102**: p. 791-803.

165. Clausen, M.R. and P.B. Mortensen, *Kinetic studies on colonocyte metabolism of short chain fatty acids and glucose in ulcerative colitis.* Gut, 1995. **37**: p. 684-689.

166. Wang, H.-B., P.-Y. Wang, X. Wang, Y.-L. Wan, and Y.-C. Liu, *Butyrate Enhances Intestinal Epithelial Barrier Function via Up-Regulation of Tight Junction Protein Claudin-1 Transcription.* Digestive Diseases and Sciences 2012 57:12, 2012. **57**: p. 3126-3135.

167. Arpaia, N., C. Campbell, X. Fan, S. Dikiy, J.v.d. Veeken, P. deRoos, . . . A.Y. Rudensky, *Metabolites produced by commensal bacteria promote peripheral regulatory T-cell generation.* Nature 2013 504:7480, 2013. **504**: p. 451-455.

168. Furusawa, Y., Y. Obata, S. Fukuda, T.A. Endo, G. Nakato, D. Takahashi, . . . H. Ohno, *Commensal microbe-derived butyrate induces the differentiation of colonic regulatory T cells.* Nature 2013 504:7480, 2013. **504**: p. 446-450.

169. Nastasi, C., M. Candela, C.M. Bonefeld, C. Geisler, M. Hansen, T. Krejsgaard, . . . A. Woetmann, *The effect of short-chain fatty acids on human monocyte-derived dendritic cells.* Scientific Reports 2015 5:1, 2015. **5**: p. 1-10.

170. Vernia, P., P.L. Fracasso, V. Casale, G. Villotti, A. Marcheggiano, V. Stigliano, . . . R. Caprilli, *Topical butyrate for acute radiation proctitis: randomised, crossover trial.* The Lancet, 2000. **356**: p. 1232-1235.

171. SHIN, R., M. SUZUKI, and Y. MORISHITA, *Influence of intestinal anaerobes and organic acids on the growth of enterohaemorrhagic Escherichia coli O157:H7.* Journal of Medical Microbiology, 2002. **51**: p. 201-206.

172. CA, C., H. M, P. GR, C. I, C.A. Cherrington, M. Hinton, . . . I. Chopra, *Short-chain organic acids at pH 5.0 kill Escherichia coli and Salmonella spp. without causing membrane perturbation.* Journal of Applied Bacteriology, 1991. **70**: p. 161-165.

173. Rolfe, R.D., *Role of volatile fatty acids in colonization resistance to Clostridium difficile.* Infection and Immunity, 1984. **45**: p. 185-191.

174. Gantois, I., R. Ducatelle, F. Pasmans, F. Haesebrouck, I. Hautefort, A. Thompson, . . . F. Van Immerseel, *Butyrate specifically down-regulates Salmonella pathogenicity island 1 gene expression.* Applied and Environmental Microbiology, 2006. **72**: p. 946-949.

175. Lamas, A., P. Regal, B. Vázquez, A. Cepeda, and C.M. Franco, *Short chain fatty acids commonly produced by gut microbiota influence Salmonella enterica motility, biofilm formation, and gene expression.* Antibiotics, 2019.

176. Yang, F., L. Yang, Z. Chang, L. Chang, and B. Yang, *Regulation of virulence and motility by acetate in enteropathogenic Escherichia coli.* International Journal of Medical Microbiology, 2018.

177. Repaske, D.R. and J. Adler, *Change in intracellular pH of Escherichia coli mediates the chemotactic response to certain attractants and repellents.* Journal of Bacteriology, 1981.

178. Umemura, T., Y. Matsumoto, K. Ohnishi, M. Homma, and I. Kawagishi, *Sensing of cytoplasmic pH by bacterial chemoreceptors involves the linker region that connects the membrane-spanning and the signal-modulating helices.* Journal of Biological Chemistry, 2002.

179. Chet, I. and R. Mitchell, *Ecological aspects of microbial chemotactic behavior.* Annual review of microbiology, 1976. **30**(1): p. 221-239.

180. Falke, J.J., R.B. Bass, S.L. Butler, S.A. Chervitz, and M.A. Danielson, *The two-component signaling pathway of bacterial chemotaxis: a molecular view of signal transduction by receptors, kinases, and adaptation enzymes.* Annual review of cell and developmental biology, 1997. **13**(1): p. 457-512.

181. Wadhams, G.H. and J.P. Armitage, *Making sense of it all: Bacterial chemotaxis.* Nature Reviews Molecular Cell Biology, 2004. **5**: p. 1024-1037.

182. Matilla, M.A. and T. Krell, *The effect of bacterial chemotaxis on host infection and pathogenicity.* FEMS microbiology reviews, 2017. **42**(1): p. fux052.

183. Adler, J. and B. Templeton, *The effect of environmental conditions on the motility of Escherichia coli.* Microbiology, 1967. **46**(2): p. 175-184.

184. Shioi, J., C. Dang, and B. Taylor, *Oxygen as attractant and repellent in bacterial chemotaxis.* Journal of bacteriology, 1987. **169**(7): p. 3118-3123.

185. Kihara, M. and R.M. Macnab, *Cytoplasmic pH mediates pH taxis and weak-acid repellent taxis of bacteria.* Journal of Bacteriology, 1981. **145**(3): p. 1209-1221.

186. Maeda, K., Y. Imae, J.-I. Shioi, and F. Oosawa, *Effect of temperature on motility and chemotaxis of Escherichia coli.* Journal of bacteriology, 1976. **127**(3): p. 1039-1046.

187. Keeney, K.M. and B.B. Finlay, *Enteric pathogen exploitation of the microbiota-generated nutrient environment of the gut.* Current Opinion in Microbiology, 2011. **14**: p. 92-98.

188. Makki, K., E.C. Deehan, J. Walter, and F. Bäckhed, *The impact of dietary fiber on gut microbiota in host health and disease.* Cell Host Microbe. **23**: p. 705-715.

189. Domka, J., J. Lee, and T.K. Wood, *YliH (BssR) and YceP (BssS) regulate Escherichia coli K-12 biofilm formation by influencing cell signaling.* Appl Environ Microbiol, 2006. **72**(4): p. 2449-59.

190. Lee, J., T. Bansal, A. Jayaraman, W.E. Bentley, and T.K. Wood, *Enterohemorrhagic Escherichia coli biofilms are inhibited by 7-hydroxyindole and stimulated by isatin.* Applied and Environmental Microbiology, 2007.

191. Lee, J., C. Attila, S.L. Cirillo, J.D. Cirillo, and T.K. Wood, *Indole and 7-hydroxyindole diminish Pseudomonas aeruginosa virulence.* Microb Biotechnol, 2009. **2**(1): p. 75-90.

192. Nikaido, E., E. Giraud, S. Baucheron, S. Yamasaki, A. Wiedemann, K. Okamoto, . . . K. Nishino, *Effects of indole on drug resistance and virulence of Salmonella enterica serovar Typhimurium revealed by genome-wide analyses.* Gut Pathogens, 2012.

193. Lee, J.H. and J. Lee, *Indole as an intercellular signal in microbial communities.* FEMS Microbiol Rev, 2010. **34**(4): p. 426-44.

194. Sridharan, G.V., K. Choi, C. Klemashevich, C. Wu, D. Prabakaran, L.B. Pan, . . . A. Jayaraman, *Prediction and quantification of bioactive microbiota metabolites in the mouse gut.* Nature communications, 2014. **5**: p. 5492.

195. Kumar, A., M. Ellermann, and V. Sperandio, *Taming the beast: Interplay between gut small molecules and enteric pathogens*, in *Infection and Immunity*. 2019.

196. Howard, M.F., X.R. Bina, and J.E. Bina, *Indole inhibits ToxR regulon expression in Vibrio cholerae.* Infection and Immunity, 2019: p. IAI.00776-18.

197. Kim, S.-K., H.-Y. Park, and J.-H. Lee, *Anthranilate deteriorates the structure of Pseudomonas aeruginosa biofilms and antagonizes the biofilm-enhancing indole effect.* Applied and Environmental Microbiology, 2015. **81**(7): p. 2328-2338.

198. Darkoh, C., K. Plants-Paris, D. Bishoff, and H.L. DuPont, *Clostridium difficile Modulates the Gut Microbiota by Inducing the Production of Indole, an Interkingdom Signaling and Antimicrobial Molecule* mSystems, 2019. **4**: p. e00346-18-e00346-18.

199. Muskavitch, M., E. Kort, M. Springer, M. Goy, and J. Adler, *Attraction by repellents: an error in sensory information processing by bacterial mutants.* Science, 1978. **201**(4350): p. 63-65.

200. Reader, R.W., W.-W. Tso, M.S. Springer, M.F. Goy, and J. Adler, *Pleiotropic aspartate taxis and serine taxis mutants of Escherichia coli.* Microbiology, 1979. **111**(2): p. 363-374.

201. Parkinson, J.S. and S.E. Houts, *Isolation and behavior of Escherichia coli deletion mutants lacking chemotaxis functions.* Journal of Bacteriology, 1982. **151**(1): p. 106-13.

202. Datsenko, K.A. and B.L. Wanner, *One-step inactivation of chromosomal genes in Escherichia coli K-12 using PCR products.* Proc. Natl Acad. Sci. USA, 2000. **97**(12): p. 6640-6645.

203. Scharf, B.E., K.A. Fahrner, L. Turner, and H.C. Berg, *Control of direction of flagellar rotation in bacterial chemotaxis.* Proceedings of the National Academy of Sciences, 1998. **95**(1): p. 201-206.

204. Ford, K.M., R. Chawla, and P.P. Lele, *Biophysical characterization of flagellar motor functions.* JoVE (Journal of Visualized Experiments), 2017(119): p. e55240.

205. Lele, P.P., R.W. Branch, V.S. Nathan, and H.C. Berg, *Mechanism for adaptive remodeling of the bacterial flagellar switch.* Proc. Natl Acad. Sci. USA, 2012. **109**(49): p. 20018-22.

206. Lele, P.P., A. Shrivastava, T. Roland, and H.C. Berg, *Response thresholds in bacterial chemotaxis.* Science Advances, 2015. **1**(9): p. e1500299.

207. Jani, S., A.L. Seely, A. Jayaraman, and M.D. Manson, *Chemotaxis to self-generated AI-2 promotes biofilm formation in Escherichia coli.* Microbiology, 2017. **163**(12): p. 1778-1790.

208. Jani, S., *Visualizing chemoattraction of planktonic cells to a biofilm*, in *Bacterial Chemosensing*. 2018, Springer. p. 61-69.

209. Wright, G.A., R.L. Crowder, R.R. Draheim, and M.D. Manson, *Mutational analysis of the transmembrane helix 2-HAMP domain connection in the Escherichia coli aspartate chemoreceptor Tar.* Journal of Bacteriology, 2011.

210. Segall, J.E., S.M. Block, and H.C. Berg, *Temporal comparisons in bacterial chemotaxis.* Proceedings of the National Academy of Sciences of the United States of America, 1986. **83**(23): p. 8987-8991.

211. Zarkan, A., S. Cano-Muniz, J. Zhu, K. Al Nahas, J. Cama, U.F. Keyser, and D.K. Summers, *Indole Pulse Signalling Regulates the Cytoplasmic pH of E. coli in a Memory-Like Manner.* Scientific reports, 2019. **9**(1): p. 3868.

212. Wilks, J.C. and J.L. Slonczewski, *pH of the cytoplasm and periplasm of Escherichia coli: Rapid measurement by green fluorescent protein fluorimetry.* Journal of Bacteriology, 2007. **189**(15): p. 5601-5607.

213. Martinez, K.A., R.D. Kitko, J.P. Mershon, H.E. Adcox, K.A. Malek, M.B. Berkmen, and J.L. Slonczewski, *Cytoplasmic pH response to acid stress in individual cells of Escherichia coli and Bacillus subtilis observed by fluorescence ratio imaging microscopy.* Applied and Environmental Microbiology, 2012. **78**(10): p. 3706-3714.

214. Berg, H.C., *The Rotary Motor of Bacterial Flagella.* Annual Review of Biochemistry, 2003. **72**: p. 19-54.

215. Lele, P.P. and H.C. Berg, *Switching of bacterial flagellar motors triggered by mutant FliG.* Biophysical Journal, 2015. **108**(5): p. 1275-80.

216. Minamino, T., K. Imada, M. Kinoshita, S. Nakamura, Y.V. Morimoto, and K. Namba, *Structural insight into the rotational switching mechanism of the bacterial flagellar motor.* PLoS Biology, 2011. **9**: p. e1000616-e1000616.

217. Yuan, J., R.W. Branch, B.G. Hosu, and H.C. Berg, *Adaptation at the output of the chemotaxis signalling pathway.* Nature, 2012. **484**(7393): p. 233-6.

218. Eisenbach, M., C. Constantinou, H. Aloni, and M. Shinitzky, *Repellents for Escherichia coli operate neither by changing membrane fluidity nor by being sensed by periplasmic receptors during chemotaxis.* Journal of Bacteriology, 1990. **172**: p. 5218-5224.

219. Lai, R.Z., J.M. Manson, A.F. Bormans, R.R. Draheim, N.T. Nguyen, and M.D. Manson, *Cooperative signaling among bacterial chemoreceptors.* Biochemistry, 2005. **44**(43): p. 14298-307.

220. Togashi, F., S. Yamaguchi, M. Kihara, S.I. Aizawa, and R.M. Macnab, *An extreme clockwise switch bias mutation in fliG of Salmonella typhimurium and its suppression by slow-motile mutations in motA and motB.* J. Bacteriol., 1997. **179**(9): p. 2994-3003.

221. Khan, S. and R.M. Macnab, *Proton chemical potential, proton electrical potential and bacterial motility.* Journal of molecular biology, 1980. **138**(3): p. 599-614.

222. Khan, S., J.L. Spudich, J.A. McCray, and D.R. Trentham, *Chemotactic signal integration in bacteria.* Proceedings of the National Academy of Sciences, 1995. **92**(21): p. 9757-9761.

223. Mao, H., P.S. Cremer, and M.D. Manson, *A sensitive, versatile microfluidic assay for bacterial chemotaxis.* Proceedings of the National Academy of Sciences of the United States of America, 2003.

224. Khan, S. and D.R. Trentham, *Biphasic excitation by leucine in Escherichia coli chemotaxis.* Journal of bacteriology, 2004. **186**(2): p. 588-592.

225. Moreira, C.G., R. Russell, A.A. Mishra, S. Narayanan, J.M. Ritchie, M.K. Waldor, . . . V. Sperandio, *Bacterial Adrenergic Sensors Regulate Virulence of Enteric Pathogens in the Gut.* mBio, 2016. **7**(3).

226. Hansen, M.C., R.J. Palmer Jr, C. Udsen, D.C. White, and S. Molin, *Assessment of GFP fluorescence in cells of Streptococcus gordonii under conditions of low pH and low oxygen concentration.* Microbiology, 2001. **147**(5): p. 1383-1391.

227. Pham, H.T. and J.S. Parkinson, *Phenol sensing by Escherichia coli chemoreceptors: A nonclassical mechanism.* Journal of Bacteriology, 2011.

228. Yang, J., R. Chawla, K.Y. Rhee, R. Gupta, M.D. Manson, A. Jayaraman, and P.P. Lele, *Biphasic chemotaxis of Escherichia coli to the microbiota metabolite indole.* Proceedings of the National Academy of Sciences, 2020. **117**(11): p. 6114-6120.

229. Maeda, K., Y. Imae, J.-I.I. Shioi, and F. Oosawa, *Effect of temperature on motility and chemotaxis of Escherichia coli.* Journal of Bacteriology, 1976. **127**: p. 1039-1046.

230. Yoney, A. and H. Salman, *Precision and variability in bacterial temperature sensing.* Biophysical Journal, 2015.

231. Berg, H.C. and S.M. Block, *A Miniature Flow Cell Designed for Rapid Exchange of Media Under High-power Microscope Objectives.* Microbiology, 1984. **130**: p. 2915-2920.

232. Weis, R.M., T. Hirai, A. Chalah, M. Kessel, P.J. Peters, and S. Subramaniam, *Electron microscopic analysis of membrane assemblies formed by the bacterial chemotaxis receptor Tsr.* Journal of Bacteriology, 2003. **185**: p. 3636-3643.

233. Gardina, P., C. Conway, M. Kossman, and M. Manson, *Aspartate and maltose-binding protein interact with adjacent sites in the Tar chemotactic signal transducer of Escherichia coli.* Journal of Bacteriology, 1992. **174**: p. 1528-1536.

234. Ward, S.M., A. Delgado, R.P. Gunsalus, and M.D. Manson, *A NarX-Tar chimera mediates repellent chemotaxis to nitrate and nitrite.* Molecular Microbiology, 2002. **44**: p. 709-719.

235. Manson, M.D., *The tie that binds the dynamic duo: The connector between AS1 and AS2 in the HAMP domain of the Escherichia coli Tsr chemoreceptor.* Journal of Bacteriology, 2008. **190**: p. 6544-6547.

236. Lozupone, C.A., J.I. Stombaugh, J.I. Gordon, J.K. Jansson, and R. Knight, *Diversity, stability and resilience of the human gut microbiota*, in *Nature*. 2012.

237. Lackraj, T., J.I. Kim, S.L. Tran, and D.E. Barnett Foster, *Differential modulation of flagella expression in enterohaemorrhagic Escherichia coli O157: H7 by intestinal short-chain fatty acid mixes.* Microbiology (United Kingdom), 2016.

238. Vaknin, A. and H.C. Berg, *Osmotic stress mechanically perturbs chemoreceptors in Escherichia coli.* Proceedings of the National Academy of Sciences of the United States of America, 2006.

239. Sourjik, V. and H.C. Berg, *Functional interactions between receptors in bacterial chemotaxis.* Nature, 2004.

240. Mello, B.A. and Y. Tu, *An allosteric model for heterogeneous receptor complexes: Understanding bacterial chemotaxis responses to multiple stimuli.* Proceedings of the National Academy of Sciences of the United States of America, 2005.

241. Neville, B.A., P.O. Sheridan, H.M.B.B. Harris, S. Coughlan, H.J. Flint, S.H. Duncan, . . . P.W. O'Toole, *Pro-Inflammatory Flagellin Proteins of Prevalent Motile Commensal Bacteria Are Variably Abundant in the Intestinal Microbiome of Elderly Humans.* PLoS ONE, 2013. **8**: p. e68919.

242. Ju, T., Y. Shoblak, Y. Gao, K. Yang, J. Fouhse, B.B. Finlay, . . . B.P. Willing, *Initial gut microbial composition as a key factor driving host response to antibiotic treatment, as exemplified by the presence or absence of commensal Escherichia coli.* Applied and Environmental Microbiology, 2017. **83**.

243. Li, X., J. Stokholm, A. Brejnrod, G.A. Vestergaard, J. Russel, U. Trivedi, . . . S.J. Sørensen, *The infant gut resistome associates with E. coli, environmental exposures, gut*

*microbiome maturity, and asthma-associated bacterial composition.* Cell Host & Microbe, 2021. **29**: p. 975-987.e4.

244. Vaknin, A. and H.C. Berg, *Direct Evidence for Coupling between Bacterial Chemoreceptors.* Journal of Molecular Biology, 2008.